Peer-reviewed version available at Crystals 2018, 8, 412; doi:10.3390/cryst8110412

Type of the Paper (Review)

Metal–organic framework membranes: from fabrication to application in gas separation.

Osama Shekhah [1], Valeriya Chernikova[1], Youssef Belmabkhout[1], Mohamed Eddaoudi[1,*]

[1] King Abdullah University of Science and Technology, Advanced Membranes & Porous Materials Center, Division of Physical Sciences and Engineering, Functional Materials Design, Discovery and Development research group (FMD[3]), Thuwal 23955-6900, KSA.

* Correspondence: mohamed.eddaoudi@kaust.edu.sa; Tel.: +966-12-808-1245

Abstract:

Gas membrane-based separation is considered one of the furthermost effective technology to address energy efficiency and large footprint challenges. Various classes of advanced materials including polymers, zeolites, porous carbons and metal–organic frameworks (MOFs) were attempted as membranes for gas separation. MOFs, among other porous materials, possess uniquely tunable nature, in which the pore size and environment can be controlled by connecting metal ions (or metal ion clusters) with organic linkers with various functionalities. This feature makes them attractive for thin membrane fabrication, as both diffusion and solubility components of permeability can be altered. It is interesting to notice that numerous reports have addressed the synthesis of different MOFs, fabrication of their corresponding thin films and their applications, nonetheless, relatively limited studies addressed their gas separation application as membranes. In this review, we provide a synopsis of the various MOF-based membranes that were fabricated in the last decade. In this review we propose a short introduction touching on the gas separation membrane technology and we shed light on (i) the various techniques developed for the fabrication of MOF as membranes and (ii) challenges and application for MOF thin film membranes in various important gas separation applications.

Keywords: MOFs; membranes; separation; gas; thin film; defects.

1. Introduction

A variety of technologies that are relevant to gas separations applications have been developed in the petrochemical industries, such as distillation and condensation. Despite maturity of these technologies, they suffer from heavy energy consumption and inefficiency.[1] Alternatively, membrane-based separation is proposed to be a potential replacement candidate, due to its facile operation, lower energy consumption and smaller footmark.[2] Despite the advances in material science and diversity of available materials, polymers have dominated more than 95% of the current industrial gas separation market. This is mainly due to the simplicity of polymers processing, low cost and scalability easiness.[2] However, polymer-based membranes have well documented disadvantages including selectivity/productivity trade-off, low thermal and chemical stabilities and short operating lifetime.[3-5] Because of their unique rigid structures with well-defined, regular pores, microporous Zeolites were also extensively explored as potential candidates for membrane-based gas separations. [6-12] The unique properties of zeolites, paved the way to explore them in the form of membranes in the lab as molecular sieves to achieve gas separation with high performance.[8-13] Additionally, their high thermal and chemical stabilities, potentially allow their use for separation processes that are operating at elevated temperatures and/or require harsh chemical conditions which typical polymers cannot withstand. Despite the advances in the zeolite membrane field, high

Peer-reviewed version available at Crystals 2018, 8, 412; doi:10.3390/cryst8110412

cost of the production of zeolite thin supported membranes (and appropriate modules) together with excellent performance does not outweigh the same parameters in polymers. Therefore, currently, zeolites are not used in industrial scale gas separation. Importantly, the zeolite chemistry is limited to only inorganic components and relies on topologically unpredictable synthetic routes for the synthesis of new compounds. Therefore, it is nearly impossible to control and design the material with targeted pore size and environment. The ability to tune the properties of rigid microporous materials might increase the value per price component of zeolite (or other microporous materials) market and give a start to their industrial use.

The research in metal–organic framework (MOF) area has unveiled tremendous development within the last 20 years.[14-17] This unique class of porous materials received an extensive attention because of their unique properties, which arise from the varied number of organic linkers and metal ions that can be applied, especially since the products of their assemblage can be gained as crystalline material that can be entirely characterized. MOFs exhibit a wide range of porosity, uniform- tunable pore sizes and distinct sorption/diffusivity features.[14-20] The MOF research field is rapidly expanding, going through all aspects of material science from discovery, property analysis, application and implementation as shown in Figure 1. Because of innovative character of this class of porous materials, the assessment of their performances in the field of separation and purification is gaining intense interest from researchers in different fields of chemistry, materials sciences, industrial and chemical engineering. MOFs are very fascinating target materials for membrane fabrication for gas separation applications. In fact, their pores can be judiciously controlled by the interchange of both inorganic and organic components, amenable to advanced control the gas diffusion/sorption in the pores. In addition, the functionalization of their pore surfaces can be easily achieved via a range of methodologies.[15,18,21,22]

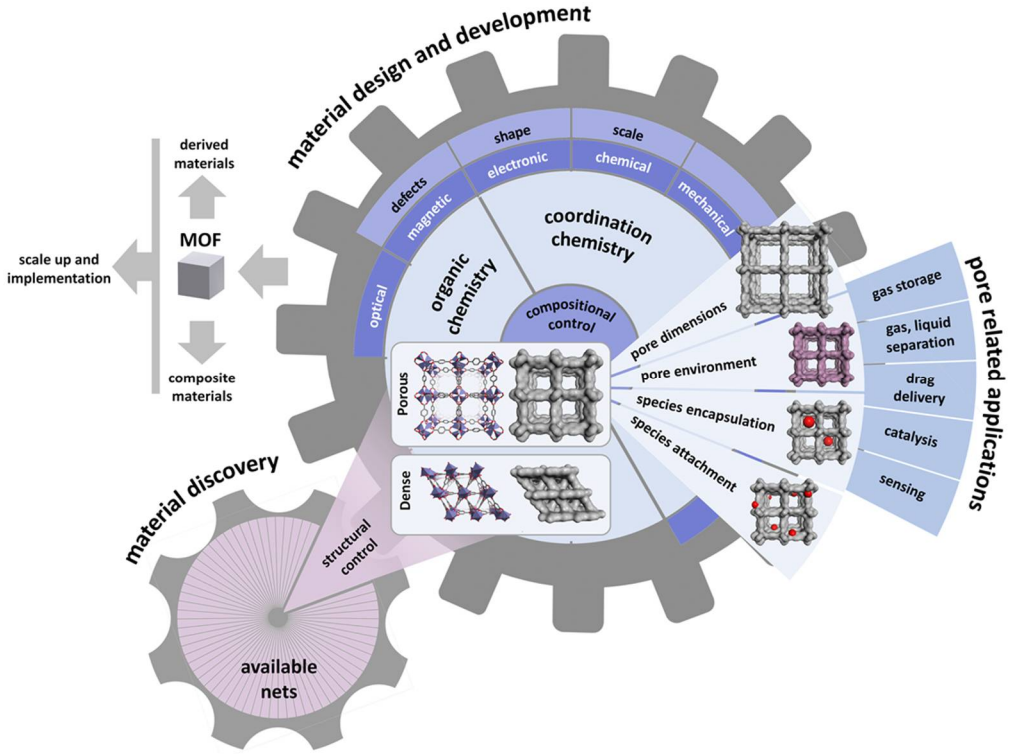

Figure 1. A landscape for MOF research areas from discovery and design to applications.

In general, gas-separation is based on two types of separations, which is diffusion-based that is controlled by the size and shape of the analyte moieties, or sorption-based that is based on the sorption affinity of the analyte in the pores. In case of microporous membranes, such as zeolites and MOFs, many aspects can contribute to their separation features, for instance molecular sieving (which is based on aperture size/shape selectivity), the structure aperture size and pore size, surface diffusion and capillary condensation. In another case, favored sorption could play the dominant role in permeation. This can happen when the adsorption of a specific analyte in gas mixture is much

stronger than the other components, resulting in blockage/hindering the path of the other components via the membrane.[23-25]

The main focus of the present MOF research was the discovery, design, synthesis and characterization of newfangled MOF structures, which is reflected in the fast increase in their number of publications. However, the number of studies about MOF films and membranes is still limited but is experiencing more growth in the last decades. Even though being in its early development stage, the current progress made in this field has proven that MOFs as membranes are promising candidates for gas separation applications.[12,19,22,26] In this review, we focus our discussion on determining the opportunities and the challenges in MOF thin films applicability as membranes. The review starts with introducing the current methodologies for the MOF membranes fabrication, then discusses their performance in different important gas separation applications like hydrogen purification, CO_2 capture, and hydrocarbon separation.

2. Basic principles for the application of MOFs for membrane-based gas separation.

For gas membrane-based separations, there are two main factors that play role on the membrane separation performance, which are solubility and the diffusivity of the analytes in single or multi-components mixtures. The solubility of the targeted gas is administrated through its thermodynamic affinity/interactions with the membrane, while its diffusivity is directed by its relative size with respect to the apertures and the pore sizes of the framework.

In principle, molecules in the gas mixture that have relatively stronger affinity/interactions with the pore framework of the membrane will adsorb strongly and diffuse faster through the membrane if the apertures and pore size are large enough than the size of the permeates.[27,28] This case can lead to good separation (i.e. solubility-based separations) if the interactions are enough mild to allow optimal desorption downstream, resulting in a permselectivity in favor of the highly absorbable analyte. Thus, the solubility-based separation can be enhanced by tuning the surface, through ligand modification or chemical functionalization.[24,29-32] This modification can lead in turn to variations in the pore aperture and volume, surface, nature or functionality, i.e. polarity, hydrophilicity or hydrophobicity which can lead to either improvement or drop in the selectivity-permeability trade-off.[24]

In the case of molecular sieving/molecular i.e. size-selective separations, where the kinetic diameters of the targeted analytes/molecules for separation, dictates the selection of the MOFs candidates with the suitable pore aperture for a given separation.[33] It is worth to mention that several reports demonstrated that even gases that have a kinetic diameter larger than that of the pore aperture are still able to permeate through the MOF membrane attributable to the well-known framework flexibility in MOFs.[34-38] The widespread flexible nature of the MOFs make the selection of the MOF for membrane-based separation extremely challenging. In addition, MOF based thin films development experience other acute challenges that should be considered in order to apply the MOFs as membranes like, the facility of fabrication, the crystallinity of the films, the directionality of the growth, the activation condition, their tunability and functionality and the flexibility of the structure.

3. Methods for the fabrication of MOFs as membranes

The successful fabrication of MOF membranes of sufficient quality is the major challenge that needs to be addressed before applying them for gas separation. In the case of MOFs, there is no universal recipe that can be used to fabricate the MOFs as membrane and for each MOF the fabrication methodology has to be explored/studied and optimized. It is important to highlight that crystalline inorganic and MOF materials are generally characterized by high brittleness and fragility in the form of self-supported (free-standing) films.[39] Therefore these materials must be attached to a highly porous, mechanically strong and rigid substrates in order to obtain membranes.

In terms of fabrication, there are several challenges that must be overcome in order to apply MOFs as membranes, like (1) the adhesion between the MOF thin film and the membrane support, (2) stability of the MOF thin film, (3) the enhancement of intergrowth of the MOF crystals and (4) the formation of macroscopic crack defects during fabrication or upon activation.[12,19,22,26,40-42] Similar to zeolites, in light of its crystalline nature a wide selection of synthesis approaches to

fabricate MOF thin film membranes were explored and developed; like (i) in situ growth solvothermal or (ii) secondary growth seeded-assisted methods.[11,13] Delightfully, the advantage of MOFs to be made under milder conditions, as compared to zeolites, afforded a larger spectrum of fabrication methodologies to grow MOFs membranes such as the layer-by-layer method.[40,43-51]

The MOF membrane fabrication involves the growth of the targeted MOF with the desired properties as a thin layer on top of different supports. In 2009 Lai and Jeong et al., reported the first MOF membrane based on MOF-5 that was grown solvothermally on a porous alumina substrate, which has been tested for gas separation.[52] Later on, many other MOF membranes have been reported using a solvothermal, a secondary growth method,[12] and a microwave-assisted solvothermal method.[53] These early reports were encouraging and have proven the possibility to prepare MOF membranes and paved the way to test them in the lab for separation applications.

In succeeding section, we present a short description of the diverse approaches that have been applied for the fabrication of MOFs as thin film membranes: (a) direct growth solvothermal method which also includes (b) secondary growth, (c) counter diffusion, (d) the gel vapor method and finally (e) the layer-by-layer growth method (Figure 2).

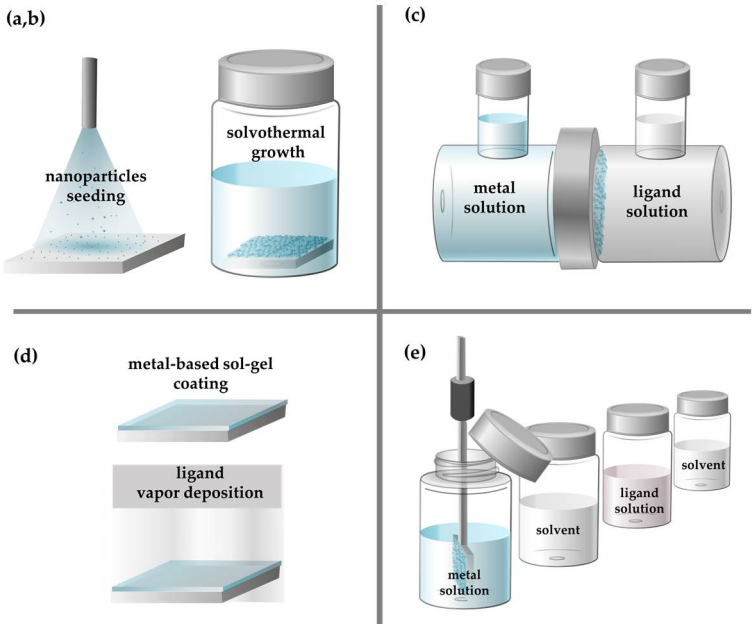

Figure 2. The schematic representation of the MOF membrane preparation methods.

3.1 In situ solvothermal growth method

This approach refers to the direct growth on the substrate, where the nucleation of MOF crystal and later on their, growth and intergrowth happen on the support immersed in the solution during the synthesis step. The substrate could have been used in some cases without any functionalization/modification, or it could be chemically functionalized/modified prior to MOF growth. This approach is built on the dipping of the support in the mother solution of the targeted MOF, then sealing and heating it to the targeted temperature.[54-57] Instead of conventional oven heating the microwave irradiation can be used.[53,58-62] In their first work Lai and Jeong et al. used this method to grow MOF-5 as a thin film on a non-modified porous alumina support, which is considered as the first reported continuous and well-intergrown membrane in MOF field (Figure 3). [52] In this study they could vary the thickness of the thin film membrane, by varying the immersion times during synthesis.

Later on, using modified synthetic conditions different MOFs membranes like HKUST-1, ZIF-8, ZIF-69, UiO-66, MOF-74 among others, were fabricated using the in situ solvothermal method on different porous supports like titania, alumina, copper net, etc. without the support modification.[63-74]

Peer-reviewed version available at Crystals 2018, 8, 412; doi:10.3390/cryst8110412

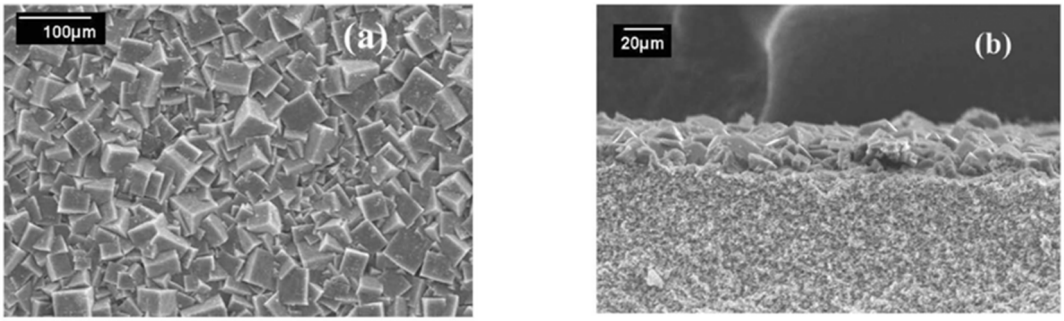

Figure 3. SEM images of the MOF-5 membrane: (a) top view, (b) cross section (adapted with permission from ref. [52]).

Alternatively, the in situ solvothermal method was also used to prepare $Ni_2(L\text{-}asp)_2(bipy)$ MOF on a Ni-based net support, that was used as the sole source for nickel and as a support at the same time (Figure 4). The Ni-based net was the sole Ni-source in the synthesis, therefore it was the limiting factor for membrane growth, where the growth stops once the membrane layer is formed and when the nickel net is becoming not accessible.[75] Similar approach was used to fabricate ZIF-8 membrane, in which zinc oxide sputtered on the polymer support served as the metal source.[76]

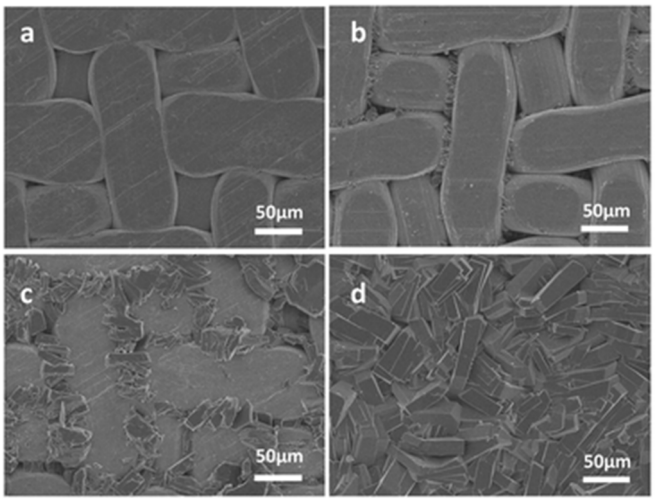

Figure 4. Top view SEM pictures of $Ni_2(L\text{-}asp)_2(bipy)$ membranes grown for (a) 1 h, (b) 2 h, (c) 3 h, (d) 4 h at 150 °C (adapted with permission from ref. [75])

In some other cases the quality of the fabricated membranes was not sufficient enough (i.e. in terms of continuity or homogeneity). This poor quality of the formed thin film membranes can be as result of many factors like bad bonding/adhesion with the support and or weak crystals intergrowth. Therefore, as an alternative strategy to overcome this problem, the supports were firstly functionalized to increase the number of functional groups (i.e. nucleation sites) on the support surface to enhance the bonding and growth of the MOF layer on the support.[39, 77-84]

The preparation of a continuous pure ZIF-67 tubular membrane was achieved by direct transformation of carbonate hydroxide nanowire arrays (Co-NWAs) in a 2-methylimidazole (Hmim) aqueous solution was reported by Zhang et al.[77] This strategy included first the growth of Co-NWAs on a porous ceramic tube and then the conversion to a continuous ZIF-67 membrane by reaction in the Hmim aqueous solution Figure 5. The obtained ZIF-67 membrane thickness was 1.7 µm and exhibits a high H_2 permeance of 5.6×10^{-7} mol m^{-2} s^{-1} Pa^{-1}, and the H_2/N_2 and H_2/CH ideal separation factors, were found to be 14.7 and 15.3, respectively.

A covalent functionalization methodology was reported by Caro et al. for fabricating ZIF-90 and ZIF-22 membrane by means of APTES (3-aminopropyltriethoxysilane) that act as covalent linkers between the MOF layer and the support (Figure 6).[78,79] In this case the APTES ethoxy functional groups reacts with the Al_2O_3 support surface-OH groups and later on these NH_2 groups on the

support surface provided nucleation sites for the MOF growth through reaction with the MOF exposed aldehyde groups from the organic linker through imine condensation reaction.[78]

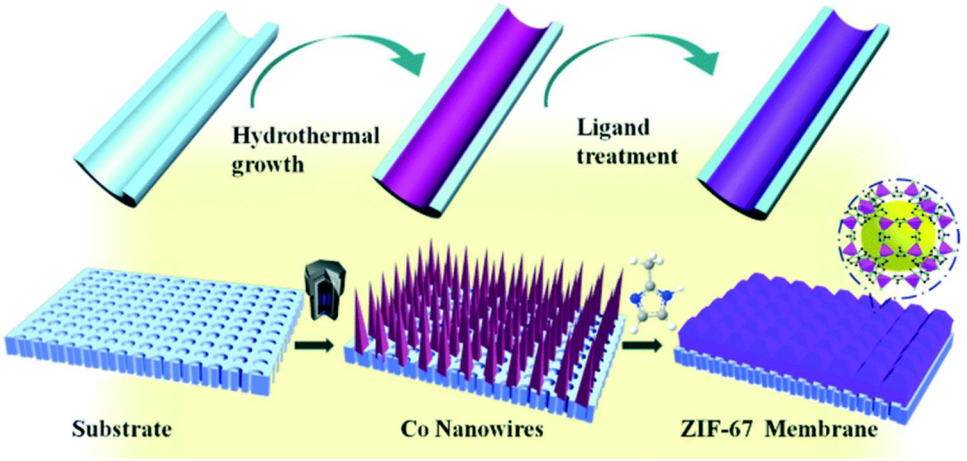

Figure 5. Schematic illustration of the preparation of a pure ZIF-67 membrane by self-conversion of Co-NWAs. (adapted with permission from ref. [77])

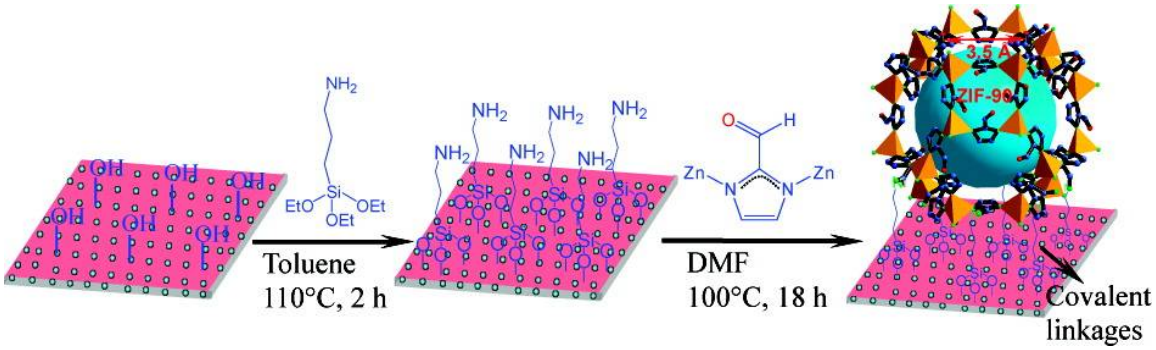

Figure 6. Scheme for preparing ZIF-90 membranes using 3-aminopropyltriethoxysilane (APTES) as a covalent linker between a ZIF-90 membrane and an Al_2O_3 support via an imine condensation reaction (adapted with permission from ref. [78]).

In 2010 Jeong et al. fabricated both of ZIF-8 and ZIF-7 membranes via the direct functionalization of the support with the organic ligand.[65] The principle is simply based on the reaction of the imidazole linkers with the preheated support to generate an Al–N bond. In order to do that the Al_2O_3 supports were heated at first to ~200 °C and then directly exposed to the solution of the ligand, which led to the fast evaporation of the solvent in the organic solution. This leaves the organic linkers covalently bonded to the Al_2O_3 support. Later on, growth on modified supports was performed using the in situ solvothermal growth approach.

The functionalization of the support with a polymer layer is another approach that has been applied by Caro et al. via the immersion of the Al_2O_3 supports in an aqueous buffered solution of dopamine at room temperature. The dopamine at pH 8.5 spontaneously polymerizes into polydopamine (PDA) and form a thin layer on the Al_2O_3 surface or any other surfaces.[80,81] Later on a ZIF-8 membrane by in situ solvothermal method was fabricated onto the PDA-modified macroporous stainless-steel-nets.[81] Post-synthetic membrane modification with graphene oxide (GO) has proven to be able to seal intercrystalline defects and in a later study, Caro et all have managed to obtain a better performing ZIF-8 membrane supported on polydopamine-functionalized support (Figure 7).[82]

Qiu et al. followed an alternative way to functionalize the support by using a spin coated poly(methyl methacrylate) (PMMA) on a substrate surface like silicon wafer in this case as support.[83] The PMMA surface was then hydrolyzed by concentrated H_2SO_4 to convert it to

poly(methacrylic acid) (PMAA). Finally, the in situ solvothermal method was applied for the growth of the MOF membrane on the PMMA–PMAA coated substrate.

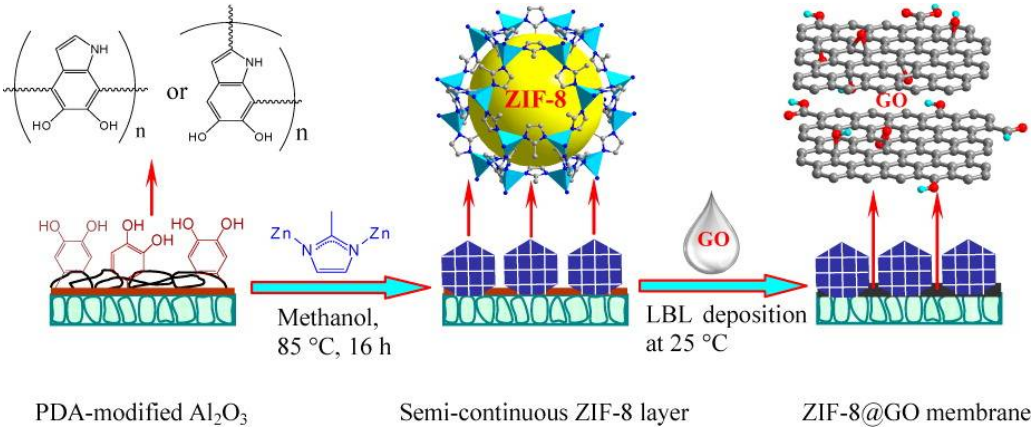

Figure 7. Scheme of preparation of bicontinuous ZIF-8@GOmembranes through layer-by-layer deposition of graphene oxide on the semicontinuous ZIF-8 layer which was synthesized on a polydopamine-modified alumina disk (adapted with permission from ref. [82])

3.2 The seed-assisted growth method

The seed-assisted growth method is another approach, which has been adapted from zeolites to grow MOF membrane.[84,85] This approach has some advantageous since it helps to grow a compact and continuous MOF membrane and a control on the MOF thin film orientation in some cases. There have been many seeding techniques that have been developed and applied including support rubbing with MOF crystals, dip coating in crystals solution, spin coating, layer-by-layer and heating, which we address them briefly in this section.

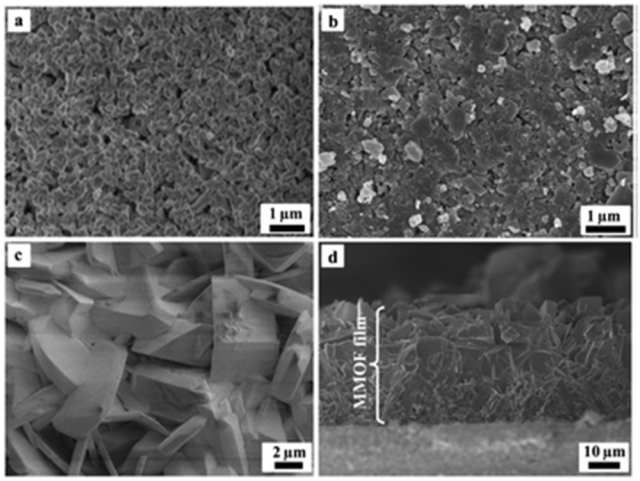

Figure 8. SEM images at different stages of MOF membrane growth: (a) α-alumina support, (b) seed layer, (c) membrane (top view) and (d) membrane (cross-section view) (adapted with permission from ref. [86]).

Tsapatsis et al. used the seed-assisted growth method via a manual rubbing approach of the MOF seed crystals onto PEI-functionalized alumina support, then applying the in situ solvothermal method MOF membrane growth (Figure 8).[86] Using assisted seed growth method through dropwise coating with colloidal seed suspension of NH_2-MIL-53(Al) MOF on macroporous glass frit disc, and a seed layer was formed after drying it under ambient condition overnight. A continuous NH_2-MIL-53(Al) membrane was fabricated later by placing the seeded support in a Teflon-lined vessel and then using the in situ solvothermal growth, a dense and well-closed MOF membrane was achieved.

Peer-reviewed version available at Crystals 2018, 8, 412; doi:10.3390/cryst8110412

Alternatively, this seeding step can be made by an in situ growth process using the solvothermal synthesis method, through producing a seeding layer by reacting firstly the support with the organic linker with no metal precursor (Figure 9). This approach has proven to be important to fabricate a homogenous, closed thin film MIL-53 MOF membrane.[87]

The layer-by-layer (LBL) process was also applied by Jin et al. as another technique to coat a homogeneous seeding layer on an alumina support. The targeted HKUST-1 membrane was grown later on the seeded support again through an in situ solvothermal method.[69]

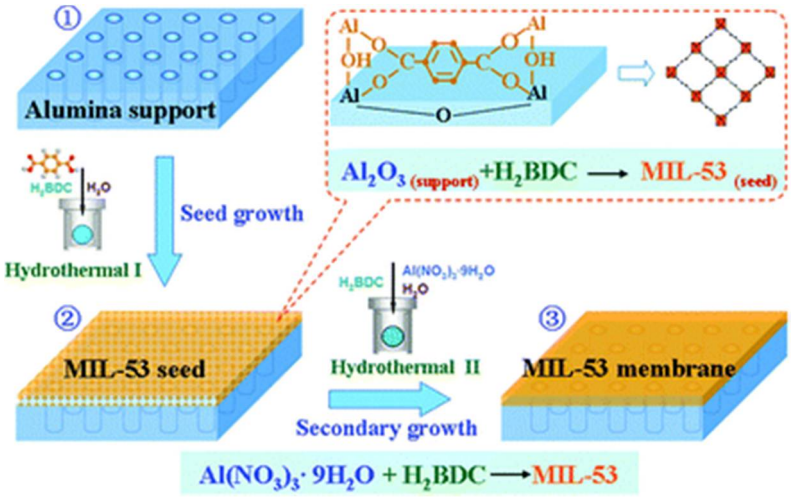

Figure 9. Schematic diagram of preparing the MIL-53 membrane on an alumina support via the reactive seeding method (adapted with permission from ref. [87])

3.3 Counter diffusion method

Counter diffusion method for synthesis of MOFs implies the slow diffusion of the reagents from different sides of the porous substrate (usually metal and ligand precursor solutions of MOFs are separated) into the substrate pores. In this case, the growth appears on one of the sides of the substrates, which can be in general controlled by means of varying the targeted reagents concentrations.[88-90]

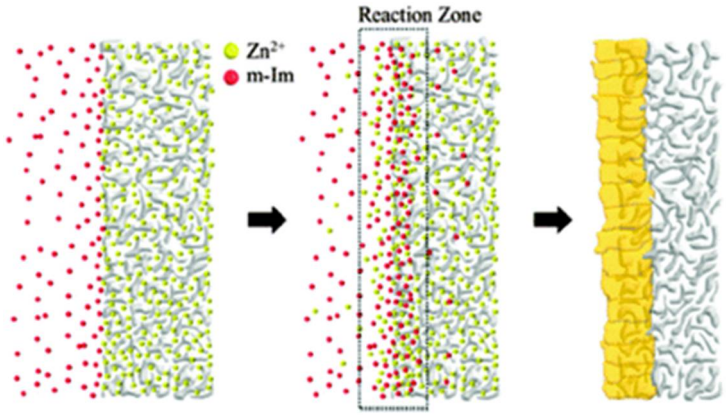

Figure 10. Schematic illustration of membrane synthesis using the counter-diffusion-based in situ method (adapted with permission from ref.[65]).

A simple method to functionalize the support was reported by Jeong et al., in 2013, which is based on soaking the support initially in the first component solution (like metal precursor in this case) for some time, then subjecting to solvothermal growth condition in another component solution like a ligand (Figure 10).[65] Upon support contact with the component solution, either metal ions or ligand molecules, as a result of concentration, can diffuse to the solution from the support or vice versa. The metal ions and ligand solutions were retained in high concentrations in the area of the

Peer-reviewed version available at Crystals 2018, 8, 412; doi:10.3390/cryst8110412

support throughout the solvothermal handling. The MOF thin film growth was completed after about 30 min of reaction and its thickness was about 1.5 μm, which did not vary, after longer growth times. Pienemann et al. have demonstrated recently, that an enhancement in the fabrication of the ZIF-8 MOF membrane, can be achieved via the polymer support modification prior to MOF growth. [11, 15] They have used a polymer than can bind zinc ions, which could provide favorable surface for ZIF-8 growth. In this study, they have used Poly-thiosemicarbazide (PTSC) polymer (Figure 11), which is form the group of thiosemicarbazide materials, which are known for their ability to chelate with various metals. In this work, they have coated PAN support with PTSC and further explore its affinity for zinc ions for ZIF-8 membrane fabrication.[91] Upon surface modification with PTSC, ultrathin and compact ZIF-8 thin films were grown via a counter diffusion method. In this method, each of the two solutions of the zinc ions and the 2-methylimidazole (HMIM) organic ligand made from the same solvent are introduced to the cell from opposite sides of the support. Upon their introduction, solution diffuse in opposite directions, leading to the ZIF-8 thin film growth on one side of the support surface. Later on, the gaps in the thin film allow further diffusion of the reactant components, leading to the filling of these gaps and formation of a dense membrane layer (Figure 12).

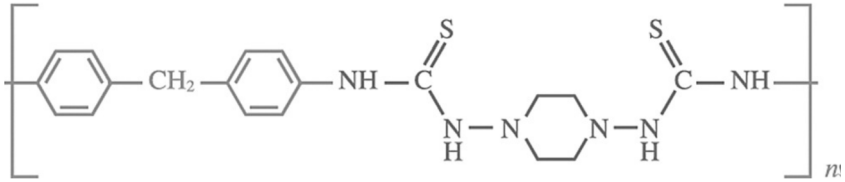

Figure 11. Structure of poly-thiosemicarbazide (adapted with permission from ref. [91]).

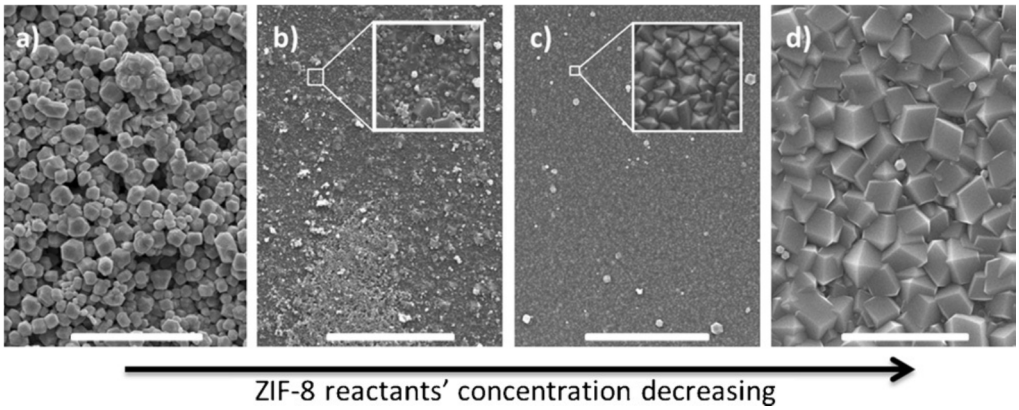

Figure 12. SEM surface images of ZIF-8/PTSC membranes prepared with different reactant concentrations: a) M1, b) M2, c) M3, and d) M4. Scale bar: 10 mm (adapted with permission from ref. [91]).

3.4 Gel vapor deposition method

A gel–vapor deposition (GVD) method was introduced by Zeng et al. for MOF membranes fabrication. The method is based on combining a free sol–gel coating with a solvent-free vapor deposition.[92] Through this method, a better control over the thickness of the MOF membranes can be achieved and in some cases, a 20 nanometer-thick MOF membrane can be fabricated via the variation of sol concentrations and coating techniques. This method proved to bring several advantages like the no need for pretreatment of supports prior to growths, compatibility between MOF and supports, low cost via the possibility to reuse MOF precursors, the facile handling of MOF layers locations and shortening the time of fabrication. The GVD approach was applied to grow ultrathin ZIF-8 membranes by using a sol precursor, which is Zn-based, prepared via the mixing of zinc acetate dihydrate precursor and ethanolamine base in ethanol solvent. This support was then coated with sol precursor and thermally treated to form the Zn-based gel. Later on, this gel thin film was converted to the MOF membrane by the deposition of the ligand vapor by heating (Figure 13, a). In this process, the produced ligand vapor reacts with the sensitive Zn-based gel thin film, which leads to the crystallization of the MOF (Figure 13, b).

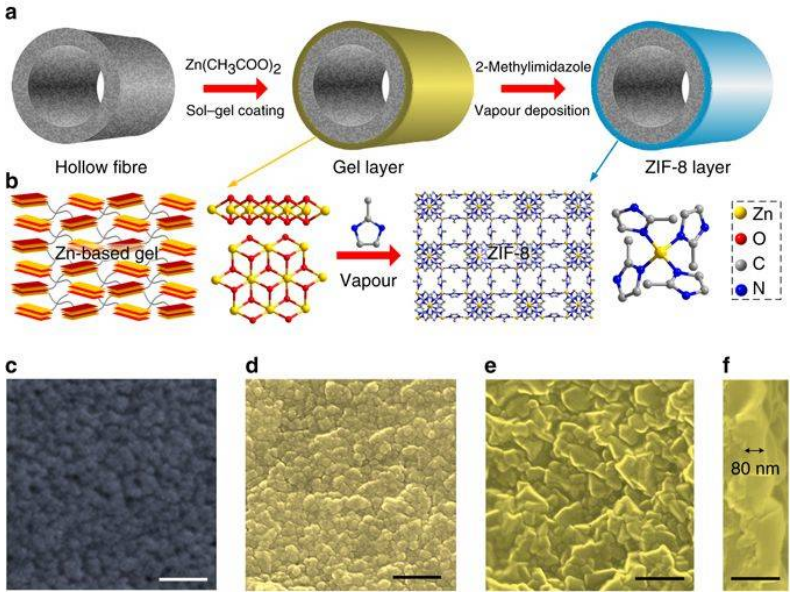

Figure 13. GVD fabrication of ultrathin ZIF-8 membrane. a) Schematic of MOF membrane formation process. b) Schematic illustration and chemical structure of Zn-based gel and crystalline structure of ZIF-8. Zn, O, C and N atoms are depicted in *yellow*, *red*, *grey* and *blue*, respectively. H atoms are not presented for clarity. Top view SEM images of (c) the PVDF hollow fiber and (d) the Zn-based gel layer. SEM images of (e) top and (f) cross-sectional view of the ZIF-8 membrane prepared with sol concentration of 1 U and coating time of 2 s. The images are colored for clarity. *Scale bar*, 200 nm (adapted with permission from ref. [96]).

3.5 Layer-by-layer method

The developed layer-by-layer (LBL) growth method in 2007 was successfully verified for fabricating thin films of HKUST-1 MOF.[43,93-97] The LBL growth method for MOFs is based on the exposing of the support surface to the reaction precursors in an alternating approach that is separated by a rinsing step for removing excess/unreacted precursors after each step. Using this approach, it was possible to grow different types of surface mounted MOFs (SURMOFs) on organic and oxide surfaces.

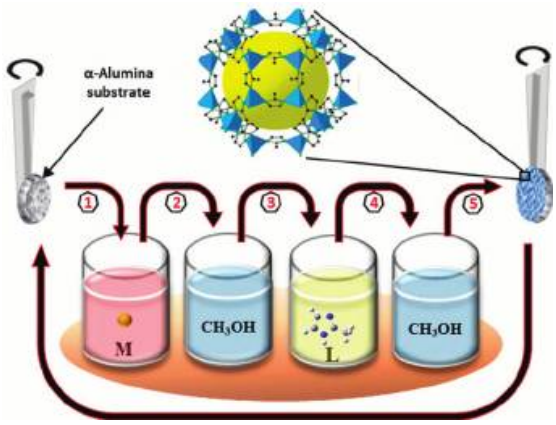

Figure 14. Schematic diagram for the automated LBL growth of MOFs thin films on substrates functionalized with SAMs. The preparation is done by repeated immersion cycles first in solution of the metal precursor and subsequently in the organic ligand solution, with solvent rinsing in between (adapted with permission from ref. [48]).

The LBL method was always used to fabricate MOF films on different substrates but not as membranes.[26,40,43-51,93-101] In a recent work, the LBL was successfully introduced to fabricate

homogenous ZIF-8 thin film on various supports like porous silica and gold.[93] Consequently, the ability to control the film thickness and continuity, has offered the possibility to apply the LBL technique for the fabrication MOF membranes on porous supports. Indeed, Shekhah et al. reported the implementation of the LBL method using a computer controlled dipping system (Figure 14) for growing a closed ZIF-8 membrane on alumina support Figure 15.[48]

Later on, an advanced LBL method for the construction of MOF membranes was introduced, based on the unique features of the traditional LBL method and the spin coating approach, for MOF membrane fabrication in a high-throughput manner Figure 16.[102] In this work a defect-free ZIF-8 membrane was grown using this developed LBL- spin coating approach was fabricated on porous alumina support as shown in Figure 17.

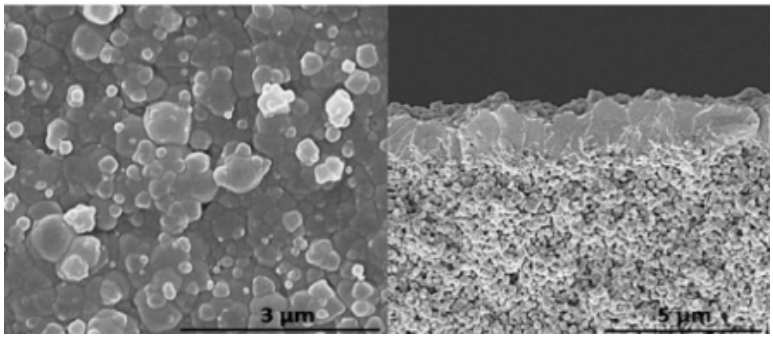

Figure 15. Representative examples of SEM micrographs of the top view (left) and cross-section (right) of the ZIF-8 membrane grown using 300 cycles of the LPE method on an alumina substrate (adapted with permission from ref. [48]).

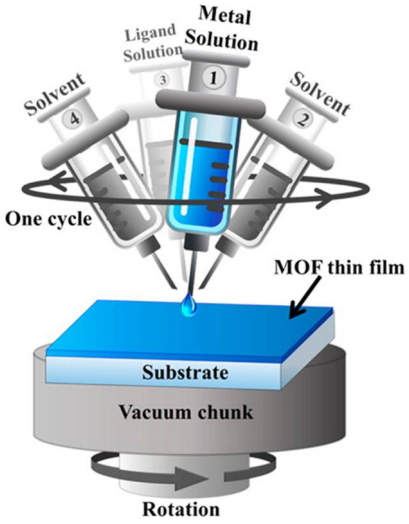

Figure 16. Schematic Representation of the Setup employed for the Fabrication of MOF Thin Films Using the LPE Approach Adapted to the Spin Coating Method (adapted with permission from ref. [[102]).

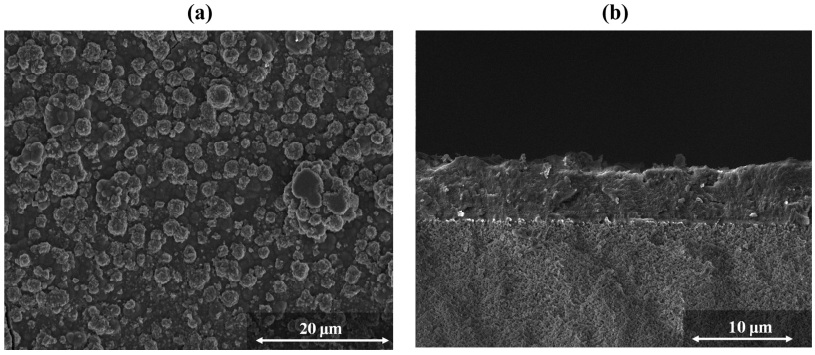

Figure 17.(a) Top view and (b) cross-section SEM image of ZIF-8 membrane grown on alumina support using the spin coating approach (adapted with permission from ref. [102]).

4. MOF membranes for gas separation application

MOF-based membranes have recently attracted the attention of different research groups around the world, as a promising candidate for many important gas separation applications. [19,26,33,103] The MOF membrane materials are based on their fabrication as thin films on porous supports like alumina. This review emphases basically on polycrystalline, pure and continuous grown MOFs membrane, that have been tested for the different gas separation applications. In the succeeding sections, we present many successful reported examples of MOF membranes used for different gas separations systems and discuss for each application the basic background and requirements.

4.1 Hydrogen purification and recycling.

Nowadays, Hydrogen (H_2) is one of the trustworthy, viable and environmental friendly energy sources, that could fulfill the world's increasing energy requirements through it application as a highly dense energy source.[104] However, it co-occurs with other un-favored gases such as N_2, CH_4, CO_2, etc., in the course of production in many industrial processes. Consequently, there is a necessity for the development/improvement of advanced separation techniques to separate it from the above-mentioned impurities and get it as pure H_2, which is the highly valuable fuel product. Provided optimal membranes are available, membranes-based separation processes that make it a promising candidate to surpass the commercially applied highly energy intensive cryogenic separation.[105] Among other materials, zeolite-based membranes that are characteristic of its well-defined pore structures, were fabricated by various techniques and investigated for H_2 refining from exhausted gas streams.[106,107] Newly, MOF-based membranes were anticipated and applied for this important gas separation; specifically, H_2 recovery.[108] Here we highlight some of the reported MOF membranes used for H_2 purification and recycling properties.

The first MOF-based membrane was reported in 2009 was a MOF-5 membrane, fabricated using an in situ solvothermal method on top of alumina support.[52] The single gas permeation were investigated and the results demonstrated that they follow Knudsen diffusion behavior, where the gases with lighter molecular weight permeates faster than other gases, which is related to that the aperture size of MOF-5 is larger than all the tested molecules in this case. As shown in Figure 18, H_2 which has the lightest molecular weight permeates faster than the heavier studied gases like CH_4, N_2, CO_2 and SF_6. Later on, the orientation of the MOF-5 membrane was controlled by using a seeding approach and the subsequent solvothermal secondary growth on various porous substrates was achieved.[58] The associated single gas permeation results of the preferentially oriented MOF-5 membrane was found to have the same behavior that is consistent with the prior report Figure 19.

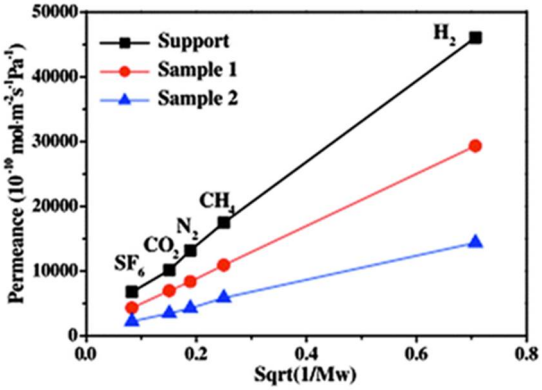

Figure 18. Single-component gas permeation results through the alumina support (square), sample 1 (circle) and sample 2 (triangle) under 800 Torr (adapted with permission from ref. [52]).

HKUST-1 MOF (also known as $Cu_3(btc)_2$ or MOF-199) was fabricated as a membrane and was grown using the 'twin copper source' solvothermal method. [109] The HKUST-1 MOF is a three-dimensional network, with two types of pores, where the small pores are not accessible and the larger ones have a window aperture of 9 × 9 $Å^2$. The single-gas permeation of HKUST-1 membrane exhibited a high permeation flux of 1 × 10^{-6}, which is expected due to that the window aperture size of HKUST-

Preprints (www.preprints.org) | NOT PEER-REVIEWED | Posted: 3 September 2018 doi:10.20944/preprints201809.0010.v1

Peer-reviewed version available at Crystals 2018, 8, 412; doi:10.3390/cryst8110412

1 large pores is much bigger than the kinetic diameter of common studied gas. The permeation results also showed a permeation selectivity in favor of H_2 with respect to other gases such as H_2/N_2 = 7, H_2/CO_2 = 6.8 and H_2/CH_4 = 5.9.

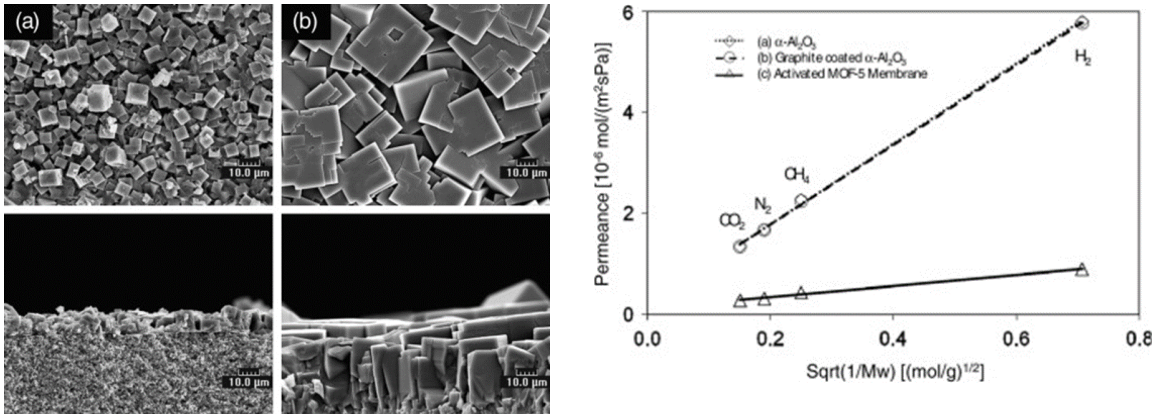

Figure 19. (left) SEM images of top views (upper) and cross-sections (lower) of (a) an oriented MOF-5 seed layer and (b) an oriented MOF-5 membrane after secondary growth for 6 h. (right) Permeation of various gas molecules through: (a) α-alumina support, (b) graphite-coated α-alumina support, and (c) activated randomly-oriented MOF-5 membrane. Note that three membrane samples were prepared under the same condition and their performance was tested and plotted (adapted with permission from ref. [58]).

Another HKUST-1 membrane prepared was grown through applying the LBL approach as a seeding layer at first and then followed by in situ solvothermal method.[69] The single gas separation performances for this membrane were also evaluated and the ideal selectivities for H_2 of this membrane were 2.9, 3.7, and 5.1 for H_2/CH_4, H_2/N_2, and H_2/CO_2, respectively. These ideal- selectivities clearly indicates that the permeation behavior of this membrane follows the Knudsen diffusion.

In another work HKUST-1 membrane was fabricated on a polymer functionalized stainless steel net-support using in situ solovothermal method.[83] This HKUST-1 membrane showed an enhanced ideal selectivities in favor of H_2 for H_2/CO_2 = 9.24, H_2/N_2 = 8.91 and H_2/CH_4 = 11.2, than earlier studies. Later on the same group has successfully fabricated a continuous HKUST-1 membrane on pre-seeded, chitosan functionalized α-Al_2O_3 hollow ceramic fibers , through a secondary growth approach.[110] The fabricated membrane exhibited a slightly higher H_2 selectivity of 8.66, 13.56 and 6.19 for the H_2/N_2, H_2/CO_2 and H_2/CH_4 gas mixtures, respectively (Figure 20).

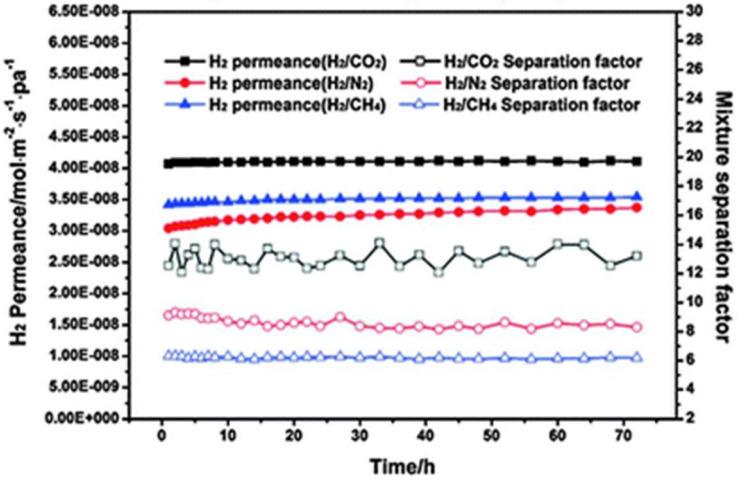

Figure 20. H_2 permeance and separation factors in the volume ratio binary gas mixture H_2–CO_2, H_2–N_2 and H_2–CH_4 systems of HKUST-1 membrane as a function of time at 40 °C with a pressure drop of 1 atm (adapted with permission from ref. [110]).

The unique properties of Zeolitic-imidazolate frameworks (ZIFs), in terms of permanent porosity, pore sizes uniformity and outstanding chemical and thermal stability, made them an

excellent candidate for their application as molecular sieve membranes.[111-114] . ZIF-8, is one of the most studied ZIF, has a sodalite topology with a~3.4 Å aperture size for the six-membered-ring as sole access to pores, which would be, theoretically, able to separate H_2 from the other larger components. [34,63,111,115] . Caro et al. fabricated the first ZIF-8 membrane via applying the in situ solvothermal method.[116] The membrane single-gas permeation results of this ZIF-8 membrane showed a higher H_2/CH_4 selectivity of 11.2, relative to earlier reported MOF membranes. Besides, Jeong et al. managed to fabricate a 1 μm thick ZIF-8 membrane, that exhibited a higher measured ideal selectivities for H_2/N_2 and H_2/CH_4 of 11.6 and 13, respectively.[67] Later on, Caro et al. established a bicontinuous ZIF-8@GO membrane by applying the LBL method using a graphene oxide (GO) suspension on a ZIF-8 membrane to close the gaps between the ZIF-8 crystals in the thin film.[82] These ZIF-8@GO membranes exhibited a higher selectivity in favor of H_2, at 250°C and 1 bar, which were 14.9, 90.5, 139.1, and 3816.6 for H_2/CO_2, H_2/N_2, H_2/CH_4, and H_2/C_3H_8,respectively with a high H_2 permeance of about 1.3×10^{-7}mol·m^{-2}·s^{-1}·Pa^{-1}. Other groups fabricated other ZIF-8 membrane using the seeding method, LBL method and counter diffusion method and the permeation results are more or less in good agreement with the H_2 selectivities reported earlier.

In a recent study, Caro et al established a simple synthesis strategy for ZIF-8 membranes fabrication that was built on improving the support hydrophobicity by functionalization with a highly hydrophobic polymer, namely 1H,1H,2H,2H-perfluoroalkyltriethoxysilanes (POTS) (Figure 21).[117] A high quality 20 μm thick ZIF-8 membrane was grown on the POTS-modified α-Al_2O_3 support, which exhibited a higher H_2 selectivity and thermal stability. The mixture separation factors of different gases like H_2/CO_2, H_2/N_2, H_2/CH_4, and H_2/C_3H_8 were measured and were found to be 15.8, 22.6, 40.6, and 549.3, at 200 °C and feed pressure of 1 bar. The effect of temperature on the H_2 permeance was investigated and showed that an increase in the temperature from 25° to 200 °C under same feed pressure of 1 bar, led to an increase in the H_2 permeance accordingly from 1.4×10^{-7} to 2.3×10^{-7} mol·m^{-2}·s^{-1}·Pa^{-1}, and an increase in the H_2/CH_4 mixture selectivity from 23.5 to 40.6 (Figure 22 (right)). This is due to the fact that, CH_4 dominates the sorption at low temperature in the ZIF-8 pores, consequently hindering the H_2 diffusion. However, at higher temperature less CH_4 can adsorb and thus more H_2 can permeate.

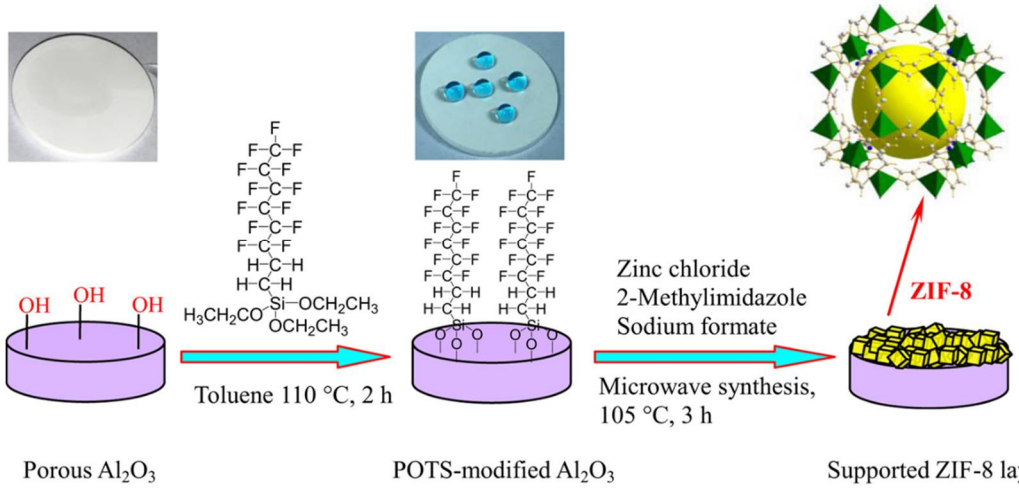

Figure 21. Scheme of the preparation of ZIF-8 membranes on hydrophobic α-Al_2O_3 supports through 1H,1H,2H,2H-perfluoroalkyltriethoxysilanes (POTS) modification (adapted with permission from ref. [117]).

Using a counter-diffusion method to fabricate ZIF-8 membrane as a composite on hollow fiber support membranes that was first functionalized with reduced graphene oxide (rGO) membranes via hydrothermal treatment was reported.[118] Using this approach, 150 nm thin membranes were grown at the interfaces. The gas permeation studies on these ultrathin ZIF-8/rGO membranes, showed an exceptional performance in H_2 separation, as indicated by a high permeance of over 60 $\times10^{-8}$ mol m^{-2}s^{-1}Pa^{-1} and selectivities for H_2/CO_2, H_2/N_2 and H_2/CH_4 of 25.3, 70.4, and 90.7, respectively (Figure 23).

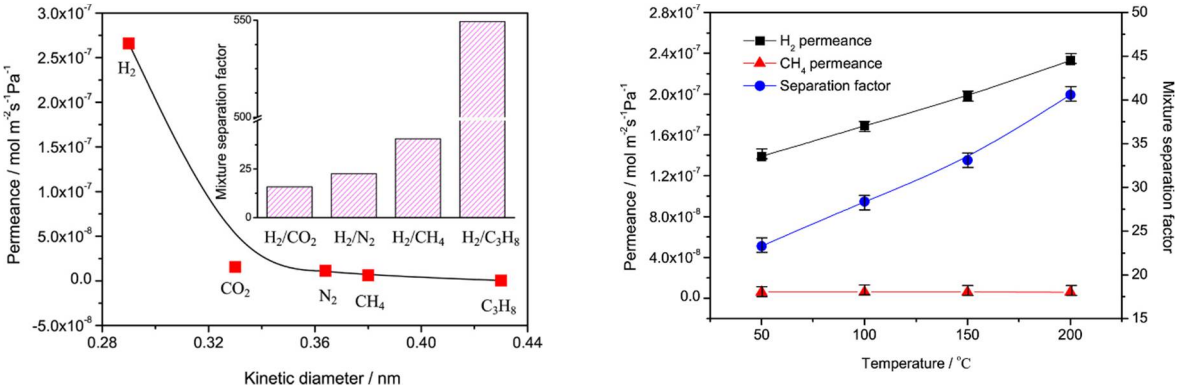

Figure 22. Single gas permeances of different gases through the ZIF-8 membrane prepared on the POTS-modified α-Al_2O_3 disk at 200 °C as function of their kinetic diameter. The inset gives the mixture separation factors (adapted with permission from ref. [117]).

Another ZIF membrane was later reported using a microwave-assisted secondary growth approach by Caro et al. using ZIF-7, which has also the same sodalite topology like ZIF-8 but with small pore aperture.[119] ZIF-7 is a hydrophobic MOF, highly thermal stability and has a pore dimension that are smaller than ZIF-8 and almost similar to the size of H_2, which is expected to achieve a higher H_2 selectivity via molecular sieving. The single- and mixed-gas permeation results for fabricated ZIF-7 membrane was tested at 200 °C and 1 bar using the Wicke–Kallenbach technique and are shown in Figure 24. The selectivities of the binary mixtures examined in this study for H_2/N_2, H_2/CO_2 and H_2/CH_4, were higher than Knudsen and found to be 7.7, 6.5 and 5.9, respectively.

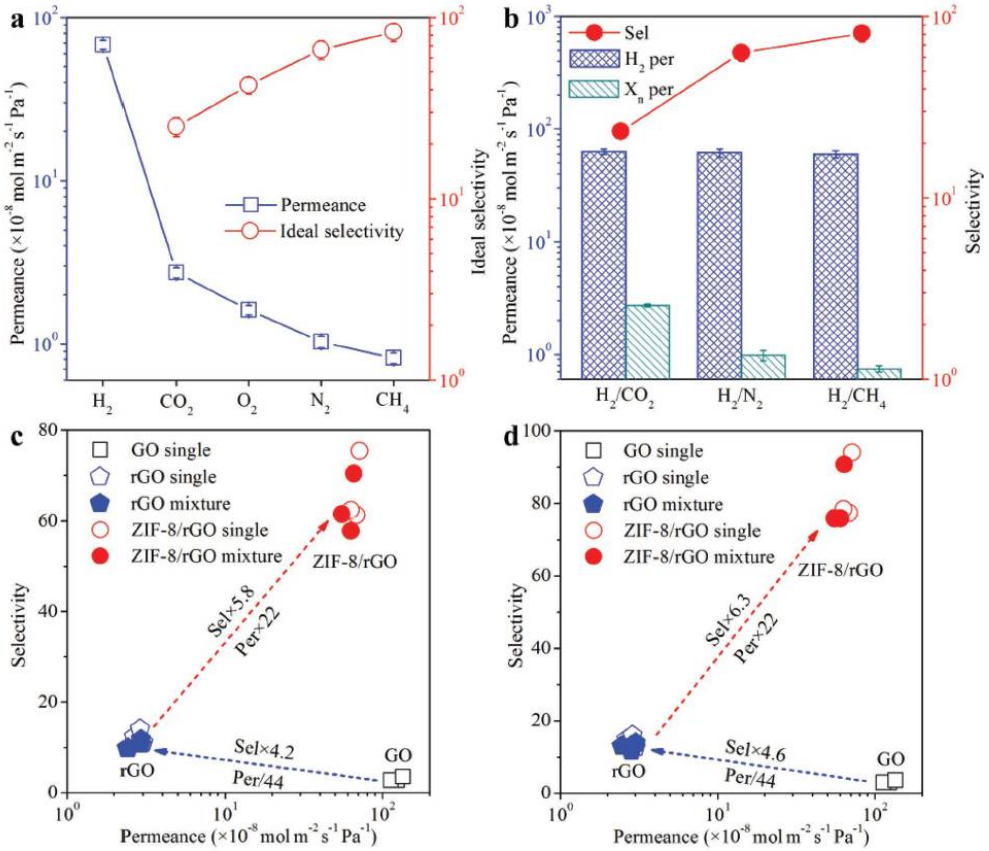

Figure 23. a) The permeation properties of various gases through the ZIF-8/rGO membrane. b) The separation performance of the ZIF-8/rGO membrane for H_2/CO_2, H_2/N_2, and H_2/CH_4 mixtures. The comparison of the GO, rGO, and ZIF-8/rGO membranes for c) H_2/N_2 and d) H_2/CH_4 separations. (adapted with permission from ref. [118]).

The results indicated that the ZIF-7 structure sodalite structure with narrow pore aperture, are accountable for this molecular sieving behavior. The non-zero permeance of gases larger than H_2 was attributed to the imperfect sealing or presence of some defects. Later on, the 220 °C activated of ZIF-

7 membrane single gas and binary mixtures permeations testes, revealed improved H_2 selectivities with slightly change in permeances. The H_2/CO_2 other binary mixtures like H_2/N_2 and H_2/CH_4 ideal selectivity and separation factor were higher than Knudsen.

ZIF-22, another ZIF isostructure with similar aperture size like ZIF-7 (0.3 nm) was fabricated by Caro et. al, as a membrane on alumina support functionalized with APTES to facilitate the MOF growth.[79] The ZIF-22 membranes gas permeation properties were evaluated and the separation factors of different mixture like H_2/CO_2, H_2/O_2, H_2/N_2 and H_2/CH_4 were tested at 323 K and found to be 7.2, 6.4, 6.4 and 5.2, respectively, with a H_2 permeance of over 1.6×10^{-7} mol m^{-2} s^{-1} Pa^{-1} (Figure 25).

ZIF-90, which has a structure like ZIF-8 and ZIF-7, that has a similar pore size of almost 0.35 nm, exhibit also high thermal and hydrothermal stability was fabricated as a membrane on alumina support by Caro group.[78] The ZIF-90 membrane gas transport properties were evaluated and exhibited molecular sieve performance with a H_2/CH_4 and H_2/CO_2 selectivity of 15 and 7.2 respectively. The performance of this membrane was improved, via post-functionalization the membrane via imine condensation, which helped enhancing the ZIF-90 H_2/CO_2 permselectivity from 7.2 to 62.5by increasing the framework interaction with CO_2 (Figure 26).

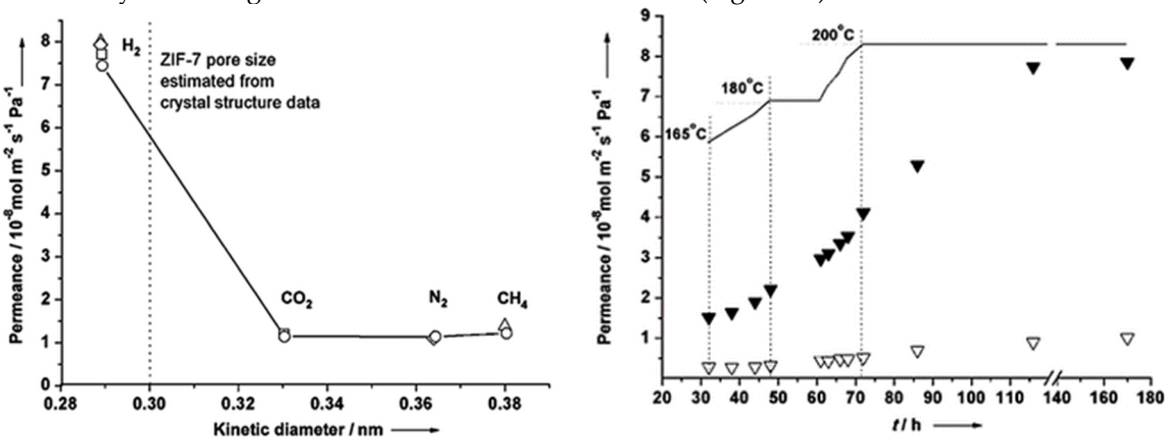

Figure 24. Left: H_2 (solid triangles) and N_2 (triangles) permeance from the mixture through the ZIF-7 membrane during the on-stream activation process with increasing temperature. Right: permeance of single gases (circles) and from mixtures (squares: H_2–CO_2 mixture, rhombuses: H_2–N_2 mixture, triangles: H_2–CH_4 mixture) of the ZIF-7 membrane at 200 °C as a function of molecular kinetic diameters (adapted with permission from ref. [119]).

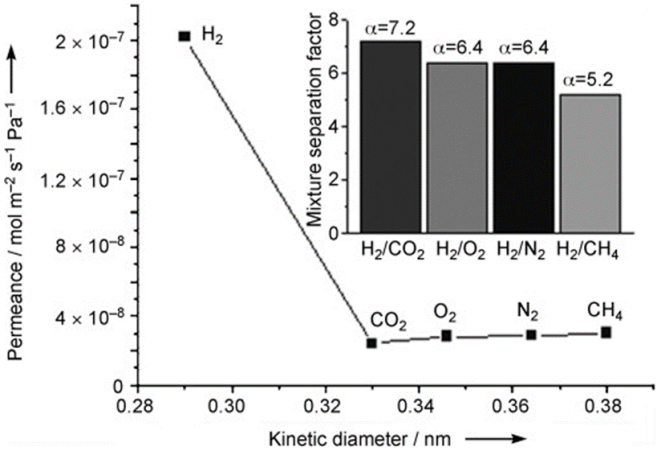

Figure 25. Single-gas permeances of different gases on the ZIF-22 membrane at 323 K as a function of the kinetic diameter. The inset shows the mixture separation factor for H_2 over other gases, determined by gas chromatography (adapted with permission from ref. [79]).

ZIF-95 is another candidate from the ZIF family that has a POZ topology, which has a 2.4 nm huge cavities, constricted aperture size (~0.37 nm) and excellent thermal stability up to 500 °C. [120] The sorption studies on pristine ZIF-95 showed that it has an extraordinary affinity and capacity for CO_2 that can strongly adsorb CO_2 and immobilized it in its big cavities. The H_2/CO_2 mixed gas

493 selectivity was measured at 1 bar and was found to increase from 8.5 to 25.7 with temperature
494 increase from 25 °C up to 325 °C. This is explained by means of the higher affinity of the framework
495 for CO_2 at lower temperatures that lead to the blockage of the highly mobile gas since mainly CO_2
496 was adsorbed (Figure 27). At higher temperature less CO_2 will be adsorbed and thus H_2 could diffuse
497 more easily.[121]

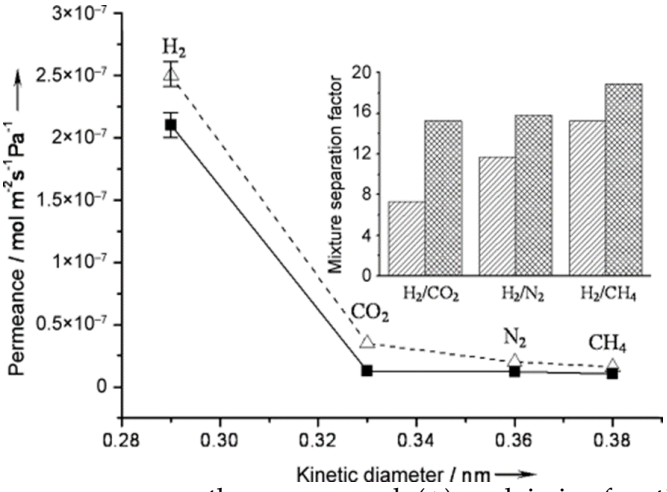

498 **Figure 26**. Single-gas permeance on the as-prepared (△) and imine-functionalized (■) ZIF-90
499 membrane at 200 °C and 1 Barrer (bar) as a function of the kinetic diameter (measured with a bubble
500 counter). The inset shows the mixture separation factors for H_2 over other gases from an equimolar
501 mixture as determined by gas chromatography using the Wicke–Kallenbach technique before
502 (hatched columns) and after (crossed columns) imine functionalization (adapted with permission
503 from ref. [78]).

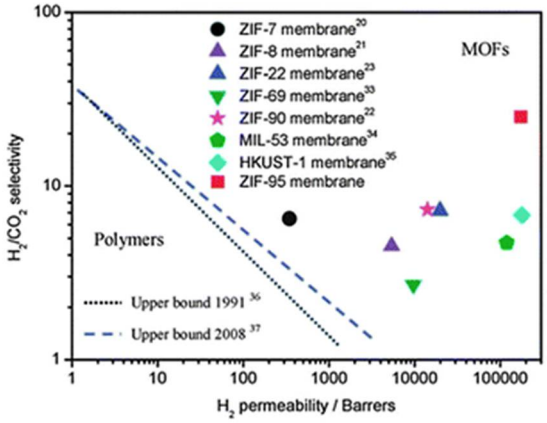

504 **Figure 27**. H_2/CO_2 selectivity versus H_2 permeability for polymeric and MOF membranes (adapted
505 with permission from ref. [121]).

506 A continuous pure ZIF-67 tubular membrane fabricated by direct transformation of carbonate
507 hydroxide nanowire arrays (Co-NWAs) in a 2-methylimidazole (Hmim) aqueous solution was
508 reported.[77] The obtained ZIF-67 membrane exhibits a high H_2 permeance of 5.59×10^{-7} mol m^{-2} s^{-1}
509 Pa^{-1}, and ideal selectivities for H_2/CH_4 and H_2/N_2 were 15.3 and 14.7, respectively. Figure 28 shows
510 the gas permeation and separation values for pure Co-ZIF-67 tubular membrane for H_2, CO_2, N_2 and
511 CH_4. The ideal selectivities for this membrane were found higher than Knudsen values for (H_2/N_2=
512 14.7) and (H_2/CH_4= 15.3). The separation factors through the pure Co-ZIF-67 tubular membrane for
513 the mixed gas permeation of H_2/N_2 and H_2/CH_4 were 11.2 and 13.7, respectively. The gas permeances
514 and separation factors in the mixed gas measurements slightly decreased compared to those from
515 single gases, which could be due the adsorption competition of gases. The ZIF-67 membrane revealed
516 a high H_2 permeance of about 55.87×10^{-8} mol m^{-2} s^{-1} Pa^{-1}, which is considered the highest with respect
517 to the reported ZIF-8 membranes having the same isostructural sodalite topology. This was attributed
518 to the good adhesion between the membrane and the support by using the Co-NWA layer as the Co^{2+}
519 ions source, leading to the fabrication of a uniform and well-intergrown thin layer (1.7 μm) of ZIF-

67. The influence of temperature was also investigated and showed that mainly the ideal selectivity to H_2/CO_2 has increased visibly with the increased temperature. This increase was related to that the kinetic diameter of CO_2 (ca. 0.33 nm) is much closer to the aperture of ZIF-67 (ca. 0.34 nm) than those of N_2 and CH_4, which are larger. The separation properties were tested under different temperatures through the as-prepared ZIF-67 membrane for the equimolar H_2/CH_4 mixture, Figure 28. Increasing the temperature from 30 to 150 °C, led to a slight enhancement in H_2/CH_4 separation factor from 13.7 to 15.4 and a decrease in H_2 permeance from 45.32 × 10^{-8} to 32.47 × 10^{-8} mol m^{-2} s^{-1} Pa^{-1}. This was explained by the difference in the adsorption and diffusion behaviors of H_2 and CH_4 in the ZIF-67 membrane.

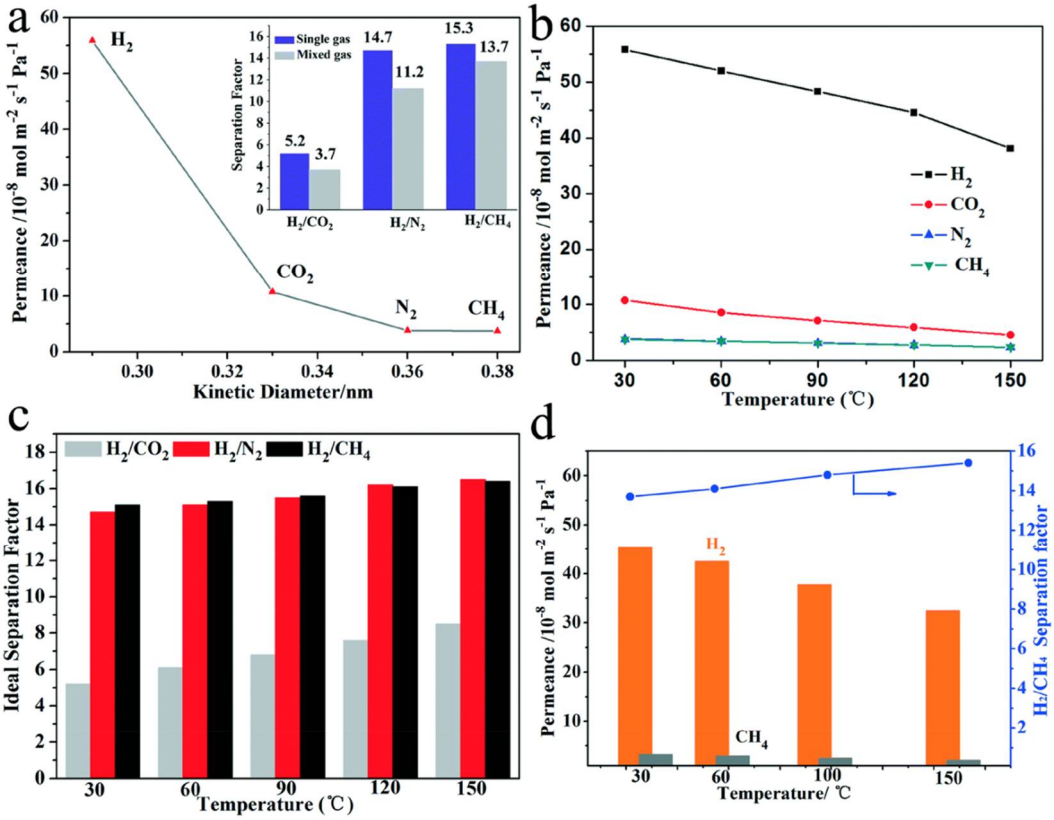

Figure 28. (a) Single gas permeabilities through the prepared ZIF-67 membrane measured at 30 °C and 0.1 MPa. The inset shows the separation factors of H_2 relative to the other gases in both the single gas and equimolar mixed gas permeation tests. (b) Single gas permeances at elevated temperature. (c) Ideal separation factors of H_2 over CO_2 (gray), N_2 (red) and CH_4 (black) at different temperatures. (d) H_2/CH_4 mixture separation as a function of temperature. (adapted with permission from ref. [77]).

ZIF-100 was also fabricated as a membrane on polydopamine-modified alumina support and tested for its H_2 separation properties. ZIF-100 has a composition of $Zn_{20}(cbIM)_{39}(OH)$ (cbIM =5-chlorobenzimidazole) and a MOZ topology with a window aperture size of 3.35 Å. The sorption studies on ZIF-100 showed that it exhibits an enhanced affinity and capacity to CO_2 that led to an exceptional CO_2 uptake.[122] The H_2/CO_2, H_2/N_2 and H_2/CH_4 mixture separation performance of this ZIF-100 membrane were evaluated at room temperature and 1 bar, their separation factors were found to be 72, 22 and 41, respectively (Figure 29). The high H_2/CO_2 selectivity is attributed to their extraordinary CO_2 uptake behavior of ZIF-100 and the small 3.35 Å window aperture.

A composite membrane of ZIF-8-on-ZIF-67 and the neat ZIF-67 membrane were grown using the LBL approach on ceramic α-Al_2O_3 discs.[123] Gas permeation of binary mixture experiments were conducted on the pure ZIF-67 and ZIF-8-on-ZIF-67 membranes (Figure 30). The permeation test was performed form both sides i.e. via either the ZIF-8 to ZIF-67 side or vice versa, in order to show that there is no difference in the membranes performance from both directions. The permeation results for different gas H_2 mixtures CO_2, CH_4, N_2, ethane, ethylene, propane and propylene were comparable (c.f. Figure 30, b–h). The permeation results were good for smaller gases like H_2/CO_2,

549 H_2/CH_4 and H_2/N_2, and for H_2/N_2 the performance of the ZIF-67 membrane was similar to reported
550 results for ZIF-8 membranes (Figure 30, c). In case of H_2/CH_4 separation the ZIF-67 membrane
551 performance is lower that ZIF-8 but still higher than Knudsen and in case of the ZIF-8-on-ZIF-67
552 membrane an improved separation performance was observed (Figure 30, b). Finally, the ZIF-8-on-
553 ZIF-67 separation performance for H_2/CO_2 separation (Figure 30, b) is better than the neat ZIF-67 and
554 ZIF-8, and is almost doubled the best reported values in literature. In case of H_2 separation from
555 hydrocarbons like ethane, ethylene, propane and propylene is higher than Knudsen but lower than
556 the literature values (Figure 30, e–h).

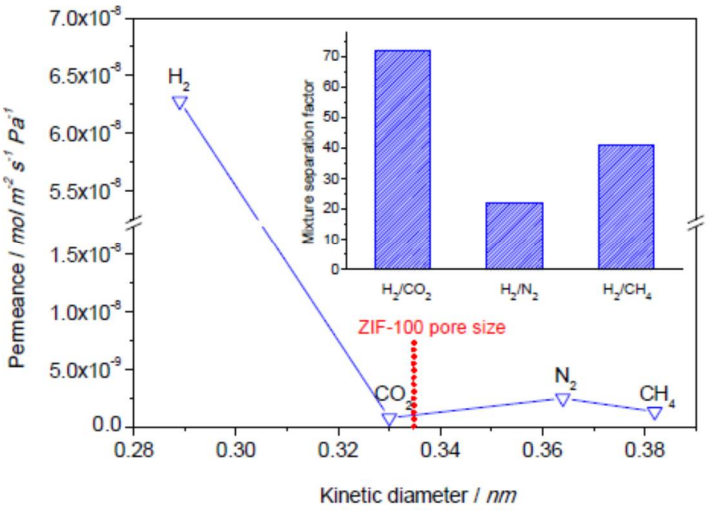

557 **Figure 29**. Single gas permeances through the ZIF-100 membrane prepared by PDA-modification at
558 25 oC and 1 bar as a function of the kinetic diameter of permeated gases. The inset shows the mixture
559 separation factors for H_2 over other gases from equimolar mixtures. (adapted with permission from
560 ref. [122]).

561 In another report, the high stability related to the MIL MOFs series like MIL-53, which was
562 fabricated as membrane. Jin et al. reported a densely-packed uniform MIL-53(Al) membrane acquired
563 by a seeding and solovothermal method (Figure 11, left).[87] The permeabilities of the small gases
564 designated a permeation behavior similar to Knudsen. This is expected since the MIL-53 channel size
565 is about 7.3 × 7.7 Å, is bigger than the kinetic diameters of tested gas (Figure 31, right).
566 Afterward, a NH_2-MIL-53(Al) membrane was fabricated on a glass frit macroporous support,
567 assisted by using seeding method.[124] The adsorption results for this pristine material showed that
568 the preferred functionalization of the MIL with the NH_2 groups has enhanced the adsorption affinity
569 of particular gases, and altered the gas interactions with the framework. Encouraged by these results
570 the NH_2-MIL-53(Al) membrane was fabricated and its permeation results are shown in Figure 32, the
571 fabricated membrane exhibited high selectivity for H_2 permeation over CO_2 with a selectivity more
572 than 20.

573 MIL-96(Al) MOF has a unique features in term of structure and hydrothermal stability up to 300
574 °C.[125] As a result MIL-96 is a good candidate for H_2 separation like precombustion CO_2 capture
575 technologies. MIL-96(Al) was fabricated as a membrane on ceramic alumina supports and tested for
576 H_2/CO_2 mixed gas separation. Figure 33 shows the permeation performance for MIL-96(Al)
577 membrane, showed that the 2 μm thick membrane has a lower permeance the 8 μm one. This finding
578 was elucidated to the dissimilar orientations of the MIL-96(Al) crystals in the membrane layer.
579 The MIL-96(Al) membrane fabricated from the toluene/water seeding, form (0*k*0)-equivalent facets
580 that allow a faster diffusion. The 100% higher permeance of this thicker membrane (toluene/water
581 seeded) than the thinner one from DMF/water seeded happens due to the variation in ratio of the
582 crystals orientation in the membrane. The pathway of the gas through the outer lattice planes in case
583 of DMF/water-seeded MIL-96 membrane are blocked since this MOF is virtually a 2D network. MIL-
584 96(Al) structure, allows an easier diffusion in the *a*-direction (i. e. perpendicular to *b*–*c* planes) and *b*-

direction (i. e. perpendicular to *a*–*c* planes), however in case of the *c*-direction (i. e. perpendicular to *a*–*b* planes), it is slower Figure 33, b.

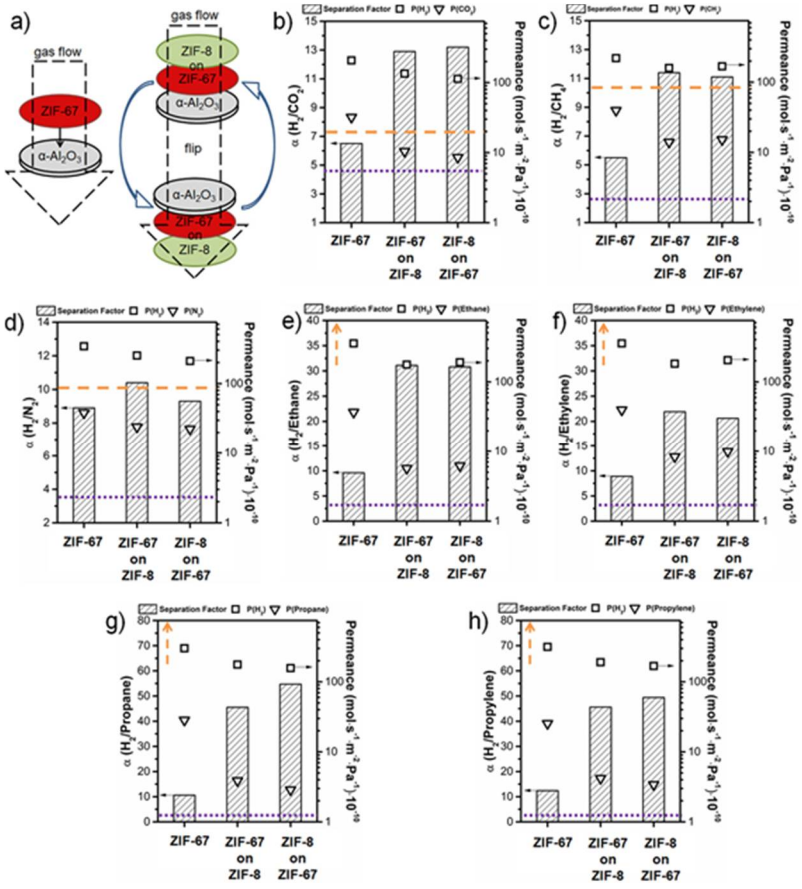

Figure 30. (a) Schematically measuring principle to clarify the permeation data in both directions of the neat, supported ZIF-67, ZIF-67-on-ZIF-8 and ZIF-67-on-ZIF-8 layers (b) Permeation data for H_2/CO_2, (c) for H_2/CH_4, (d) for H_2/N_2, (e) for H_2/ethane, (f) for H_2/ethylene, (g) for H_2/propane, and (h) for H_2/propylene. All membranes show clearly a separation factor α above Knudsen (purple, dotted line). The orange dashed line shows the performance of conventionally prepared neat ZIF-8 membrane taken from comparable literature data. (adapted with permission from ref. [123])

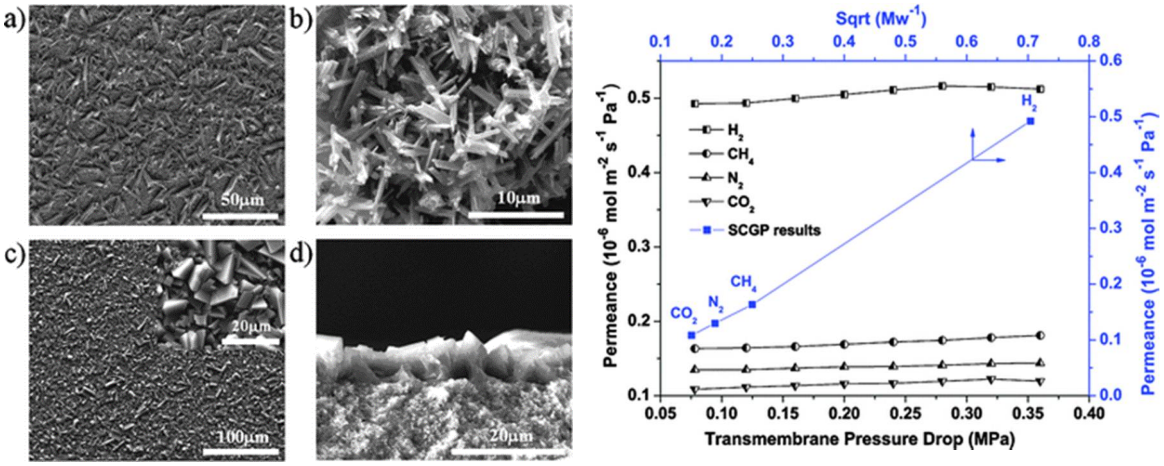

Figure 31. (Left). SEM images of the MIL-53 seed layer (a), MIL-53 powders (b), MIL-53 membrane surface (c) and cross-section (d). (right) Permeances of small gas molecules through an MIL-53 membrane at different trans-membrane pressure drops, and the single-component gas permeation (SCGP) results through the MIL-53 membrane under 0.8 MPa (adapted with permission from ref. [87]).

The MIL-96(Al) membrane fabricated from the toluene/water seeding, form (0*k*0)-equivalent facets that allow a faster diffusion. The 100% higher permeance of this thicker membrane (toluene/water seeded) than the thinner one from DMF/water seeded happens due to the variation in ratio of the crystals orientation in the membrane. The pathway of the gas through the outer lattice planes in case of DMF/water-seeded MIL-96 membrane are blocked since this MOF is virtually a 2D network. MIL-96(Al) structure, allows an easier diffusion in the *a*-direction (i. e. perpendicular to *b*–*c* planes) and *b*-direction (i. e. perpendicular to *a*–*c* planes), however in case of the *c*-direction (i. e. perpendicular to *a*–*b* planes), it is slower Figure 33, b.

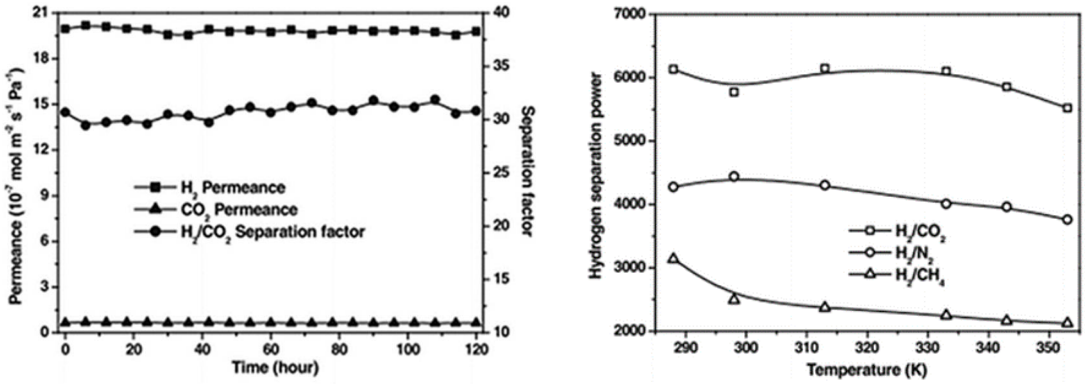

Figure 32. left: plot of H_2/CO_2 permeance and separation factors for the NH_2-MIL-53(Al) membrane versus test time. right: hydrogen separation power of the NH_2-MIL-53(Al) membrane as a function of the permeation temperature (adapted with permission from ref.[124]).

A thin NH_2-MIL-125 MOF membrane was fabricated and tested its separation performance for a H_2/CO_2 gas mixture with equimolar ratios, at different temperatures.[126] Additionally, permeation tests were done by varying feed pressures (3, 4, 5 bar) at 150 °C, in order to simulate the pre-combustion process for CO_2 sequestration application. The presence of free amine groups in the NH_2-MIL-125 MOF is enhancing framework affinity with CO_2, since it is a polar acidic molecule, which will help in retaining it compared to H_2 and as a result enhancing the separation of H_2/CO_2. The NH_2-MIL-125 membrane showed a higher H_2 permeability of almost 8 times more than CO_2 at room temperature Figure 34.

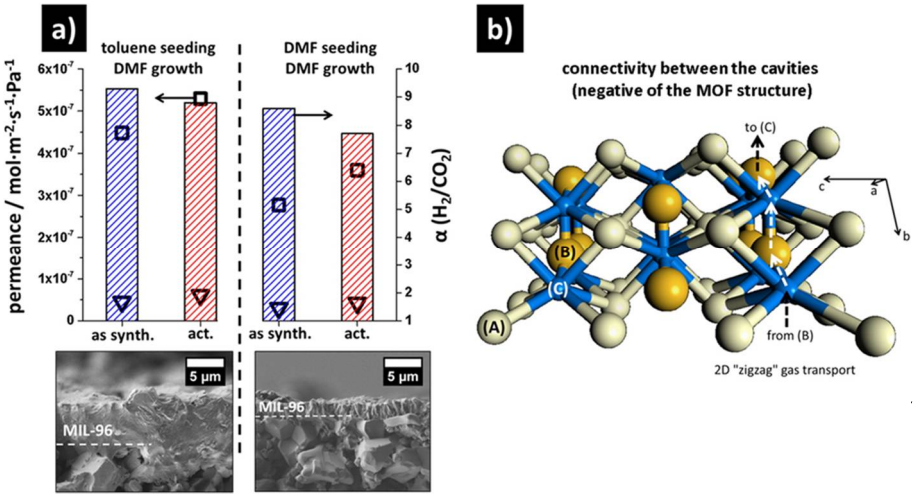

Figure 33. (a) H_2/CO_2 mixture separation factor α (columns) and H_2 (□) and CO_2 ( ) permeances for the two neat supported MIL-96(Al) membranes (left, toluene/water seeding; right, DMF/water seeding) at room temperature. Measurements carried out directly after synthesis (as synth.) and after 24 h activation at 150 °C in a nitrogen flow (act.). (b) Schematic connectivity between the three different cavities (A), (B), and (C), showing that the 3D pore structure is a virtual 2D pore structure since the gas transport is limited to a "zigzag" pathway (arrows) between the two cavities (B) and (C) (adapted with permission from ref. [125])

Preprints (www.preprints.org) | NOT PEER-REVIEWED | Posted: 3 September 2018 doi:10.20944/preprints201809.0010.v1

Peer-reviewed version available at Crystals 2018, 8, 412; doi:10.3390/cryst8110412

The H_2 permeability in single gas permeation measurement is slightly than the mixed gas measurements, which indicating the absence of strong adsorptive interaction between H_2 and the framework. However, in case CO_2 the single gas permeation results are almost double the mixed gas one, which attributed to the stronger affinity of CO_2 molecules with the restricted number of NH_2 functional groups in the framework.

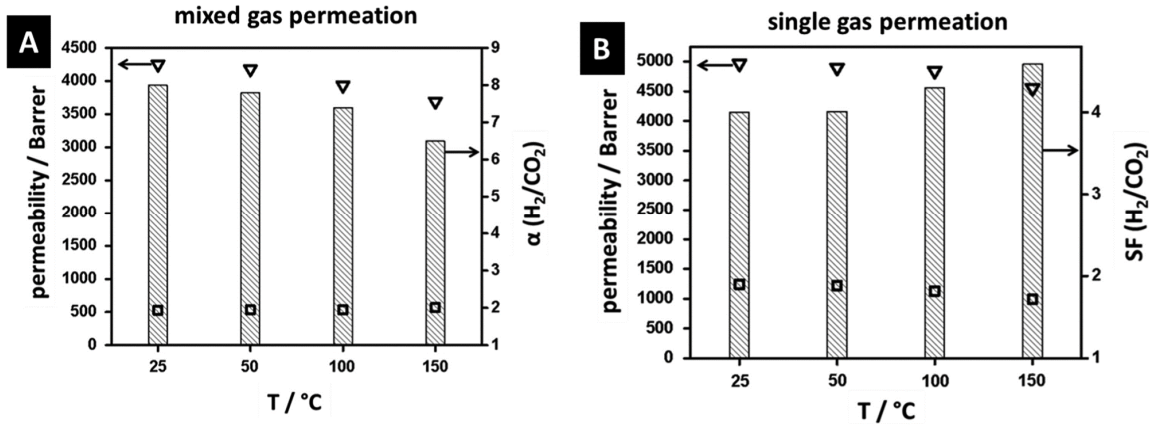

Figure 34. Mixed (A) and single gas permeabilities (B) for H_2 (∇) and CO_2 (□) and ideal/real separation factors (columns) for an equimolar mixture of H_2/CO_2 at different temperatures for the neat supported NH_2-MIL-125 membrane. (adapted with permission from ref. [126]).

Li et al. used the strategy of MOF transformation for bulk and applied it to membranes.[127] In this case CuBTC membrane, fabricated on hollow fiber polymeric support, was applied as a sacrificial layer for the transformation to MIL-100 membrane. Figure 35, a–c shows the CuBTC membrane SEM images of the CuBTC/MIL-100 as-synthesized and after purification. After post-transformation, the CuBTC/MIL-100 membrane (as-synthesized) became denser due to the presence of some $FeCl_3$ residue. However, after the $FeCl_3$ removal, and when the transformation period was extended to 48 h, a complete transformation to MIL-100 was achieved. The gas separation performance of transformed MOF membranes, for H_2, CO_2, etc. was investigated. Figure 36, d, e shows the gases permeance and selectivities of the different gas mixtures with H_2 for the neat CuBTC and transformed CuBTC/MIL-100 membranes. The results show smaller permeances values of all gases for the transformed CuBTC/MIL-100 membranes than for neat CuBTC membrane, and H_2 has the highest permeance of 8.8×10^{-8} mol m^{-2} s^{-1} Pa^{-1}. In case of selectivities they showed a good improvement in case of H_2/CO_2, H_2/O_2, H_2/N_2 and H_2/CH_4 that were found to be 77.6, 170.6, 217.0 and 335.7, respectively. The effect of temperature on the selectivities was investigated and was found to increase and reached 89.0 for H_2/CO_2 and 240.5 for H_2/N_2, with temperature increase to 85 °C. Additionally, the H_2 permeance increased to 10.5×10^{-8} mol m^{-2} s^{-1} Pa^{-1} with the temperature increase (Figure 36, f). The performance of the transformed MIL-100 membrane was found better than most reported membranes for separation systems like H_2/CO_2, H_2/N_2 and H_2/CH_4.

An aluminum base MOF, namely CAU-10-H (CAU stands for Christian-Albrechts-University, Kiel, Germany) was fabricated as a membrane using *in situ* solvothermal method.[128] The gas separation performance of this membrane was studied for ternary mixture of $H_2/CO_2/H_2O$ under different feed pressures and temperatures. Figure 36 shows the gas permeance with respect to gas molecular size, which reveal a permeance cut-off edge for gases larger than H_2, which is due to the size-exclusive molecular sieving of the membrane. The selectivities for the mixed gas measurements for H_2/CO_2 was 10.5 and for H_2/CH_4 was found 74.7, which are higher than Knudsen. The H_2 permeance in case H_2/CO_2 binary mixture was found to be lower than H_2/CH_4 one due to the blocking effects caused by the strongly adsorbed CO_2. The increase in the temperature or feed pressure led to an enhancement in the H_2 and CO_2 permeances and a reduction in the selectivities Figure 37. A dense and continuous membrane of Mg-MOF-74 was fabricated by using seeding method of magnesium oxide and tested for hydrogen separation Figure 38.[73] The measured single gas permeances of this membrane showed a H_2 permeance of 1.2×10^{-7} mol m^{-2} s^{-1} Pa^{-1}. The H_2/CO_2 mixture separation factor was the highest among other mixtures like H_2/CH_4 and H_2/N_2 (inset in Figure 39).

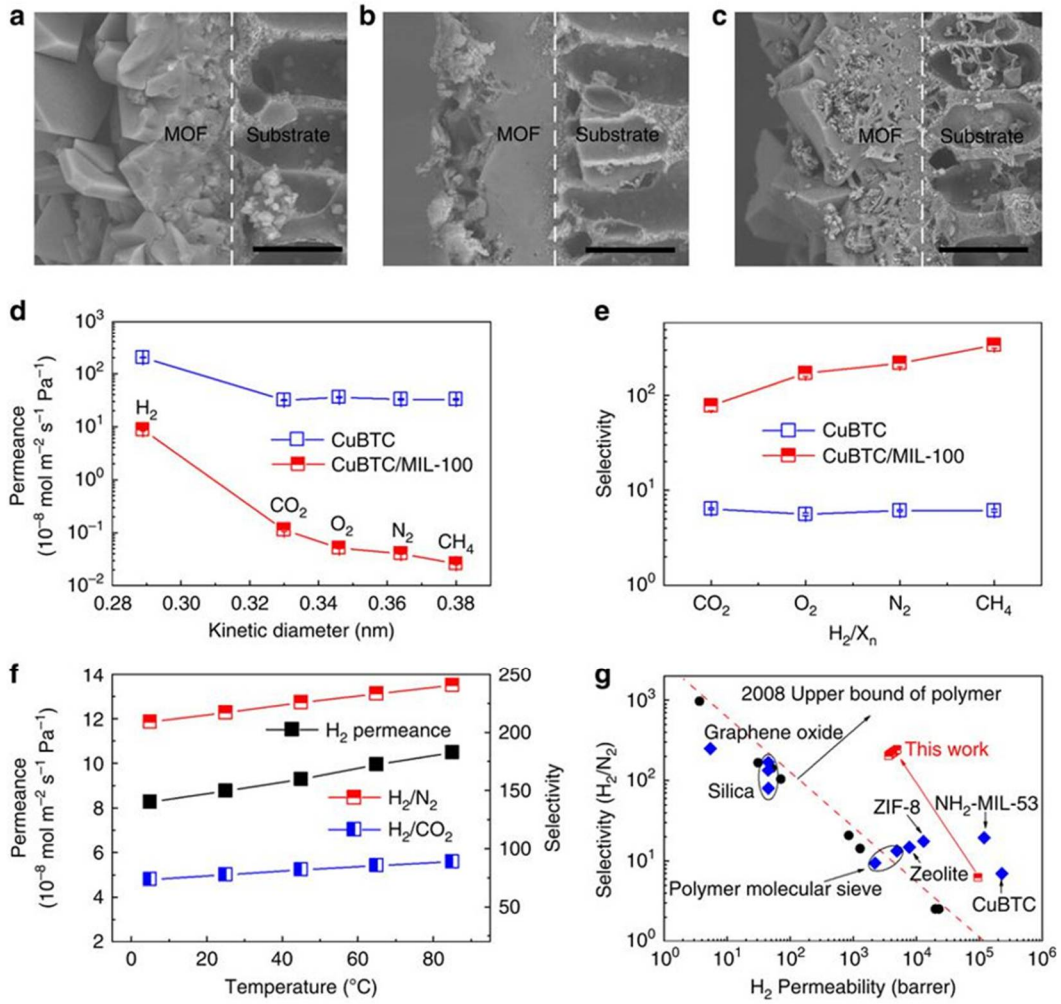

Figure 35. (a–c) SEM images of original CuBTC membrane, transformed CuBTC/MIL-100 membrane and transformed CuBTC/MIL-100 membrane after purification, respectively. Scale bar, 20 μm. (d,e) Gas permeance and selectivities of the CuBTC and CuBTC/MIL-100 membranes. All the average permeation results with standard deviation were calculated from three measurement data. (f) Effect of temperature on H_2 permeance and H_2/CO_2 and H_2/N_2 selectivities for CuBTC/MIL-100 membrane. (g) Comparison of CuBTC/MIL-100 membrane with polymeric, silica, zeolite, other MOF and graphene oxide membranes for H_2/N_2 system. 1 barrer=3.348 × 10^{-16} mol m^{-2} s^{-1} Pa^{-1}, the red dotted line is the Robeson's upper-bound reported in 2008. (adapted with permission from ref. [126])

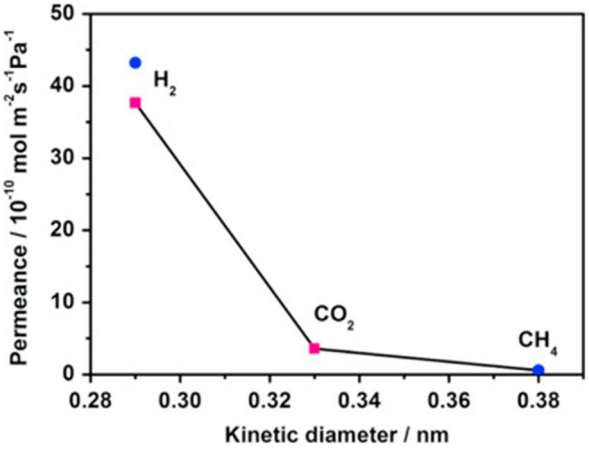

Figure 36. H_2, CO_2 and CH_4 mixed gas permeances from equimolar binary mixtures (H_2/CH_4 or H_2/CO_2) of the CAU-10-H membrane as a function of the kinetic diameter (circles: H_2/CH_4 mixture, squares: H_2/CO_2 mixture).(adapted with permission from ref. [128])

Peer-reviewed version available at Crystals 2018, 8, 412; doi:10.3390/cryst8110412

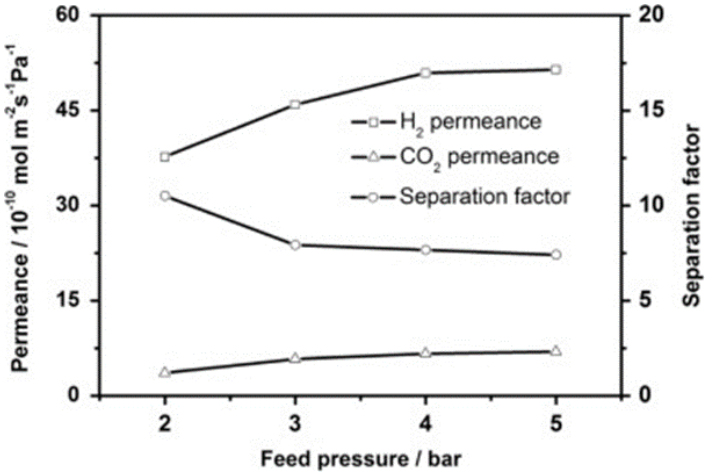

Figure 37. H_2 and CO_2 permeances from equimolar binary mixtures and H_2/CO_2 mixed gas separation factor of the CAU-10-H membrane as a function of the feed pressure at 200 °C.(adapted with permission from ref. [128])

The mixed gas selectivities of H_2/CO_2 mixture were enhanced by ethylenediamine post-modification of the Mg-MOF-74, where the introduced amine functionality enhance the adsorption affinity for acidic CO_2 molecules. After post-functionalization, the membrane performance was clearly enhanced, as indicated by increase in the H_2/CO_2 selectivity from 10.5 to 28 (Figure 40).

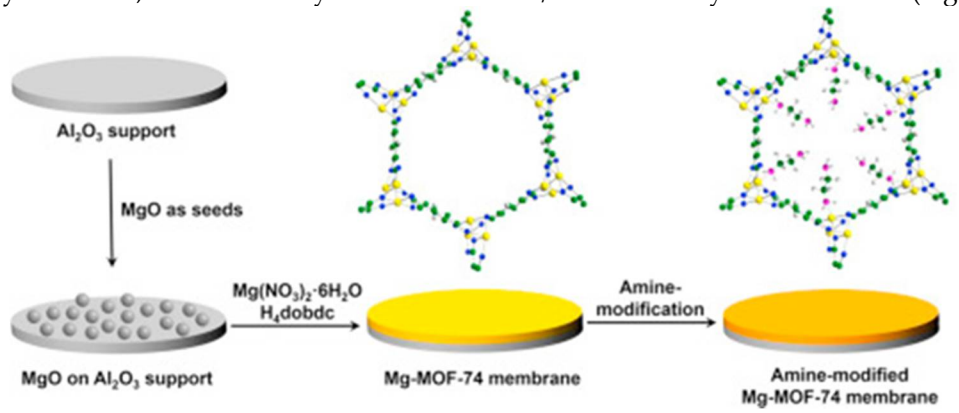

Figure 38. Scheme of the synthesis of Mg-MOF-74 membrane on MgO-seeded Al_2O_3 supports and amine-modification of the as-prepared Mg-MOF-74 membrane. (adapted with permission from ref. [73])

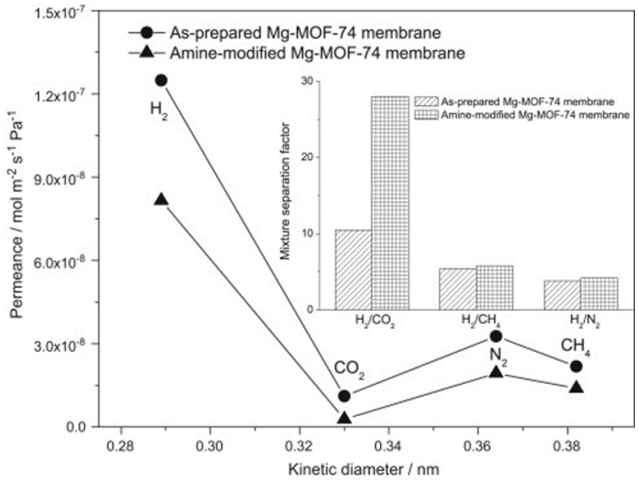

Figure 39. Single gas permeances on the as-prepared and amine-modified Mg-MOF-74 membranes at 25 °C and 1 bar as a function of the kinetic diameter. The inset shows the mixture separation factors for H_2 over other gases from equimolar mixtures (for the temperature dependence of the H_2/CO_2 mixed gas selectivities) (adapted with permission from ref. [73]).

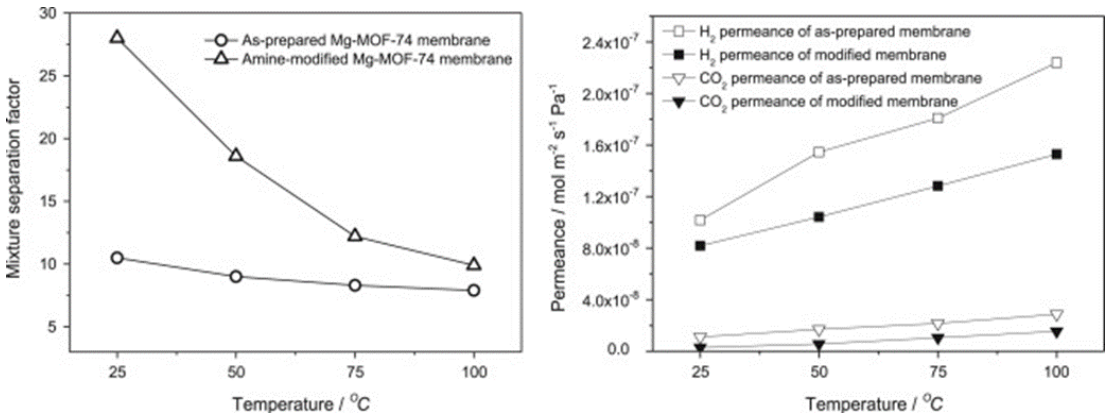

691 **Figure 40**. Mixture separation factors for H_2/CO_2 from equimolar mixture (left) and single gas
692 permeances of H_2 and CO_2 (right) on the as-prepared and amine-modified Mg-MOF-74 membranes
693 at 1 bar as a function of temperature. (adapted with permission from ref. [73]).

694 Using the LBL seeding approach and a solvothermal secondary growth method, a continuous
695 Ni-MOF-74 membrane was fabricated on α-alumina support.[129] The gas permeation of the
696 fabricated membranes was tested for gases like H_2, N_2, CH_4 and CO_2, were measured. The CO_2
697 permeation was found to be the lowest one, which is due to the stronger adsorption affinity for CO_2
698 and as a result a high ideal selectivity for H_2/CO_2 was obtained for this membrane (Figure 41).
699

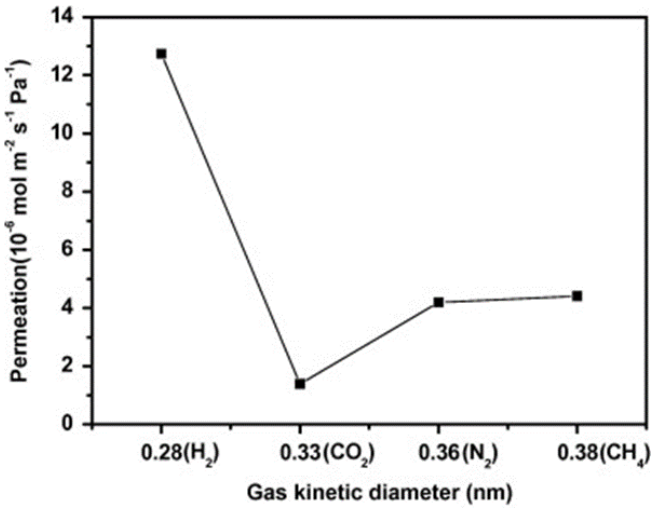

700 **Figure 41**. Single gas permeation of Ni-MOF-74 membrane (S-4) at 25 °C and 1 bar of feed pressure
701 (adapted with permission from ref. [129]).

702 Layer-pillar based MOFs structures can also be tuned to create isoreticular structures with
703 different pore sizes via tuning the length of the pillars, like for example the $Cu(bipy)_2(SiF_6)$ MOF, that
704 showed an extraordinary CO_2 sorption selectivity over other gases like N_2, H_2 and CH_4, even under
705 humid conditions.[130] This $Cu(bipy)_2(SiF_6)$ MOF was successfully fabricated as a membrane by Sung
706 et al. by in situ solvothermal synthesis method (Figure 13). The fluoridation of the support by
707 $(NH_4)_2SiF_6$ was used the source of SiF_6^{2-}, which was used to control the growth and enhances the
708 linkage between the membrane and support. The H_2 permeation tests with respect to other gases
709 showed separation factors of 8.0, 7.5 and 6.8 for H_2/CO_2, H_2/CH_4 and H_2/N_2, respectively. The
710 membrane showed a high H_2 permeance of 2.7×10^{-7} mol m^{-2} s^{-1} Pa^{-1} and an excellent thermal stability
711 (Figure 42).

Preprints (www.preprints.org) | NOT PEER-REVIEWED | Posted: 3 September 2018 doi:10.20944/preprints201809.0010.v1

Peer-reviewed version available at Crystals 2018, 8, 412; doi:10.3390/cryst8110412

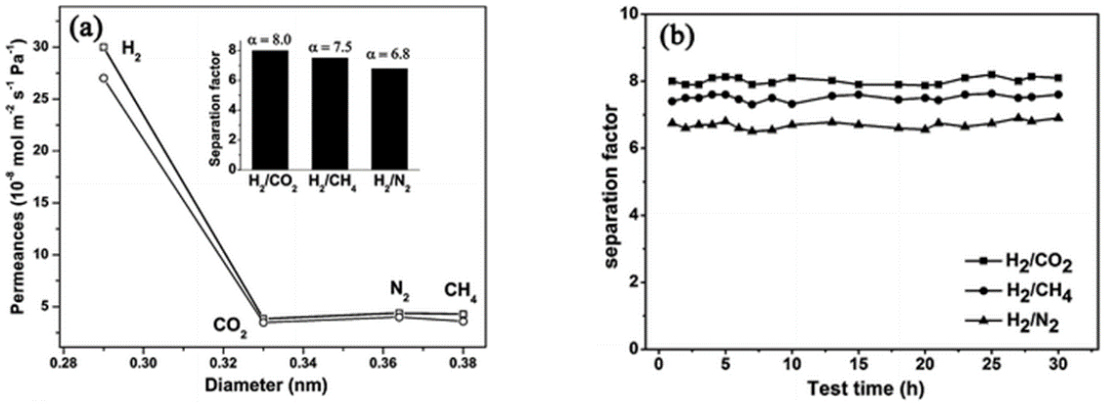

712 **Figure 42**. (a) Single- (□) and binary- (○) gas permeances of different gases on the $Cu(bipy)_2(SiF_6)$
713 membrane at 293 K as a function of the kinetic diameter (inset: the separation factor for H_2 over other
714 gases by binary gases tests). (b) Plot of H_2–CO_2, H_2–CH_4 and H_2–N_2 separation factors of the
715 $Cu(bipy)_2(SiF_6)$ membranes (average values of five different membranes) at different test times.
716 Permeation temperature = 293 K, feed pressure = 1×10^5 Pa (adapted with permission from ref. [130]).

717 Takamizawa et al. [131] report the fabrication of an oriented membrane from a single-crystal of
718 $[Cu_2(bza)_4(pyz)]_n$ MOF, having high permeance one-dimensional (1D) channels; this membrane
719 unveils an anisotropic gas permeation via the 1D channels, that showed a high permselectivity for H_2
720 and CO_2. Though the narrow channels smaller aperture size is than the tested gases kinetic diameters
721 of, many of them were able to pass via these 1D channels (Figure 43). Permeability values measured
722 along the channels were found to be 7–60 times more than those measured perpendicular to the
723 channels.
724

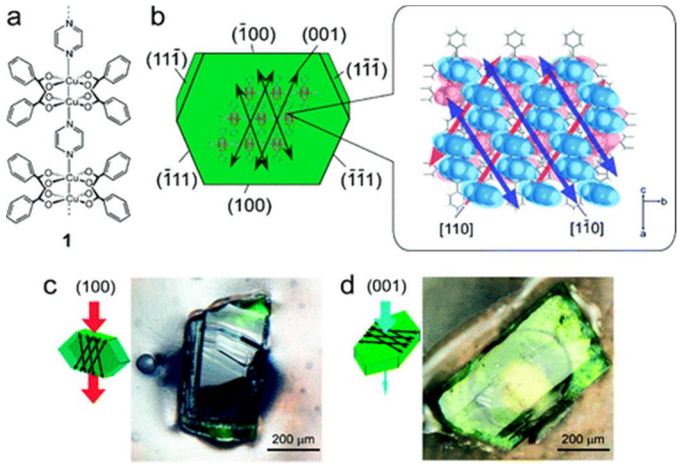

725 **Figure 43**. (a) Chemical structure and (b) crystal structure of $[Cu_2(bza)_4(pyz)]_n$ (1) showing the
726 determined numbers of the crystal planes and the channel direction. (c, d) Photographs of single-
727 crystal membranes of 1: (c) exposed (100) crystal surface (channel membrane); (d) (001) crystal surface
728 (nonchannel membrane) (adapted with permission from ref. [131]).

729 The permeability measure perpendicular to the channels for several gases under the experimental
730 conditions were undetectable. The results indicated that for He, H_2 and CO_2 gases, they permeate
731 slightly faster when they are in the orientation is perpendicular to the channels, which could be
732 related to a minimum number of crystal defects in this route. This clearly indicated the possibility for
733 the gases to permeate through the membrane channels, even though the channel aperture size is
734 smaller than the kinetic diameters of the tested gases (Figure 44).

735

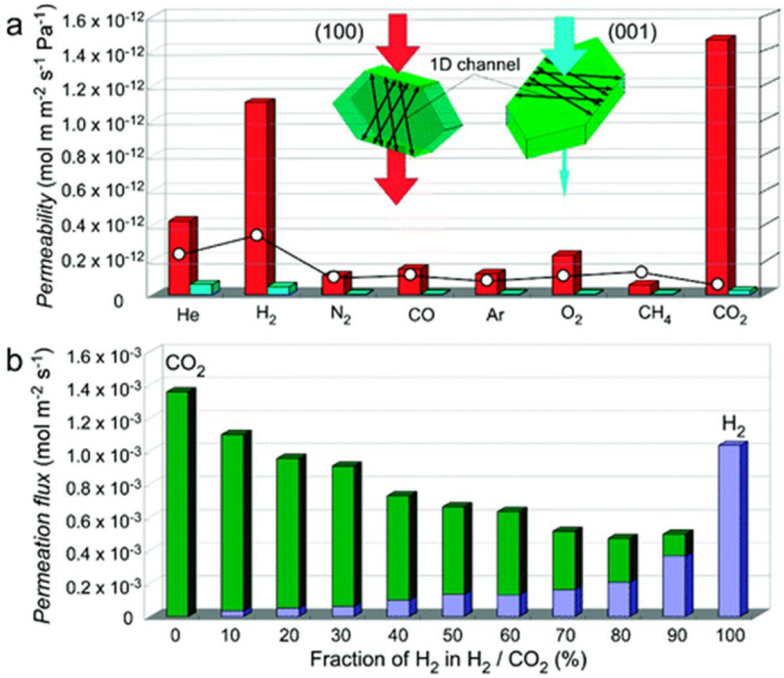

Figure 44. (a) Comparison of the permeabilities of crystal membrane 1 for various gases: (red) along the channels (channel membrane); (light-blue) perpendicular to the channels (nonchannel membrane). The inset plot (○) is the calculated permeability based on the Knudsen model. (b) Comparison of the permeation fluxes of H_2 and CO_2 along the channels of gas mixtures for various mixing ratios (H_2, purple; CO_2, green) (adapted with permission from ref. [131]).

The $[Ni_2(L\text{-asp})_2(bipy)]$ MOF (L-asp=L-aspartic acid, and bipy=4,4'-bipyridine), which is a chiral MOF was investigated by Qui et al. who take a chance to try to alter the pores in this parent MOF by use of a shorter pillar like pyrazine (pz). As expected, this new MOF of the same framework topology $[Ni_2(L\text{-asp})_2(pz)]$ (named JUC-150, JUC=Jilin University China) was successfully synthesized and structurally characterized Figure 45.[132] This ultra-microporous JUC-150 membrane exhibited a favored permeation of H_2 against other tested due to its excellent size sieving properties, which enhanced its selectivity performance from 26.3, 17.1 and 38.7 for the case of H_2/CH_4, H_2/N_2 and H_2/CO_2, respectively. These values represent one of the best separation selectivity with respect to prior reported MOF membranes. Furthermore, JUC-150 membrane showed an outstanding thermal stability separation performance at higher temperatures of 200ºC (Figure 46-47).

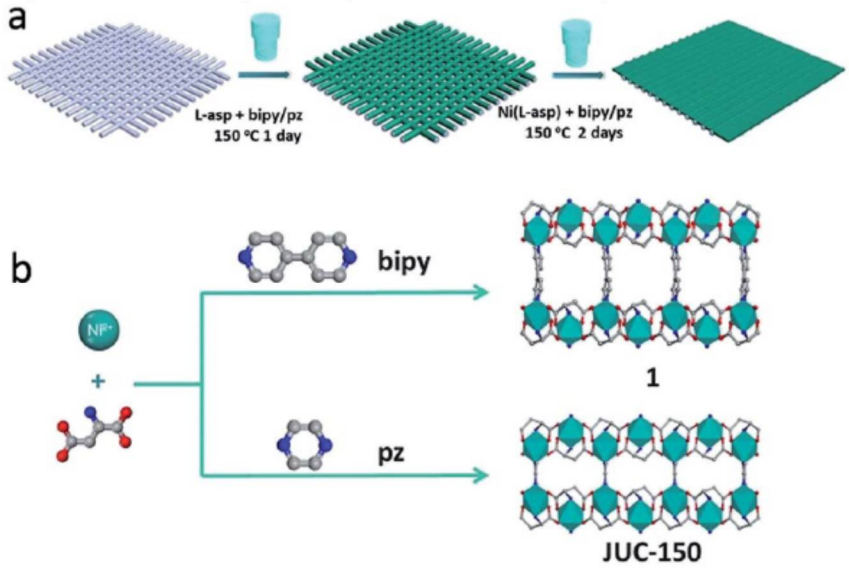

Figure 45. (a) Schematic diagram of the preparation of $Ni_2(L\text{-asp})2P$ (P= bipy or pz) membranes on nickel screens. (b) Schematic description of compound 1 and JUC-150 structure. Ni cyan, C gray, N blue, and O red; the H atoms are omitted for clarity (adapted with permission from ref. [132]).

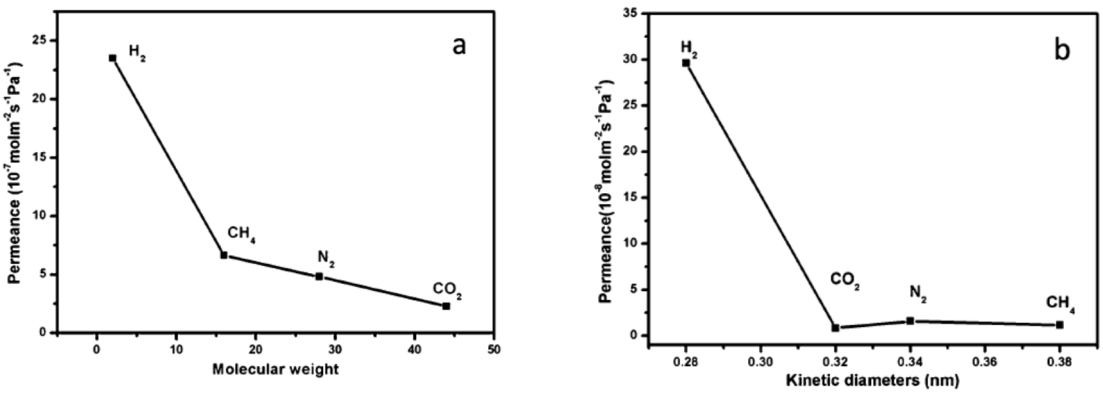

Figure 46. (a) The permeances of single gases through the 1 membrane at 298 K as a function of the molecular weight. (b) The permeances of single gases through the JUC-150 membrane at 298 K as a function of the kinetic diameters. (adapted with permission from ref. [132]).

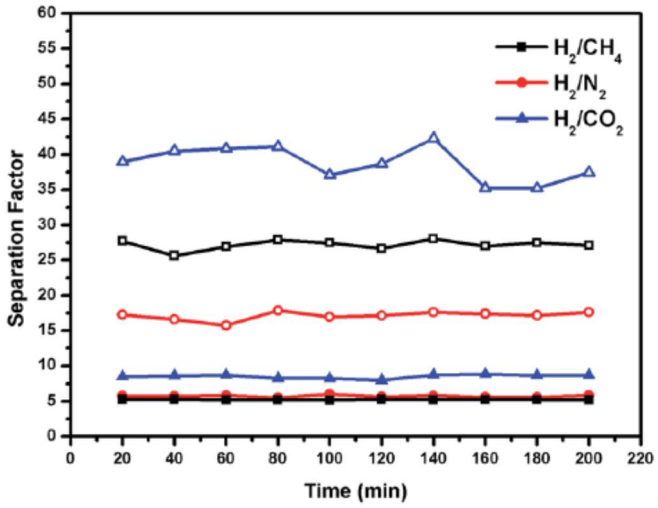

Figure 47. H_2/CH_4, H_2/N_2, and H_2/CO_2 separation factors of the 1 membrane (solid) and the JUC-150 membrane (hollow) over time (adapted with permission from ref. [132]).

Covalent organic frameworks (COFs), is a subclass of the porous materials that consist of strong covalent bonds between light elements like C, B, N, etc. These porous materials are credited with excellent properties in terms structural tunability, low density and stability. Recently, COF-MOF composite membranes was fabricated and tested for H_2 separation from CO_2 was reported by Qiu et al.[133] (Figure 48-49). The excellent performance was not only in terms of very high selectivity compared to the neat COF and MOF membranes, but it has beat the Robeson upper bound for other materials like polymer-based membranes for this separation. The separation factors for the H_2/CO_2 (1:1) binary mixture for two composite membranes form [COF-300]-[$Zn_2(bdc)_2(dabco)$] and [COF-300]-[ZIF-8] were found to be around 12.6 and 13.5, respectively (Figure 50). This noteworthy performance is attributed probably to the fabrication method of, that implicates the strong chemical bonding induced between the support, COF and MOF, since the COF material can cooperate via imine groups with polyaniline, while in case of the ZIF the HN-Zn-imidazole bonds could help in sealing the interface with the COF.

Recently, the interest in two dimensional (2D) MOF nanosheets is increasing due to their unique properties in terms of large surface areas, nanometer-sized cavities, uniform channels, stability, and chemical tunability, which made them potential candidates for their application in gas separation as membranes.[134,135] A highly oriented tubular membrane of $Zn_2(bIm)_4$ (bIm= benzimidazole) ZIF nanosheet was fabricated by the self-conversion of ZnO nanoparticles (NPs) using a graphene oxide (GO) guided method (Figure 51).[118]

Preprints (www.preprints.org) | NOT PEER-REVIEWED | Posted: 3 September 2018 doi:10.20944/preprints201809.0010.v1

Peer-reviewed version available at Crystals 2018, 8, 412; doi:10.3390/cryst8110412

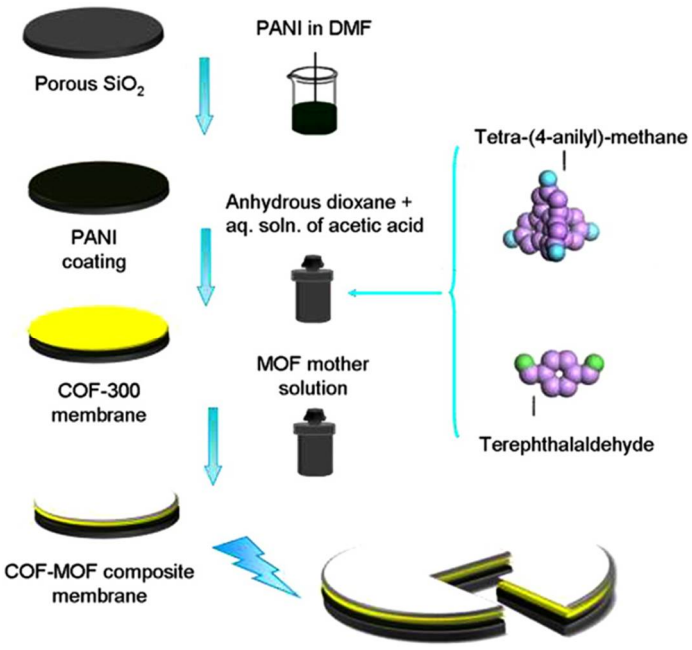

778 **Figure 48**. Schematic representation of the fabrication of COF-MOF composite membranes. (adapted
779 with permission from ref. [133]).

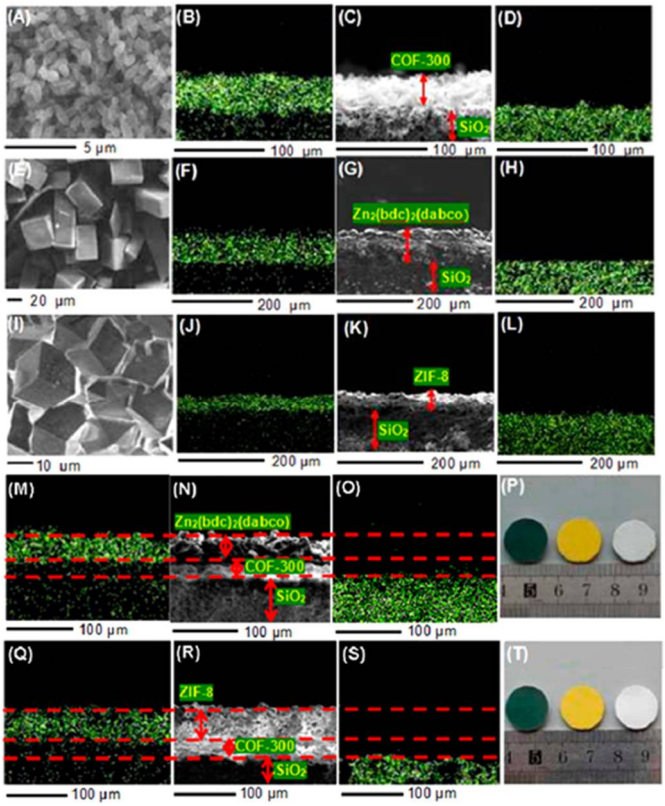

780 **Figure 49**. COF-300 membrane: (A) SEM top view, (B) elemental mapping image (carbon), (C) SEM
781 cross-sectional view, and (D) elemental mapping image (silicon). $Zn_2(bdc)_2(dabco)$ membrane: (E)
782 SEM top view, (F) elemental mapping image (zinc), (G) SEM cross-sectional view, and (H) elemental
783 mapping image (silicon). ZIF-8 membrane: (I) SEM top view, (J) elemental mapping image (zinc), (K)
784 SEM cross-sectional view, and (L) elemental mapping image (silicon). [COF-300]-[$Zn_2(bdc)_2(dabco)$]
785 composite membrane: (M) elemental mapping image (zinc), (N) SEM cross-sectional view, (O)
786 elemental mapping image (silicon), and (P) photo image. [COF-300]-[ZIF-8] composite membrane:
787 (Q) elemental mapping image (zinc), (R) SEM cross-sectional view, (S) elemental mapping image
788 (silicon), and (T) photo image. (adapted with permission from ref. [133]).

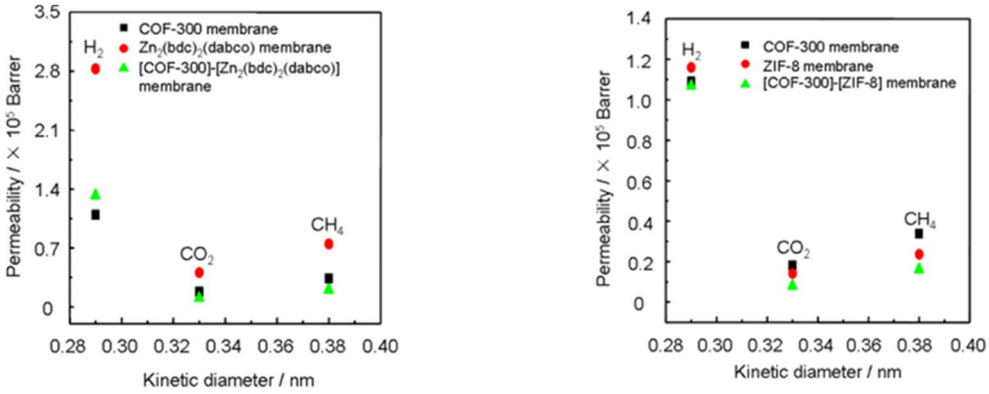

789 **Figure 50**. (top) Single gas permeability of various gases through the COF-300 membrane,
790 $Zn_2(bdc)_2(dabco)$ membrane, and [COF-300]-[$Zn_2(bdc)_2(dabco)$] composite membrane at room
791 temperature and 1 bar as a function of their kinetic diameters. (bottom) Single gas permeability of
792 various gases through the COF-300 membrane, ZIF-8 membrane, and [COF-300]-[ZIF-8] composite
793 membrane at room temperature and 1 bar as a function of their kinetic diameters. (adapted with
794 permission from ref. [133]).

795

796 **Figure 51**. Scheme depicting the preparation procedure of highly oriented $Zn_2(bIm)4$ nanosheet
797 membranes by ZnO self-conversion growth in a GO confined space (adapted with permission from
798 ref. [118]).

799 An oriented nanosheet tubular membrane fabricated using the solvothermal growth for 9 hours
800 (denoted as M-9) was tested for its single and binary mixtures gas permeation performances,
801 respectively. Figure 52 displays the permeances of H_2, N_2, CO_2 and CH_4, which showed that H_2 has
802 the highest one. The lower permeances of larger gases than H_2, indicates molecular sieve performance
803 of this membrane exhibited. The ideal selectivities were 106, 126 and 256 for H_2/CO_2, H_2/N_2 and
804 H_2/CH_4, respectively, which are higher than Knudsen. Moreover, binary mixtures through the M-9
805 membrane confirmed the molecular sieve performance of this membrane, and the separation
806 selectivities for H_2/CO_2, H_2/N_2 and H_2/CH_4 were found to be 89, 103 and 221, respectively.
807 The results show that changing the feed partial pressure for H_2 from 0.5 to 1.5 bar did not affect both
808 the gas permeances and H_2/CO_2 separation selectivity, thus proving their excellent mechanical
809 stability. The increase in testing temperature from 30 to 150 ^{0}C did not affect significantly the
810 permeation for both H_2 and CO_2, however, the H_2 permeance and separation selectivity of H_2/CO_2
811 increased slightly Figure 52, b. This is could be due to some structural flexibility of the nanosheets
812 that could cause some slight increase in their effective pore size. This small change of pore size can

affect in the permeance of H_2 (small kinetic diameter) and barely influence the permeance of CO_2 (larger kinetic diameter), however slightly enhanced the separation selectivity of H_2/CO_2.

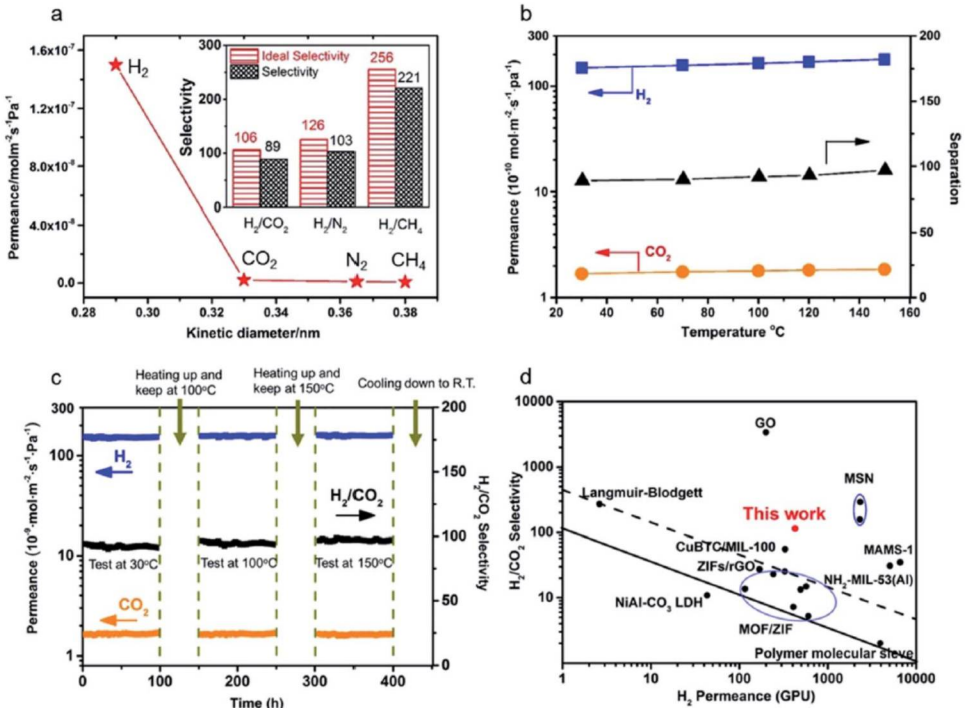

Figure 52. (a) Single gas permeances of the M-9 membrane (inset: ideal separation factors for single gases and separation selectivities for binary gas mixtures for H_2 over CO_2, N_2 and CH_4); (b) permeances of binary gas mixtures as a function of temperature difference; (c) long-term operating stability of the M-9 membrane for the separation of an equimolar H_2/CO_2 mixture in the range of temperatures from 30 to 150 _C at 0.1 MPa; (d) comparison of our M-9 membrane with the reported molecular sieve membranes for the separation of H_2/CO_2 mixtures. The black solid line represents the 2008 upper bound of polymeric membranes for H_2/CO_2. The black dashed line represents the 2010 upper bound of microporous inorganic membranes for the separation of H_2/CO_2 mixtures. (adapted with permission from ref. [118]).

4.2 MOF membranes for CO_2 separation.

Carbon dioxide (CO_2) is considered as the foremost contributor for greenhouse gas emissions, its continuous concentration buildup in our atmosphere is expected to produce severe global warming concerns. CO_2 is known to be one of the main impurities in natural gas and need to be separated before the gas is pumped to the pipeline, in order to prevent major corrosion issues. Thus, it is of great meaning to develop processes to effectively separate and recycle CO_2 from the different sources. [136] Membrane-based separation technology is considered as an encouraging alternate to the conventional separation processes, since it compromises a more energy effective route and a superb reliability. The removal of CO_2 with minimum energy spending is principally highly desirable. Therefore, many materials have been developed as membranes for CO_2 separation like polymers and zeolites, however plasticization decreases the performance of polymers while zeolites suffer from low permeability. [2,13,137-139]

Many MOFs have been explored to be fabricated as membranes and applied to separate CO_2 from other common gases like CH_4, N_2, etc. Among these MOFs are ZIFs, which possess very much porous framework with reachable pore volume.[111,140] The pore apertures of different ZIFs, as an example in ZIF-8, lies within the kinetic diameter range of common gas molecules. Moreover, ZIF-8 is chemically stable material even in the presence of water and some aromatic hydrocarbons like benzene, the classic impurities in natural gas refining, making this MOF a potential candidate for separating CO_2 from CH_4. [63,113,115,141]

Carreon et al. fabricated ZIF-8 membranes via the in situ solvothermal method on tubular alumina supports, that were functionalized via hydrothermal seeding.[63] In their study, all of the

fabricated membranes (Figure 29), displayed a high CO_2 permeance of ~2.4×10^{-5} mol m^{-2} s^{-1} Pa^{-1} and a selectivity for CO_2/CH_4 of ~4 - 7 under their experiment conditions. The density functional theory simulation data on ZIF-8 suggested that, the ZIF-8 smaller pores were the favored adsorption spots for CO_2. Consequently, the small pore aperture will favor the diffusion of CO_2 over CH_4.

Achieving molecular separation of CH_4 and CO_2 is difficult due to the similarity in their molecular sizes in a membrane-based process. Advantageously, the MOFs tunable composition of wide-ranging metal ions and organic ligands, have managed to exhibit selective adsorption between these two gases, paving the way that they may be applied for CO_2 separation from CH_4 separate through sorption-based separation mechanism. Continuous and well intergrown membranes of $Co_3(HCOO)_6$ MOF were fabricated on a macroporous glass support (Figure 53).[142] The overall framework of the $Co_3(HCOO)_6$ MOF has a 1D zigzag channels with an aperture size of 5.5 Å. This channel structure was found to favor CO_2 separation from CH_4 via preferential adsorption. As shown in Figure 54, the microporous $Co_3(HCOO)_6$ membrane showed a high permeation flux of 2.09×10^{-6} mol m^{-2} s^{-1} Pa^{-1} and outstanding permeation selectivity for CO_2 over CH_4 of 10.37–15.95 at 0–60 °C. This is because CO_2 molecules permeate faster through the 1D zigzag channels as compared to CH_4. This faster permeation of CO_2 was as a result was of the preferential adsorption of CO_2 in the micropores and external surfaces of the MOF membrane, which repressed CH_4 sorption from the mixture. These results revealed that the suitable pore size combined with the pore shape in case of the $Co_3(HCOO)_6$ MOF has prevented the two molecules to permeate through it simultaneously, i.e. once CO_2 permeates through the pores, the permeation of CH_4 molecules was hindered.

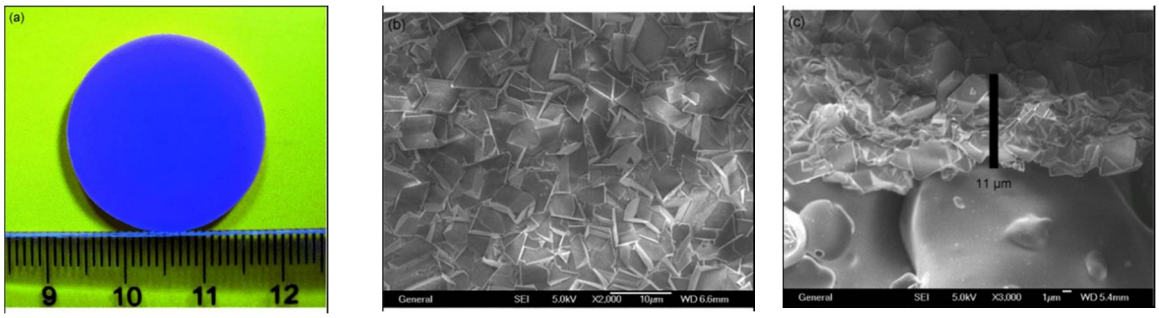

Figure 53. a) Optical image of a $CO_3(HCOO)_6$ membrane grown on a glass frit. b) Top and c) side view SEM images of the intergrown layer (adapted with permission from ref. [142]).

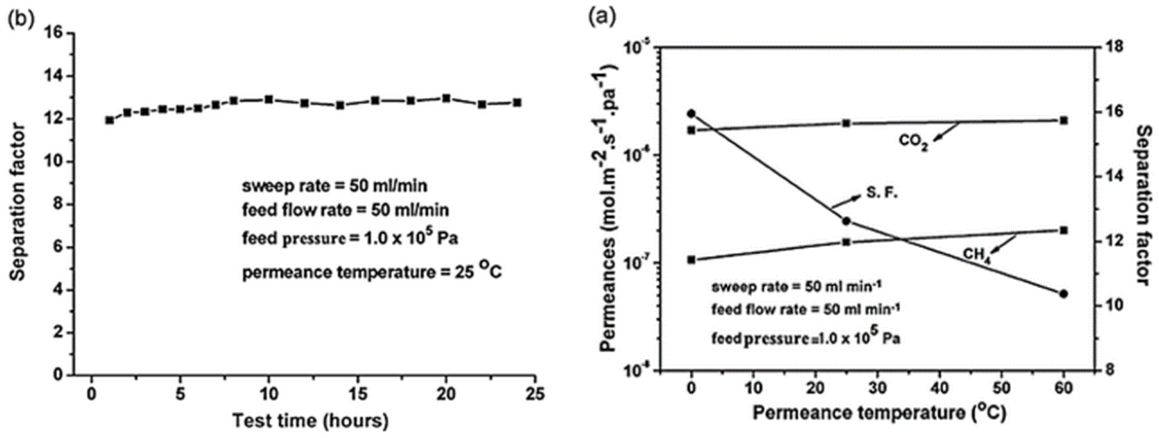

Figure 54. (a) CO_2/CH_4 permeance and separation factor (SF) of the $Co_3(HCOO)_6$ membrane versus permeation temperature. (b) Plot of the CO_2/CH4 separation factor of the $Co_3(HCOO)_6$ membrane as a function of test time (adapted with permission from ref. [142]).

The orientation of fabricated membranes has shown to influence their separation performance. Highly oriented MOF membrane of ZIF-69 was reported for gas separation by Lai et al.[143] The ZIF-69 possessed a zeolite GME topology with 12 and 8MRchannels along the c-axis and the a- and b-axes, respectively. The aperture size along the c-axis is about 0.78 nm, which means that in order to

achieve an outstanding gas permeation performance, it is required to fabricate a c-oriented ZIF-69 membrane; which will have the straight channels line up perpendicular, with respect to the support surface. The ZIF-69 membranes were fabricated by using oriented seeds at first and then a secondary growth step (Figure 55). The single-gas permeation results of N_2, CO_2 and CH_4 showed that they have Knudsen behavior, whereas in case of CO_2 permeation was dominated by surface diffusion as a result of the high adsorption affinity of ZIF-69. The separation of equimolar gas mixture of CO_2 and N_2, CO and CH_4 were measured and found to be 6.3, 5.0 and 4.6, respectively, with a permeance of ~1.0×10^{-7} mol m^{-2} s^{-1} Pa^{-1} for CO_2 (Figure 56 and 57). A comparison of the non-oriented grown ZIF-69 with the c-oriented ZIF-69 membrane, showed that the oriented one exhibited a better selectivity and higher permeance.

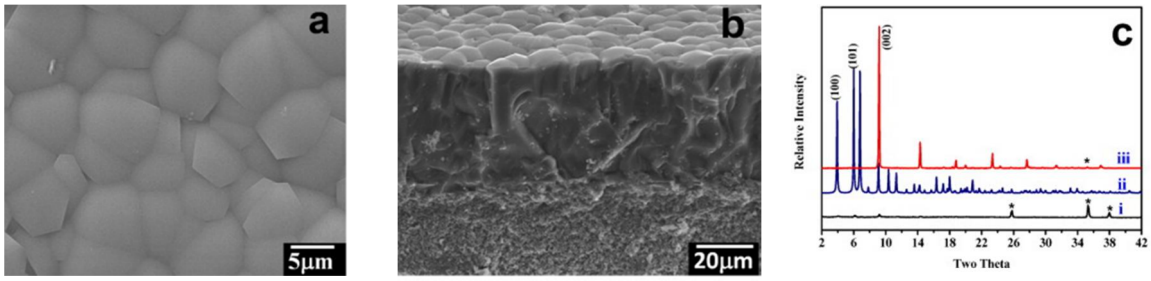

Figure 55. (a) Top view of ZIF-69 membrane by secondary growth. (b) Cross section view of ZIF-69 membrane by secondary growth. (c) XRD patterns for (i) ZIF-69 seeded α-alumina substrate, (ii) ZIF-69 powder by simulation from Mercury Software (Cambridge Crystallographic Data Centre), (iii) Highly oriented ZIF-69 membrane by secondary growth in this study. * are peaks from α-alumina substrate (adapted with permission from ref. [143]).

Recently, the LBL method was used for the fabrication of membranes of $[Cu_2(ndc)_2(dabco)]$ or $[Cu_2(BME\text{-}bdc)_2$ $(dabco)]$.[144] The $[Cu_2(ndc)_2(dabco)]$ is a MOF with a large-pore where no affinity exists between the gases and the framework. As expected with such systems they were found to follow the Knudsen behavior. However, in case of the BME-bdc, which is composed of a benzene ring functionalized with two ether side groups ($O(CH_2)_2OCH_3$), that are expected to enhance the framework affinity toward CO_2 in $[Zn_2(BME\text{-}bdc)_2$ $(dabco)]$ MOF. The fabricated membrane of $[Cu_2(BME\text{-}bdc)_2$-$(dabco)]$ has shown higher selectivity toward CO_2, compared with CH_4. The gas mixtures tests of equimolar CO_2/CH_4, exhibited a 4.5 selectivity factor that is higher than the corresponding Knudsen coefficient. The separation cannot be credited only to molecular sieving effect, since the flexibility of the ether groups make it difficult to estimate the effective pore size, but also to enhanced affinity of the framework and CO_2 (Figure 58).

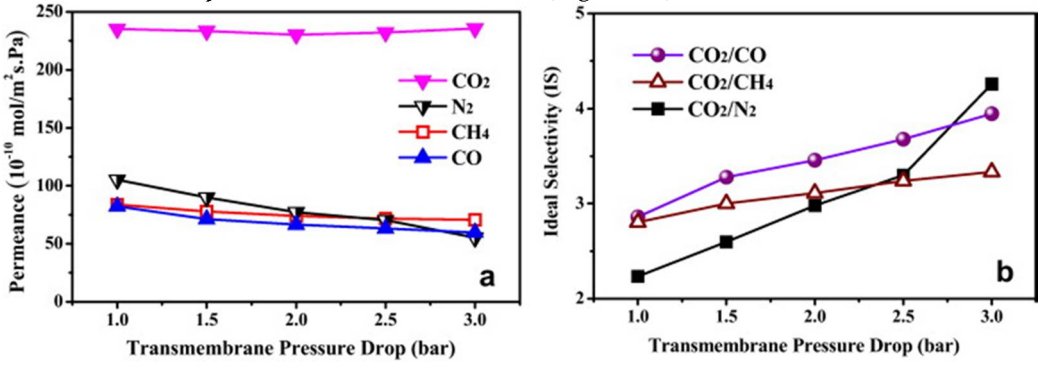

Figure 56. (a) Single gas permeances of CO_2, N_2, CH_4 and CO through a ZIF-69 membrane as a function of transmembrane pressure drop at 298 K. (b) The ideal selectivities of CO_2/CO, CO_2/CH_4, and CO_2/N_2 for a ZIF-69 membrane as a function of transmembrane pressure drop at 298 K (adapted with permission from ref. [143]).

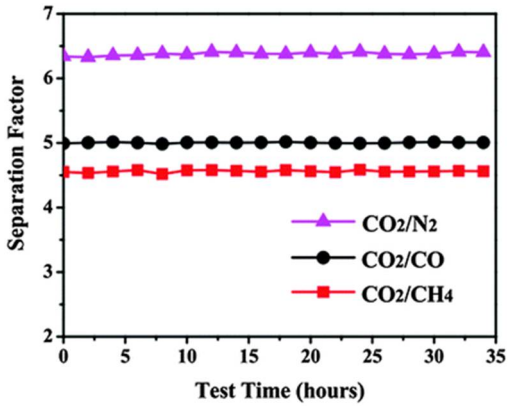

Figure 57. Separation factors for the CO_2–CO, CO_2–CH_4 and CO_2–N_2 gas mixtures (50% molar each) as a function of test time for the ZIF-69 membrane at 298 K (adapted with permission from ref. [143]).

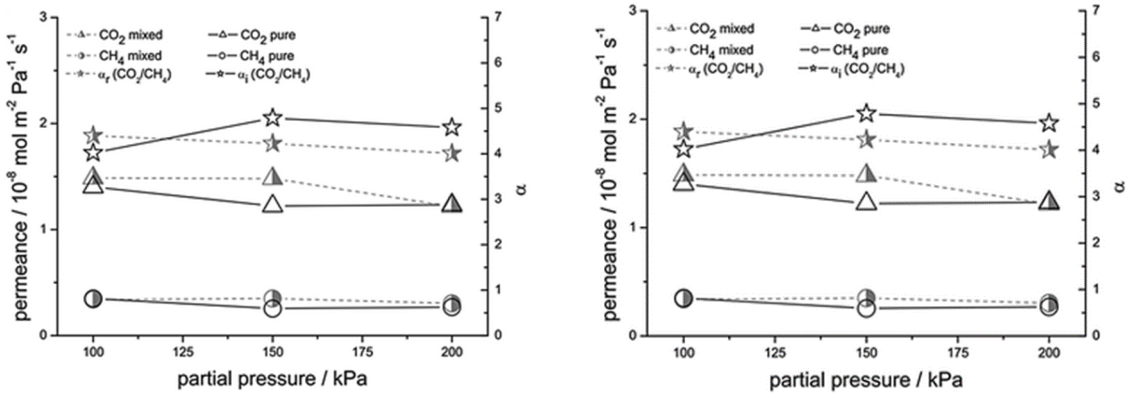

Figure 58. (Left) permeance of pure and equimolar mixed CO_2 and CH_4 measured for the $[Cu_2(ndc)_2(dabco)]_n$ (1) membrane at room temperature (T = 298 K) as a function of pressures at the feed side (total pressures for pure gases, partial pressures for the gas mixture). The ideal and mixed gas separation factors αi and αr were calculated from the corresponding ratio of the CO_2/CH_4 permeance. (Right) permeance of pure and equimolar mixed CO_2 and CH_4 measured for the $[Cu_2(BME\text{-}bdc)_2(dabco)]_n$ (2) membrane at room temperature (T = 298 K) as a function of pressures at the feed side (total pressures for pure gases, partial pressures for the gas mixture). The ideal and mixed gas separation factors αi and αr were calculated from the corresponding ratio of the CO_2/CH_4 permeance (adapted with permission from ref. [144].

Bio-MOF-1 membranes were prepared by a secondary seeded growth method and tested for gas mixture separation, by Carreon et al.[145] These Bio-MOF-1 membranes exhibited high CO_2 permeances and separation selectivity over CH_4. The measured CO_2/CH_4 separation selectivities were higher than one, which is higher than Knudsen selectivity. The CO_2 preferential adsorption in this MOF, driving separation mechanism, was credited to the existence of organic ligand amino basic sites in the Bio-MOF-1 structure. The Robson plot and showed that the Bio-MOF-1 membrane has same performance like most conventional polymeric membranes and smaller than most zeolite membranes (Figure 59).

Later on, the same group reported the fabrication of cobalt–adeninate MOF (bio-MOF-13 (I) and bio-MOF-14 (II)) membranes.[146] The fabricated membranes exhibited high CO_2 permeabilities and low CO_2 separation selectivities over CH_4. These observed high CO_2/CH_4 selectivities were credited to the favored CO_2 adsorption in case of the bio-MOF-13 framework. These membranes displayed CO_2 permeances as high as 4 10^6 mol m^2s^1Pa with CO_2/CH_4 separation selectivities in the 3–4 range at 295 K (Figure 60). The enhanced CO_2 adsorption in these frameworks was again credited to the presence of basic linkers, although the type of this specific nature between the CO_2 and framework is unclear.

Peer-reviewed version available at Crystals 2018, 8, 412; doi:10.3390/cryst8110412

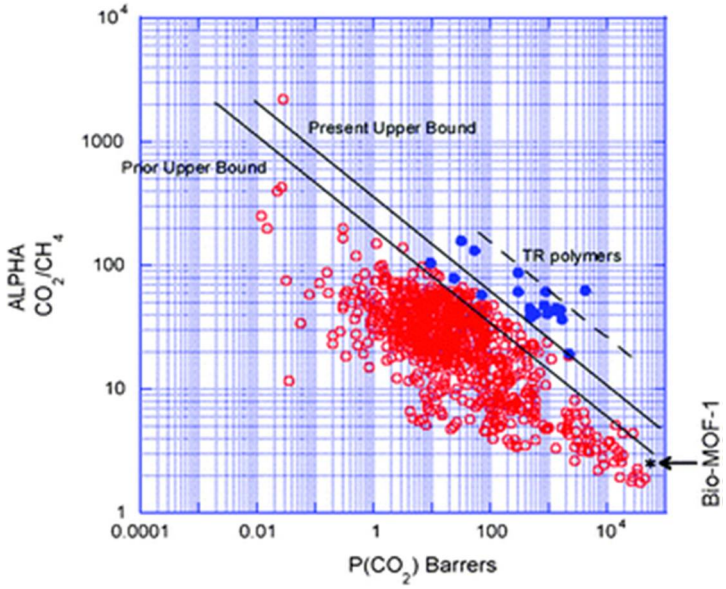

933 **Figure 59**. Robeson plot for CO_2/CH_4 mixtures. For comparison, data point for a Bio-MOF-1
934 membrane is shown (adapted with permission from ref. [145]).

935 Recently Jeon et al. also used a rapid one-pot solvothermal microwave growth approach to
936 fabricate a mixed-linker ZIF membranes.[62] The mixed-linker ZIF was consisting of the ZIF-8 linker
937 the 2-methylimidazolate (mIm) and the ZIF-7 linker the benzimidazolate (bIm), and these were
938 termed as the ZIF-7-8 membranes (Figure 61). Using this rapid synthesis approach, they were able
939 via varying the ratios of bIm to mIm linkers in the mixed linker frameworks to alter the ZIF-7-8
940 membranes separation properties. The permeances of H_2, CO_2, N_2, and CH_4 was reduced, and the
941 ideal selectivities increased with increasing the bIm/mIm ratios. The mixture gas permeation study
942 for H_2/CH_4 and CO_2/CH_4 on ZIF-7-8 membranes showed an increase in the selectivity with increasing
943 the bIm linker ratio, suggesting the change in the separation behavior of the membrane with the
944 variation of the linkers ration (Figure 62).

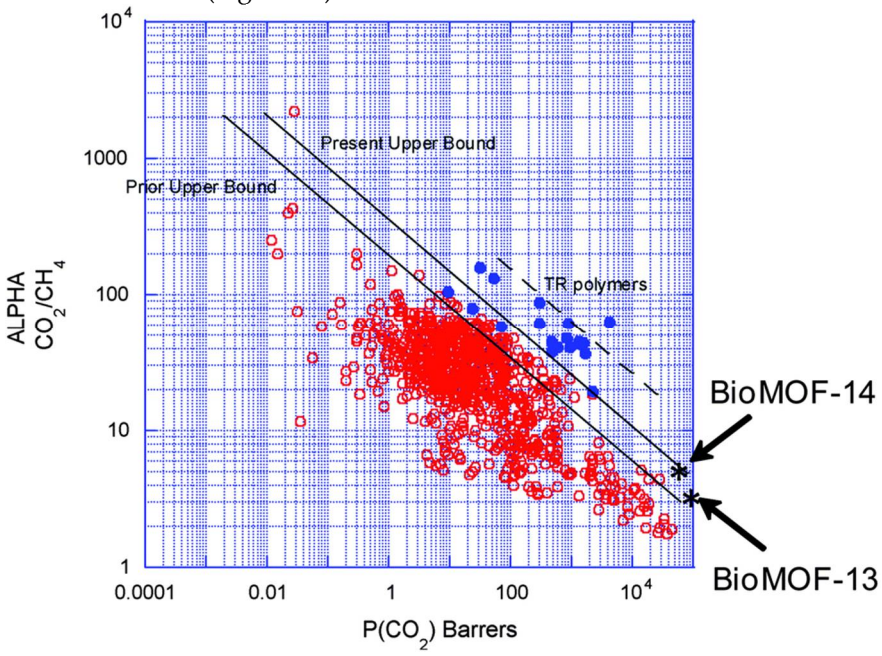

945 **Figure 60**. Revisited Robeson plot for CO_2/CH_4 mixtures. The separation performance for I and II
946 membranes is included in the plot (adapted with permission from ref. [146]).

947 Upon comparison with the mono linker neat ZIF membranes like ZIF-7 and ZIF-8, the mixed
948 linker ZIF-7-8 membranes still shows a reasonable performance for both H_2/CH_4 and CO_2/CH_4 gas
949 separations, which indicates the good quality of ZIF-7-8 membranes (Figure 63).

Peer-reviewed version available at Crystals 2018, 8, 412; doi:10.3390/cryst8110412

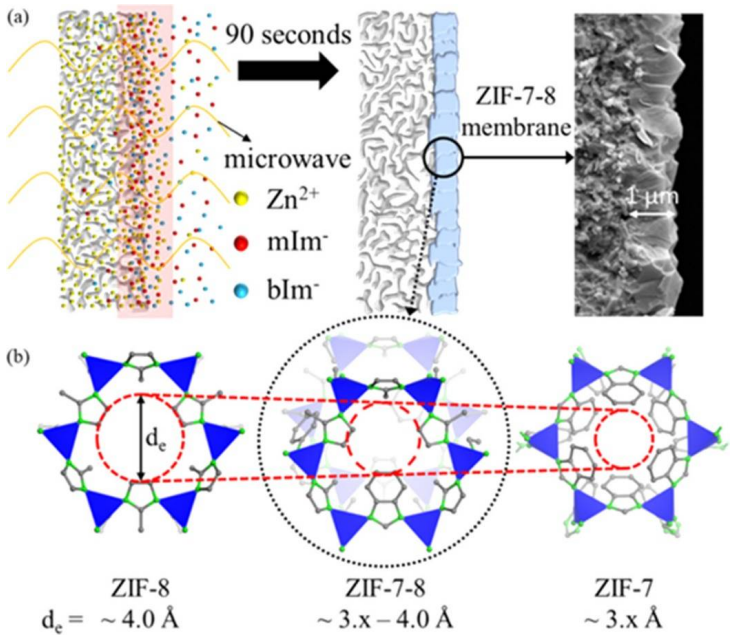

Figure 61. Schematic illustration for the rapid microwave-assisted in situ synthesis of mixed linker ZIF-7-8 membranes and (b) comparison of effective pore aperture of ZIF-8, ZIF-7, and mixed linker ZIF-7-8. de = effective aperture size. (adapted with permission from ref. [62]).

Post- and precombustion carbon capture and natural gas upgrading applications are very important separation applications. However, few studies on the application of MOF membranes for the CO_2 gas separations from N_2, CH_4 and H_2 were stated. An efficient membrane for CO_2 capture from above mentioned predominately gas feeds, should unveil an excellent separation for CO_2 over other gases, in order to concentrate these valuable gases such as CH_4, O_2, and H_2 more efficiently. According to literature, the separation selectivity that favor CO_2 permeation was reported firstly using $[Cu_2(bza)_4(pyz)]_n$ as a single crystal MOF membrane.[131]

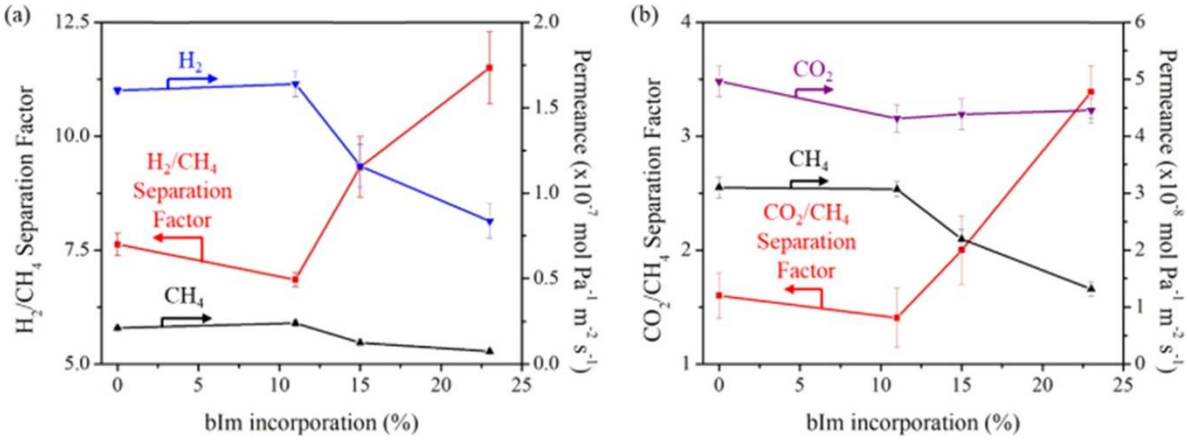

Figure 62. Binary testing of (a) H_2/CH_4 and (b) CO_2/CH_4 for ZIF-7-8 membranes with varying bIm incorporation (adapted with permission from ref. [62]).

Later on, Lin et al. reported thin MOF-5 membranes fabricated by a secondary growth method.[147] They investigated the permeation and separation features of this membrane towards mixtures of CO_2/H_2 and CO_2/N_2. The MOF-5 membranes were tested with CO_2/H_2 or CO_2/N_2 mixture feed, showed a more permeability to CO_2 over H_2 or N_2. The CO_2/H_2 separation factors were more than 1, i.e. CO_2 was more permeable not H_2. Which was related to that MOF-5 has a favored adsorption for CO_2 over H_2, as derived from a saturated sorption capacity of 2 mmol/g for CO_2 and 0.1 mmol/g for H_2 at 298 K and 1 atm). Later on using a post CO_2 annealing means, they managed to increase both the permeance and separation factor of MOF-5 membranes for CO_2 separation over

H_2.[148] The post-treatment of the membrane (PMOF-5) was done by annealing the MOF-5 under a high pressure CO_2 stream at 100 °C, which led to decrease the H_2 permeance and increase CO_2 permeance, leading to improvement in both CO_2/H_2 separation factor from 721 up to 5781 and CO_2 permeance from 5.67×10^{-7} up to 9.38×10^{-7} mol m^{-2} s^{-1} Pa^{-1} under CO_2 molar fraction of 98%, feed pressure of 5 atm and 298 K Figure 64. The uncommon separation performance is again related to the enhanced CO_2 adsorption selectivity over H_2 and the formation of surface carbonate anions caused by the CO_2 treatment. The separation factor of CO_2/H_2 for the no post-treated membrane (MOF-5) increases drastically from ~2 at a below 0.94 sharply to about 721 at an of 0.985 and CO_2 permeance of 5.67×10^{-7} mol m^{-2} s^{-1} Pa^{-1}, and then deceases with a further increase in CO_2 mole fraction.

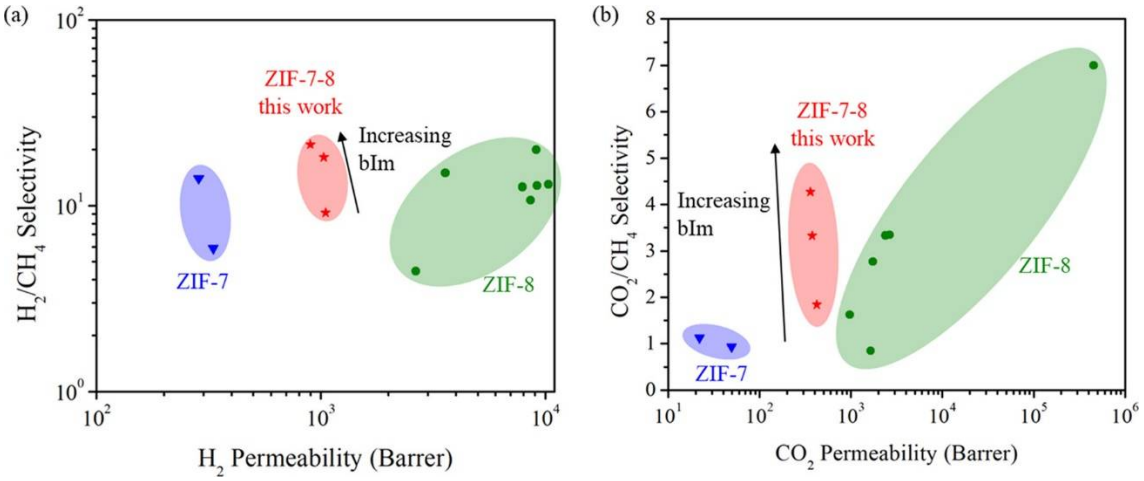

Figure 63. Comparison of (a) H_2/CH_4 and (b) CO_2/CH_4 separation performance for mixed-ligand ZIF-7-8 membranes with the parent ZIF membranes (ZIF-7 and ZIF-8). 1 Barrer = 3.348×10^{-16} mol m m^{-2} s^{-1} Pa^{-1} (adapted with permission from ref. [62]).

Recently, the first zeolite-like MOF (ZMOF) membrane with a sodalite topology was prepared via a solvothermal crystallization approach on porous alumina support.[149] ZMOFs were pioneered by Eddaoudi and represent a subclass of MOFs, which are topologically related to pure zeolites. ZMOFs exhibit unique properties like; extra-large cavities, chemical stability, and cation exchange ability. Their anionic character allows the tuning of the pore system via extra-framework cations exchange, which will, in turn, tune their host–guest interactions. The **sod**-ZMOF-1 is made from the reaction of In^{3+} cations and imidazoledicarboxylate ($ImDC^{2-}$) linkers with the help of a structure directing agents (SDAs).

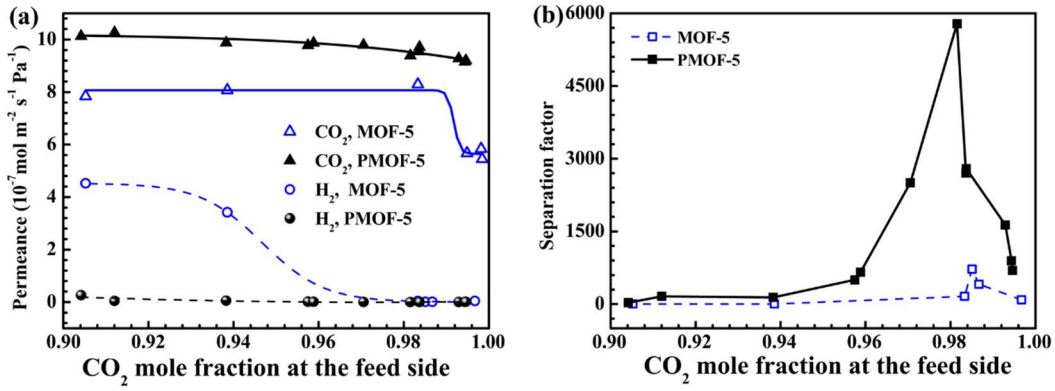

Figure 64. Performance comparison of MOF-5 and PMOF-5 membranes for CO_2/H_2 gas mixture separation at 298 K and a feed pressure of 5 atm: (a) permeance and (b) separation factor (adapted with permission from ref.[147]).

The **sod**-ZMOF-1 incorporates large β-cavities, which are only accessible via 6MR windows that has a 4.1 Å diameter aperture size and it has a 4MR window that not accessible. The **sod**-ZMOF-1 6MR narrow size is expected to provide some selective diffusion and thus allows for separation of small molecules versus larger ones. Furthermore, the **sod**-ZMOF-1 anionic character will affect the

adsorption/diffusion of some gases molecules, which will, in turn, alter its permeation and separation properties. The single gas permeation results showed a high CO_2 permeability and a higher ideal selectivities in favor of CO_2 over other gases above Knudsen (Figure 65 and 66). The calculated separation factors were 8.7 for CO_2/N_2, 5.1 for CO_2/O_2 and 3.6 for CO_2/CH_4. The gas mixture permeation experiments confirmed the preferential CO_2 selective permeation for CO_2/CH_4), and CO_2/N_2 of 4 and 10.5 (at 3.4 bar), respectively. In case of the CO_2/H_2 mixture, the CO_2 permeability was faster than H_2 and the ideal permeation selectivity for CO_2/H_2 was 2.6. The CO_2/H_2:30/70 mixture permeation confirmed the CO_2/H_2 observed reverse-selectivity and showed a 5.2 CO_2/H_2 selectivity. This enhancement in the mixed-gas permeation selectivity, was credited to the favored CO_2 adsorption over H_2. Supplementary permeation tests at more two temperatures confirmed these results, where the selectivity of CO_2/H_2 decreased with increasing the temperature increase and vice versa.

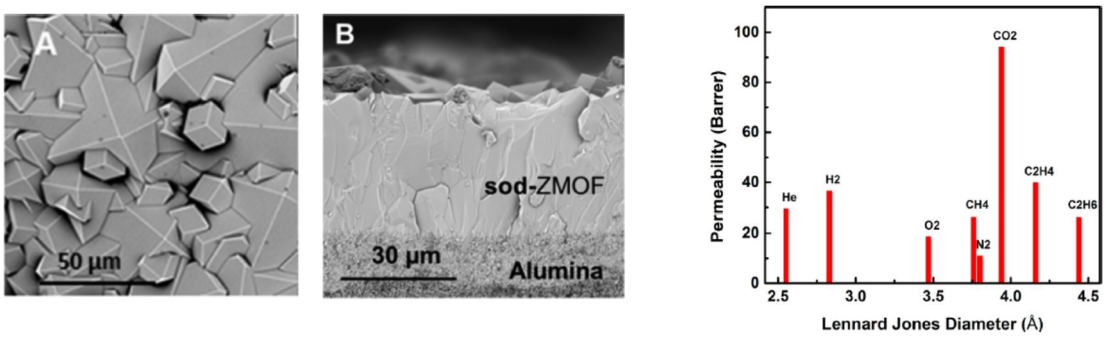

Figure 65. SEM images of sod-ZMOF-1 membrane supported on alumina substrate, top view (A) and cross-section (B) Single gas permeability vs Lennard-Jones diameter of relevant gases (at 308 K) on sod-ZMOF-1 membranes (adapted with permission from ref. [149]).

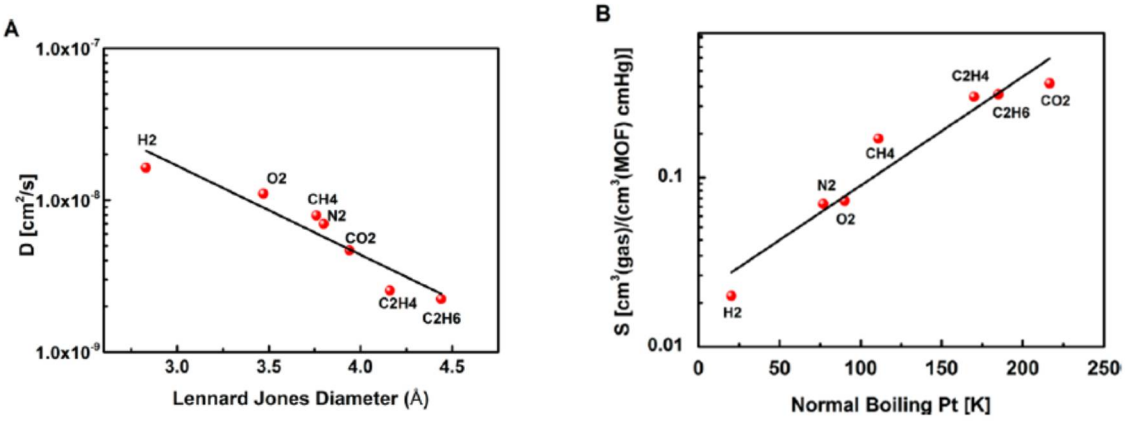

Figure 66. (A) Diffusion coefficients (D) vs Lennard-Jones diameter. (B) Solubility coefficients (S) (from sorption data) vs normal boiling point as determined from CV/VP permeation technique at 2 bar (adapted with permission from ref. [149]).

4.3 Hydrocarbons separation

The hydrocarbon gas mixtures separation is considered as one of the energy-intensive process in different industrial sections like petroleum refining, petrochemical and natural gas production. Nowadays, petrochemical refineries need to separate hydrocarbon mixtures on a huge scale to produce of fuels and chemicals for the market. For example, the cryogenic distillation process for paraffin/olefin separation is considered as the most energy and cost demanding practices.[150] In the production of propylene, the cost comes from the difficulty of separating it from propane due to their similar boiling points. The course of industrial distillation demands about 200 separation trays, which makes it one of the most energetically costly processes in the petrochemical industry.[151] The same is the case for C_4 isomers such as butane and isobutane for which the physical properties are also similar. Thus, the separation of such compounds by distillation extremely costly. Alternatively, energy efficient membrane-based separation offers the possibility to reduce the cost of separation.

Thus far, different types of membranes were tested for these types of separations including polymers, zeolites, carbon molecular sieves, and mixed matrix materials, however most of them have drawbacks that limit their performance.[152,153] In case of polymeric membranes, they suffer from plasticization. This process refers to a change of polymer structure and, thus, a loss in separation performance, caused by the swelling of the space between polymer chains by CO2 and other heavy hydrocarbons. Thus, polymers do not possess the required durability. Zeolites, carbon molecular sieve, and mixed matrix membranes although have shown high compare to the polymers selectivity/permeability performance, require the optimization of the preparation procedure and new membrane-modules designs.[154] Higher performing materials should be discovered in order to justify the investments into the changes of well-established distillation industry. Additional, carbon based membranes are extremely fragile, which makes their scale-up even more difficult than in case of other materials.[155]

Great diversity of pore environments and geometries in MOFs affords various types of adsorption-based separations. In an excellent recent review Adil et al. have highlighted major achievements made in the field of adsorption-based separation, highlighting the advances made with MOFs in the area of hydrocarbon separation. [33,156] MOFs have been also examined in a form of membranes. Recently Caro et al. fabricated a 25 μm thick ZIF-8 layer on asymmetric titania support (Figure 67) and used the measured permeation selectivity for ethane/ethylene separation for a correlation study with the grand canonical Monte Carlo simulations and infrared microscopy, diffusion and adsorption data.[141] The ethene/ethane separation factor α dependency on pressure were investigated and are shown Figure 68. By increasing the gas feed pressure, a slight decrease in separation factor from 2.8 to 2.4 was observed. The single gas permeation without applying a sweep gas showed an ideal separation factor of 4.2. The dissimilarity in separation efficiency observed between the single gas and the mixed gas measurements were attributed to the difference in experimental conditions. Later on the transport properties of ethane/ethylene separation in the same (ZIF-8) membrane were studied by James et al. at different temperatures ranging from 25 to 100 °C and different pressures.[157]

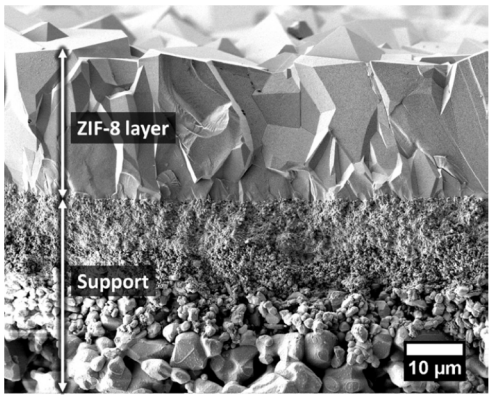

Figure 67. Cross-section of the supported ZIF-8 membrane (adapted with permission from ref. [141])

In the case of propane/propylene separation system, where a propylene permeability of 1 Barrer and a selectivity of 35 are the minimum requirement for the deployment of a membrane for commercial application. Accordingly, the innovative material development are vital to fruitfully fulfill the requirements for this highly energy-intensive important separation.[2] The separation of propylene and propane using ZIF-8 membranes was first reported by Li *et al.* and was based on the kinetic separation based on adsorption studies on ZIF-8 powder.[153] The size difference is around 0.02 nm between these two gases, however the reported selectivity was 150.

Jeong et al. reported a one-step in situ synthesis procedure, for the fabrication of high-quality ZIF-8 membranes using counter diffusion method.[65] The fabricated membranes were tested for the separation of a propylene/propane (50/50) mixture and revealed a high separation selectivity ~55. Figure 69 shows these ZIF-8 membranes propylene/propane separation performance that were fabricated at room-temperature with variable growth times. The increase in the membranes growth time increased the separation factor, however reached a plateau after 1 hour. The separation factor

and the propylene permeability of these ZIF-8 membranes has outperformed the reported values for polymeric and zeolite membranes (Figure 70).

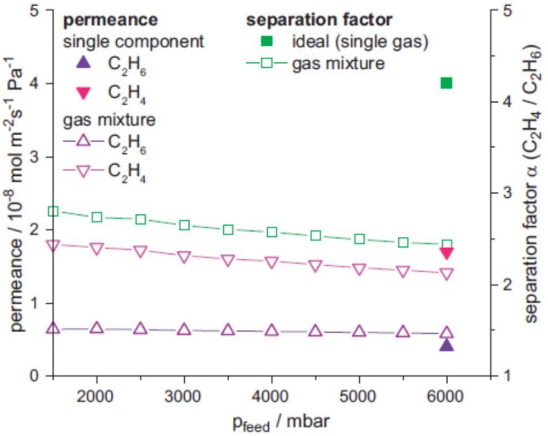

Figure 68. Permeances and separation factors at T = 298K of the ZIF-8 membrane as shown in Fig. 1 for ethene and ethane as pure component as well as in equimolar mixture for different feed pressures. The mixture measurements were carried out by the Wicke–Kallenbach technique (partial pressure of the C_2 component ≈0 at the permeate side) while for the single gas measurement no sweep gas was used (partial pressure of the C_2 component≈1 bar at the permeate side). For gas mixtures, the permeances were calculated at T = 293.15K and p = 1.013 bar from the applied partial pressure difference (for equimolar composition this is 1/2 feed pressure) and for pure component from the total pressure difference (p = 5 bar) (adapted with permission from ref. [141]).

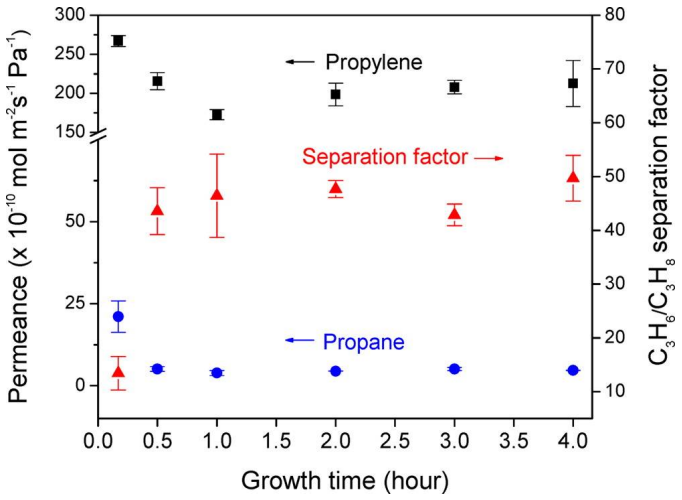

Figure 69. Propylene/propane separation performance of ZIF-8 membranes as a function of growth time at room temperature. ZIF-8 membranes show excellent propylene/propane separation factors (~50) even after growing for 30 min (adapted with permission from ref. [65]).

In another study high-quality ZIF-8 membranes were fabricated using rapid thermal deposition method by Jeong et al.[158] The separation of propylene/propane tests for these membranes were found to exhibit a selectivity ~30. Later on, using a rapid and simple microwave-assisted seeding technique they managed to synthesis high-quality ZIF-8 membranes that showed an enhancement in the propylene/propane selectivity of ~40.

Hara et al. used the counter diffusion approach to fabricate an 80 μm-thick ZIF-8 layer on a alumina capillary support.[159] They have managed to isolate the contribution of the diffusive separation for propylene/propane from the permeation features of these membranes. The single- gas permeation for C_3H_6 and C_3H_8 at temperatures were measured from 298 to 363 K. The ideal separation factors for C_3H_6/ C_3H_8 at 298 K were found to be 59. The analysis of the permeation results showed that the diffusion separation factor has increased to 23 with reducing the temperature, while the

solubility separation factor of 2.7 did not changed, which indicates that the separation of propylene/propane is mainly directed by diffusive separation.

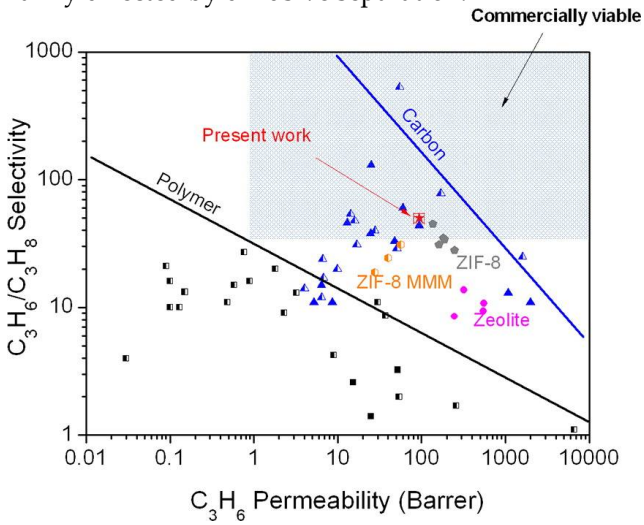

Figure 70. Comparison of the propylene/propane separation performance of our ZIF-8 membranes with those of other membranes reported in the literature. Half- and full-filled symbols indicate separation data from single and binary gas permeation measurements, respectively. The shaded area in the graph implies the performance requirement of a membrane (a minimum permeability of 1 bar and a selectivity of 35) for commercial application. The solid lines are the so-called Robson upper bound, the triangle is the carbon membrane, the circle is a zeolite membrane, the rectangle is a polymer membrane, the pentagon is a ZIF-8 membrane, the hexagon is a ZIF-8 mixed matrix membrane the star is the ZIF-8 membrane in this work (adapted with permission from ref. [65]).

In another study by Lin et al. ZIF-8 membranes were fabricated using a secondary growth method in water and were tested for the C_3H_6/C_3H_8 separation.[160] The measured single gas permeance for C_3H_6 and C_3H_8 declined with the increasing pressure, which is related to the pressure reliance of the adsorption isotherms for individual gas. The ZIF-8 membranes showed a high C_3H_6/C_3H_8 selectivity of a 30 and a high C_3H_6 permeance of 1.1×10^{-8} mol m^{-2} s Pa when an equal-molar binary feed was used exhibited a consistent (Figure 71). The C_3H_6/C_3H_8 selectivity decreased with the increasing feed pressure and temperature, while permeance also decreased when the feed pressure was increased. The stability and durability testes on these membrane for more than a month-showed a stable performance for these membranes.

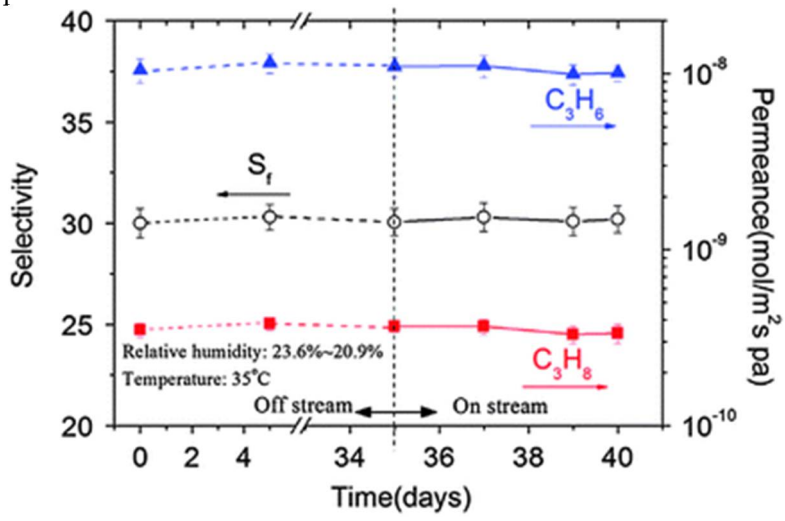

Figure 71. Off-stream stability and on stream stability test of C_3H_6–C_3H_8 mixture gas permeances on the ZIF-8 membrane at 35 °C (adapted with permission from ref. [160])

Nair et al. reported also the fabrication of ZIF-8 membranes using the interfacial microfluidic membrane processing technique in engineered polymeric hollow fibers (Figure 72).[161] Using

optimized synthetic conditions these hollow fiber membranes exhibited a separation factor of about 180. This excellent separation was even maintained high (separation factor of 60) at 120 °C. Furthermore, these membranes were tested under high-pressure operation conditions and a 4- times enhancement in the flux and an excellent C_3H_6/C_3H_8 separation factor of 90 at 9.5 bar. These membranes have also demonstrated long-term stability in permeance and selectivity for testing operation of a month (Figure 73).

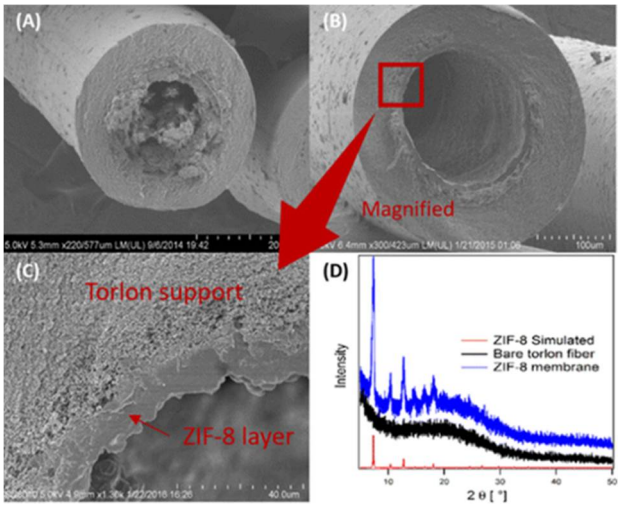

Figure 72. Cross-sectional SEM images of (a) Case 2 ZIF-8 hollow fiber membrane showing crystal overgrowths inside the fiber bore; (b,c) Case 3 ZIF-8/hollow fiber membrane; and (d) XRD patterns of bare PAI membrane and Case 3 ZIF-8 membrane, with a simulated XRD pattern of ZIF-8 shown for comparison (adapted with permission from ref. [161]).

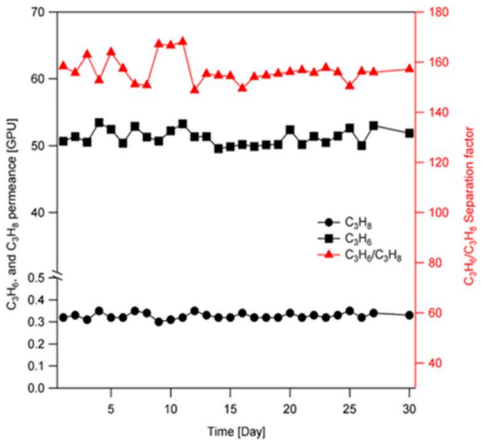

Figure 73. Permeance and separation factor of a ZIF-8 hollow fiber membrane operated continuously for 30 days under an equimolar C_3H_6/C_3H_8 mixture feed at 25 °C and 1 bar feed pressure. (adapted with permission from ref. [161]).

In another study Nair et al. have fabricated ZIFs membranes on carbon hollow fibers using the fluidic processing technique.[162] ZIF-8 membranes prepared in aforementioned way was tested for dehydration of ethanol and furfural, while the ZIF-90 have been tested for the butane isomer separation. The measured permeability of butane in ZIF-90 was comparable to the predicted data (192 vs 206 Barrer), while the selectivity was significantly lower, indicating the presence of defects (7000 vs 12). Nevertheless, the described membrane, to the best of our knowledge, is the only pure MOF membrane study reporting the separation of butane isomer mixtures.

Separation of condensable hydrocarbons like, C_2H_6, C_3H_8 and n-C_4H_{10} from supercritical CH_4 is an important industrial process in the upgrading of natural gas. Recently Shekhah et al. showed that n-C_4H_{10} exhibit an extremely slow adsorption kinetics in ZIF-8 in comparison to other hydrocarbons like C_3H_8 and C_2H_6.[49] The study showed that there is a real adsorption kinetic cut-off at 4.8–4.9 Å, which is the Lennard-Jones diameter of n-C_4H_{10}. Accordingly, for the first time the CH_4/n-C_4H_{10}

mixture separation properties on ZIF-8 membrane were explored. The ZIF-8 membrane exhibited a high selectivity (ca. 250) for CH_4 using a 75/25 CH_4/nC_4H_{10} feed, in the first 2-4 hours of the experiments, which was showed then a rapid decrease with time and exhibited a selectivity of 4 at the steady state after 30 hours (Figure 74). The analysis of the permeation results showed that permeability of n-C_4H_{10} increased from 0.01 Barrer at 6 hours to 0.35 Barrer after 30 hours, which led to a partially blocking of the CH_4 transport in the membrane, as revealed form its 40% permeability drop. A noticeable enhancement in the selectivity of CH_4 in the mixture separation from 4 to 16 was achieved the temperature increase to 323 K, under the same feed pressures.

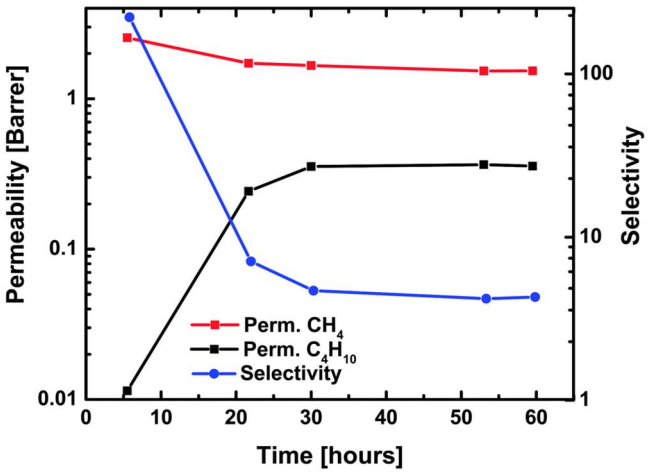

Figure 74. Permeability and selectivity for a 75/25 CH_4/n-C_4H_{10} mixture over time, measured using the time-lag method on ZIF-8 membrane at 308 K (adapted with permission from ref. [49]).

The exciting separation features of the soc-MOF platform has motivated Belmabkhout et al to fabricate them as membranes and evaluate their gas transport separation properties in particular for refinery-off gases.[163]

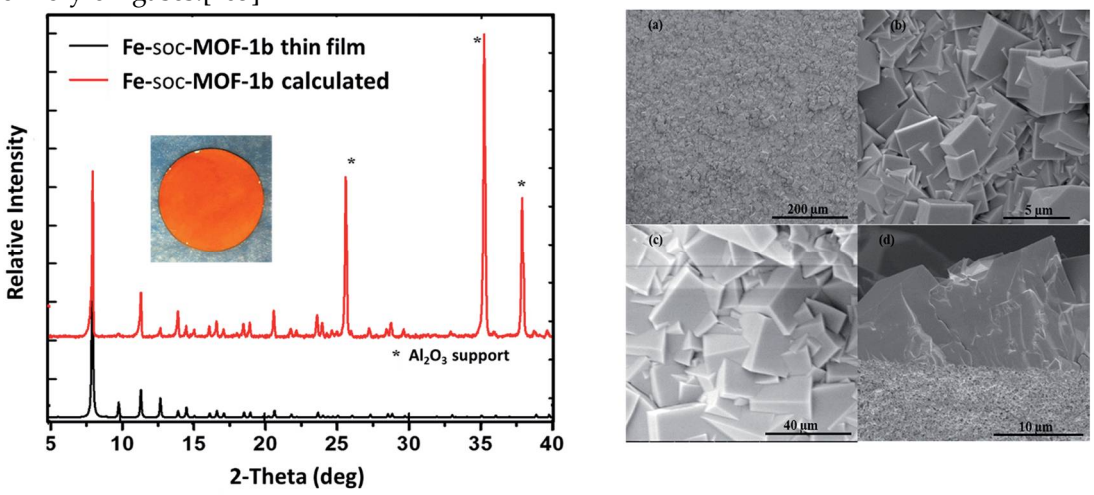

Figure 75. (left) Fe-soc-MOF-1b membrane grown on alumina support and its PXRD pattern compared to the bulk material. (Right) Top-view (a–c) and (d) cross-sectional SEM images of the Fe-soc-MOF membrane grown on the alumina support (adapted with permission from ref. [163]).

The in situ solvothermal approach was used for the growth of highly crystalline and closed Fe(III) and Al(III) soc-MOF analogues as membranes as proven by XRD and SEM in Figure 75. The single gas permeation properties for the Fe-soc-MOF membrane were studied and evaluated using the time-lag method. The single gas permeation results for diverse gases like H_2, O_2, N_2, CH_4, CO_2, C_2H_4, C_2H_6, C_3H_6, C_3H_8 and C_4H_{10} were measured and the Fe-soc-MOF membranes was found to exhibit a decrease in permeability as the Lennard-Jones diameter of the gases increased from H_2 to CH_4 (Figure 76 (left)). However, in the case of hydrocarbons the permeability was found to increase with increasing the boiling point of the gas increased, (Figure 76 (right)). Through deriving the

solubility and diffusivity coefficients from the permeability and the time lag measurements, which revealed a rise in the permeability of C_{2+} hydrocarbon is predominantly governed by solubility. The permeation of the ROG constituents followed the Knudsen behavior, though a high n-C_4H_{10}/CH_4 adsorption selectivity was revealed for the pristine Fe-soc-MOF-1b, however, the selectivity of the Fe-soc-MOF-1b membrane was only 2.2. This behavior is due to the somewhat large aperture size of the 1D channels in the soc-MOF.

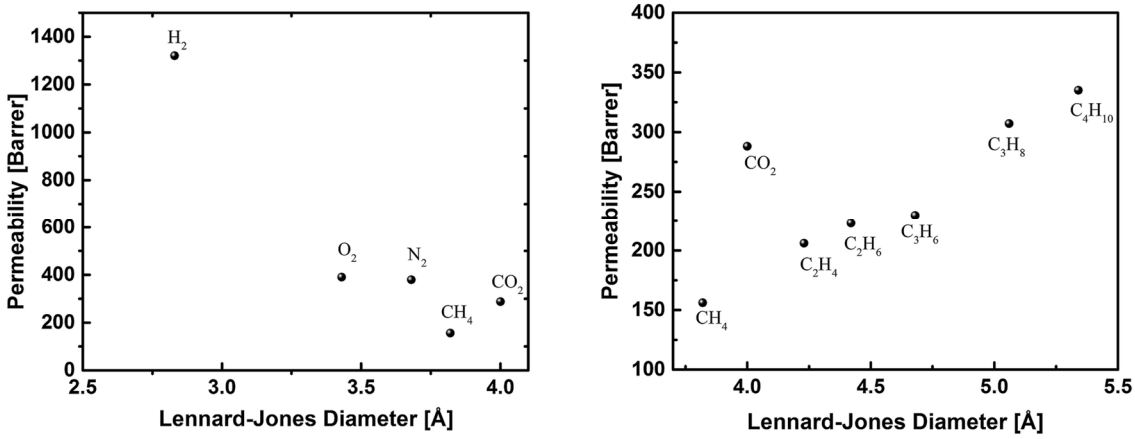

Figure 76. Permeation properties of Fe-soc-MOF-1b as a function of the kinetic diameters of H_2, O_2, N_2, CH_4, CO_2, C_2H_4, C_2H_6, C_3H_6, C_3H_8 and n-C_4H_{10} (adapted with permission from ref. [163]).

5. Discussion

As the foremost limitation for preventing the usage of polymers in the area of carbon dioxide and hydrocarbon separation is plasticization, the rigid membranes with uniform pore structures, such as made from MOFs, are expected to be more effective than polymers.[164] The robustness of these microporous materials affords the unremitting permeability of the gases, while the uniformity of the pore windows controls the passage of certain gases over others. Depending on the size and environment of the MOF structure with the targeted gas; the diffusion- or sorption-controlled selectivity can be achieved, which can be clearly witnessed by the analysis of the reported research articles concerning H_2/CO_2 separation (Figure 77).

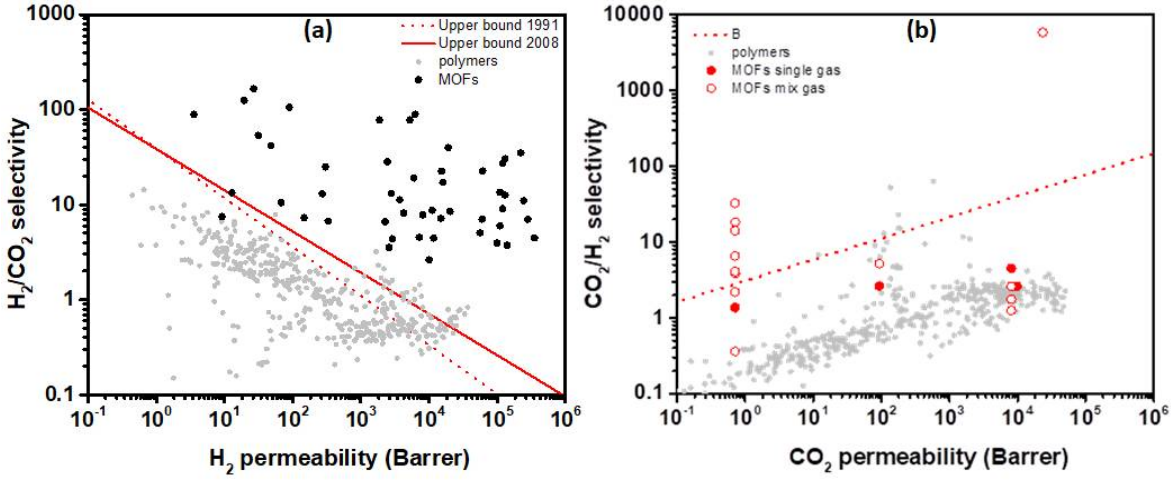

Figure 77. Comparison of permeation properties of MOFs to the performance of polymeric materials reported in the literature for membrane-based: (a) diffusion-driven H_2/CO_2 separation (b) sorption-driven reverse selective CO_2/H_2 separation. All the data points are listed in the supporting information (Table S1-S2).

The majority of MOF-based membranes are reported to act as a molecular sieve, i.e. possessing higher permeabilities for smaller hydrogen molecule compare to the larger one like carbon dioxide due to the dominant diffusion component of H_2 (Figure 77, a). The selectivity of such membranes

often does not undergo significant changes upon the increase of the temperature or the changes in the composition of mixed gases versus the single gases. It should be noted that the performance of MOF hydrogen selective membranes is significantly higher than performance of reported polymers in the literature, which make them potentially used for the Hydrogen purification.

The CO_2 gas separations from N_2, CH_4 and H_2 using MOF membranes were investigated rarely and only few examples have been reported. An efficient membrane for application, should reveal an excellent separation selectivity for CO_2 over other gases, in order to be able to concentrate these valuable gases such as H_2 more efficiently. According to literature, the performance of some MOF membranes, especially for the mixed gases is better than most of polymers in terms of selectivity Figure 77, b). In case of CO_2 separation from N_2 and CH_4, still the performance of most of the reported MOF membranes is still similar or below the performance of polymers and under the Robeson upper bound for both gas separations Figure 78 a and b.

Hydrocarbon separation using MOFs-based membranes is still in its infancy and has not been explored intensively as the limited number of studies mentioned in the above section has demonstrated Figure 79. ZIFs membranes represent so far one of the rare MOF membrane examples, where it was exceptionally stable and it was investigated for the separation of ethane/ethylene (Figure 79a) and for propylene/propane separation (Figure 79b) under different conditions. The excellent stability separation performances, made the ZIF-8 membrane a very eye-catching material for propylene/propane separation, even though there is a huge discrepancy between the values reported. In case of butane/isobutane separation there is only one example reported (Figure 79c), which shows a moderate performance.

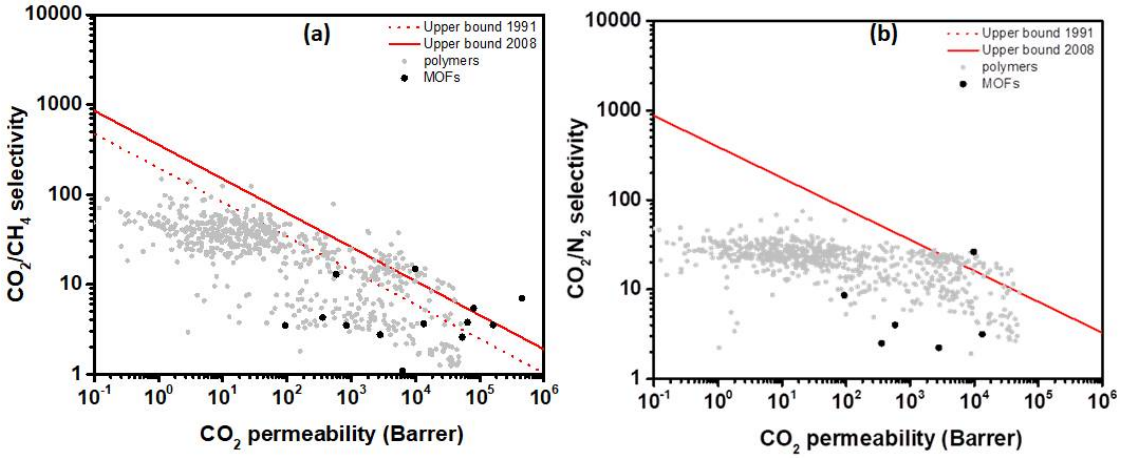

Figure 78. Comparison of permeation properties of MOFs to the performance of polymeric materials reported in the literature for membrane-based: (a) CO_2/CH_4 separation (b) CO_2/N_2 separation. All the data points are listed in the supporting information (Table S3-S4).

Although the trade-off concept is originally conveyed for polymer-based membranes, via comparing both of permeability and selectivity data for a specific gas pair on upper bound plots [4,165], it remains a popular way to estimate different membrane material performance. It is important to highlight the difference between permeance and permeability. The permeance is used in industry and academia to compare the performance of the membranes as the end-products and does not depend on their thickness. Thus, membranes with smaller thickness outperform the thicker membranes made from the same material in terms of the rate of gas transport.

In realistic separation systems, mixtures and conditions are very complex and test experiments to simulate such real conditions are needed, however very difficult to perform. Recently, Liu et al. simulated the effects of the presence of H_2O vapor and other typical gas impurities (such as SO_2 and O_2) in flue gas on the performance of CO_2 adsorption on the ZIF-68 material.[153] The results revealed that O_2 has almost a negligible effect, however, H_2O affects the CO_2 adsorption on ZIF-68 in two opposite ways, where it reduces the CO_2 adsorption ability, but increases the CO_2/N_2 separation factor. Nevertheless, the presence of SO_2 inhibits both the CO_2 adsorption and the CO_2/N_2 separation abilities of ZIF-68.

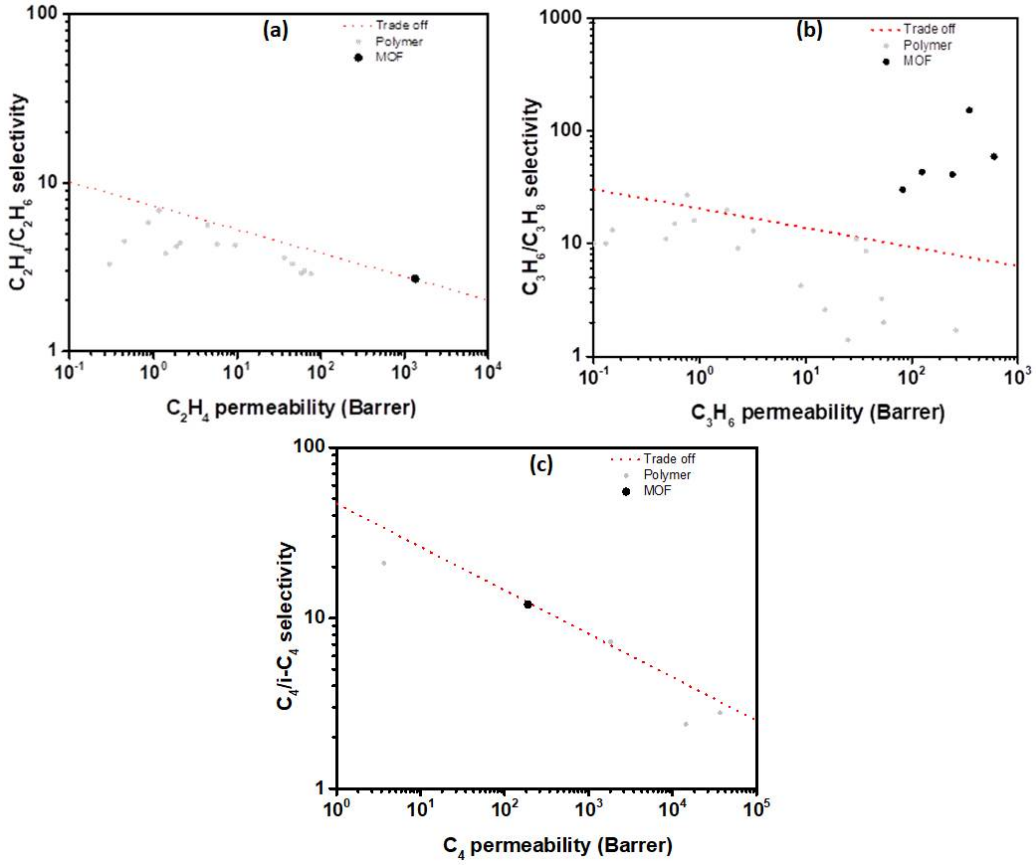

Figure 79. Comparison of permeation properties of MOFs to the performance of polymeric materials reported in the literature for membrane-based: (a) C_2H_4/C_2H_6 separation (b) C_3H_6/C_3H_8 separation, (a) C_4H_{10}/i-C_4H_{10} separation. All the data points are listed in the supporting information (Table S5-S8).

There are few challenges in the MOF-based membrane area that still need to be addressed and more work is needed to advance this filed. The low stability (thermally and chemically) of most of reported MOFs has limited there application as membranes, therefore the development of high stable MOFs as membranes is an important research topic for practical separation applications. Additionally the development of new healing methods for different defects in membrane fabrication, is another topic that need to be addressed, and further development is a need. Additionally, as for now the estimated profit from the implementation of MOF-based membranes over its production costs is still not competitive with a relatively cheap and easily produced polymers.[4] Thus, there is a tremendous need for the development of better materials, which can inverse the tendency in favor of the rigid materials. Particularly, for hydrocarbons separations, in which polymer membranes are completely impractical, microporous membranes have the potential to completely or partially substitute energy intensive distillation process.

6. Conclusions

The distinctive properties of MOFs in terms of surface area, chemical and structure designability and tunability, made them as perfect candidates for application as membranes in separation practices. The curiosity for the progress in MOFs as membranes is increasing and more and more methods are developed for their fabrication and further MOFs are studied and reported. The methods and supports have been expanded and new methods like the gel vapor deposition and LBL methods have been developed for the preparation of defect-free MOF membranes. In case of H_2 purification, an important separation for energy and the environment, the performance of MOF-based membranes has been considerably enhanced through design of MOFs with suitable structures or post-functionalization methods. Recently, the fabrication of CO_2 selective MOF-based membrane was a good advancement in this field, but still more development is needed to improve their selectivity and permeability. The application of MOF-based membranes not limited to separation of small gas

molecules like CO_2, but has been extended also for the separation of hydrocarbons and especially propane/propylene and methane/butane.

Although, there was much progress in this field in the last decade, the way to reach and apply MOF membranes in separation methods under practical application is long. The development of facile, cheap methods to fabricate MOFs on large-scale and on inexpensive supports is of great importance of their progress.

Acknowledgments: The authors acknowledge King Abdullah University of Science and Technology (KAUST) for financial support.

Author Contributions: All authors contributed equally to this manuscript.

Conflicts of Interest: The authors declare no conflict of interest.

References

1. Council, N.R. *Separation technologies for the industries of the future*. The National Academies Press: Washington, DC, 1998.
2. Baker, R.W. Future directions of membrane gas separation technology. *Ind. Eng. Chem. Res.* **2002**, *41*, 1393-1411.
3. Freeman, B.D. Basis of permeability/selectivity tradeoff relations in polymeric gas separation membranes. *Macromolecules* **1999**, *32*, 375-380.
4. Park, H.B.; Kamcev, J.; Robeson, L.M.; Elimelech, M.; Freeman, B.D. Maximizing the right stuff: The trade-off between membrane permeability and selectivity. *Science* **2017**, *356*, 1137-1147.
5. Robeson, L.M. Correlation of separation factor versus permeability for polymeric membranes. *J. Memb. Sci.* **1991**, *62*, 165-185.
6. Corma, A. Zeolites in oil refining and petrochemistry. *Zeolite Microporous Solids: Synthesis, Structure, and Reactivity* **1992**, *352*, 373-436.
7. Egeblad, K.; Christensen, C.H.; Kustova, M.; Christensen, C.H. Templating mesoporous zeolites. *Chem. Mater.* **2008**, *20*, 946-960.
8. Matsukata, M.; Kikuchi, E. Zeolitic membranes: Synthesis, properties, and prospects. *Bull. Chem. Soc. Jap.* **1997**, *70*, 2341-2356.
9. Lin, Y.S.; Kumakiri, I.; Nair, B.N.; Alsyouri, H. Microporous inorganic membranes. *Sep. Purif. Methods* **2007**, *31*, 229-379.
10. Caro, J.; Noack, M. Zeolite membranes – recent developments and progress. *Microporous Mesoporous Mater.* **2008**, *115*, 215-233.
11. Caro, J.; Noack, M.; Kölsch, P.; Schäfer, R. Zeolite membranes - state of their development and perspective. *Microporous Mesoporous Mater.* **2000**, *38*, 3-24.
12. Rangnekar, N.; Mittal, N.; Elyassi, B.; Caro, J.; Tsapatsis, M. Zeolite membranes - a review and comparison with mofs. *Chem. Soc. Rev.* **2015**, *44*, 7128-7154.
13. Kosinov, N.; Gascon, J.; Kapteijn, F.; Hensen, E.J.M. Recent developments in zeolite membranes for gas separation. *J. Memb. Sci.* **2016**, *499*, 65-79.
14. Férey, G. Hybrid porous solids: Past, present, future. *Chem. Soc. Rev.* **2008**, *37*, 191-214.
15. Zhou, H.C.; Long, J.R.; Yaghi, O.M. Introduction to metal-organic frameworks. *Chem. Rev.* **2012**, *112*, 673.
16. Guillerm, V.; Kim, D.; Eubank, J.F.; Luebke, R.; Liu, X.; Adil, K.; Lah, M.S.; Eddaoudi, M. A supermolecular building approach for the design and construction of metal-organic frameworks. *Chem. Soc. Rev.* **2014**, *43*, 6141-6172.
17. Yaghi, O.M.; O'Keeffe, M.; Ockwig, N.W.; Chae, H.K.; Eddaoudi, M.; Kim, J. Reticular synthesis and the design of new materials. *Nature* **2003**, *423*, 705-714.

18. Silva, P.; Vilela, S.M.; Tome, J.P.; Almeida Paz, F.A. Multifunctional metal-organic frameworks: From academia to industrial applications. *Chem. Soc. Rev.* **2015**, *44*, 6774-6803.
19. Zhao, X.; Wang, Y.; Li, D.S.; Bu, X.; Feng, P. Metal-organic frameworks for separation. *Adv. Mater.* **2018**, 1705189-1705195.
20. Eddaoudi, M.; Kim, J.; Rosi, N.; Vodak, D.; Wachter, J.; O'Keeffe, M.; Yaghi, O.M. Systematic design of pore size and functionality in isoreticular mofs and their application in methane storage. *Science* **2002**, *295*, 469-472.
21. Kuppler, R.J.; Timmons, D.J.; Fang, Q.-R.; Li, J.-R.; Makal, T.A.; Young, M.D.; Yuan, D.; Zhao, D.; Zhuang, W.; Zhou, H.-C. Potential applications of metal-organic frameworks. *Coord. Chem. Rev.* **2009**, *253*, 3042-3066.
22. Qiu, S.; Xue, M.; Zhu, G. Metal-organic framework membranes: From synthesis to separation application. *Chem. Soc. Rev.* **2014**, *43*, 6116-6140.
23. Zhang, J.P.; Zhu, A.X.; Lin, R.B.; Qi, X.L.; Chen, X.M. Pore surface tailored sod-type metal-organic zeolites. *Adv. Mater.* **2011**, *23*, 1268-1271.
24. Huang, A.; Caro, J. Covalent post-functionalization of zeolitic imidazolate framework zif-90 membrane for enhanced hydrogen selectivity. *Angew. Chem. Int. Ed.* **2011**, *50*, 4979-4982.
25. Aguado, S.; Canivet, J.; Farrusseng, D. Engineering structured mof at nano and macroscales for catalysis and separation. *J. Mater. Chem.* **2011**, *21*, 7582.
26. Shekhah, O.; Liu, J.; Fischer, R.A.; Woll, C. Mof thin films: Existing and future applications. *Chem. Soc. Rev.* **2011**, *40*, 1081.
27. Geus, E.R.; Jansen, A.E.; Jansen, J.C.; Schoonman, J.; van Bekkum, H. Permeability studies on a silicalite single crystal membrane model. *Stud. Surf. Sci. Catal.* **1991**, *65*, 457-466.
28. Sawamura, K.I.; Izumi, T.; Kawasaki, K.; Daikohara, S.; Ohsuna, T.; Takada, M.; Sekine, Y.; Kikuchi, E.; Matsukata, M. Reverse-selective microporous membrane for gas separation. *Chemistry - An Asian Journal* **2009**, *4*, 1070-1077.
29. Cohen, S.M. Postsynthetic methods for the functionalization of metal-organic frameworks. *Chem. Rev.* **2012**, *112*, 970-1000.
30. Du, N.; Park, H.B.; Robertson, G.P.; Dal-Cin, M.M.; Visser, T.; Scoles, L.; Guiver, M.D. Polymer nanosieve membranes for co2-capture applications. *Nat. Mater.* **2011**, *10*, 372-375.
31. Nouar, F. Design, synthesis and post-synthetic modifications of functional metal-organic materials. University of South Florida, 2010.
32. Wang, Z.; Liu, J.; Arslan, H.K.; Grosjean, S.; Hagendorn, T.; Gliemann, H.; Brase, S.; Woll, C. Post-synthetic modification of metal-organic framework thin films using click chemistry: The importance of strained c-c triple bonds. *Langmuir* **2013**, *29*, 15958-15964.
33. Adil, K.; Belmabkhout, Y.; Pillai, R.S.; Cadiau, A.; Bhatt, P.M.; Assen, A.H.; Maurin, G.; Eddaoudi, M. Gas/vapour separation using ultra-microporous metal-organic frameworks: Insights into the structure/separation relationship. *Chem. Soc. Rev.* **2017**, *46*, 3402-3430.
34. Moggach, S.A.; Bennett, T.D.; Cheetham, A.K. The effect of pressure on zif-8: Increasing pore size with pressure and the formation of a high-pressure phase at 1.47 gpa. *Angew. Chem. Int. Ed.* **2009**, *48*, 7087-7089.
35. Chen, B.; Ma, S.; Hurtado, E.J.; Lobkovsky, E.B.; Liang, C.; Zhu, H.; Dai, S. Selective gas sorption within a dynamic metal-organic framework. *Inorg. Chem.* **2007**, *46*, 8705-8709.
36. Matsuda, R. Materials chemistry: Selectivity from flexibility. *Nature* **2014**, *509*, 434-435.
37. Schneemann, A.; Bon, V.; Schwedler, I.; Senkovska, I.; Kaskel, S.; Fischer, R.A. Flexible metal-organic frameworks. *Chem. Soc. Rev.* **2014**, *43*, 6062-6096.

38. Lin, Z.J.; Lu, J.; Hong, M.; Cao, R. Metal-organic frameworks based on flexible ligands (fl-mofs): Structures and applications. *Chem. Soc. Rev.* **2014**, *43*, 5867-5895.
39. Liu, J.; Woll, C. Surface-supported metal-organic framework thin films: Fabrication methods, applications, and challenges. *Chem. Soc. Rev.* **2017**, *46*, 5730-5770.
40. Zacher, D.; Shekhah, O.; Woll, C.; Fischer, R.A. Thin films of metal-organic frameworks. *Chem. Soc. Rev.* **2009**, *38*, 1418-1429.
41. Betard, A.; Fischer, R.A. Metal-organic framework thin films: From fundamentals to applications. *Chem. Rev.* **2012**, *112*, 1055-1083.
42. Bradshaw, D.; Garai, A.; Huo, J. Metal-organic framework growth at functional interfaces: Thin films and composites for diverse applications. *Chem. Soc. Rev.* **2012**, *41*, 2344-2381.
43. Shekhah, O.; Wang, H.; Kowarik, S.; Schreiber, F.; Paulus, M.; Tolan, M.; Sternemann, C.; Evers, F.; Zacher, D.; Fischer, R.A., *et al.* Step-by-step route for the synthesis of metal-organic frameworks. *J. Am. Chem. Soc.* **2007**, *129*, 15118-15119.
44. Munuera, C.; Shekhah, O.; Wang, H.; Woll, C.; Ocal, C. The controlled growth of oriented metal-organic frameworks on functionalized surfaces as followed by scanning force microscopy. *Phys. Chem. Chem. Phys.* **2008**, *10*, 7257-7261.
45. Shekhah, O. Layer-by-layer method for the synthesis and growth of surface mounted metal-organic frameworks (surmofs). *Materials* **2010**, *3*, 1302-1315.
46. Shekhah, O.; Hirai, K.; Wang, H.; Uehara, H.; Kondo, M.; Diring, S.; Zacher, D.; Fischer, R.A.; Sakata, O.; Kitagawa, S., *et al.* Mof-on-mof heteroepitaxy: Perfectly oriented $[zn_2(ndc)_2(dabco)]_n$ grown on $[cu_2(ndc)_2(dabco)]_n$ thin films. *Dalton Trans.* **2011**, *40*, 4954-4958.
47. Shekhah, O.; Fu, L.; Sougrat, R.; Belmabkhout, Y.; Cairns, A.J.; Giannelis, E.P.; Eddaoudi, M. Successful implementation of the stepwise layer-by-layer growth of mof thin films on confined surfaces: Mesoporous silica foam as a first case study. *Chem. Commun.* **2012**, *48*, 11434-11436.
48. Shekhah, O.; Eddaoudi, M. The liquid phase epitaxy method for the construction of oriented zif-8 thin films with controlled growth on functionalized surfaces. *Chem. Commun.* **2013**, *49*, 10079-10081.
49. Shekhah, O.; Swaidan, R.; Belmabkhout, Y.; du Plessis, M.; Jacobs, T.; Barbour, L.J.; Pinnau, I.; Eddaoudi, M. The liquid phase epitaxy approach for the successful construction of ultra-thin and defect-free zif-8 membranes: Pure and mixed gas transport study. *Chem. Commun.* **2014**, *50*, 2089-2092.
50. Chernikova, V.; Shekhah, O.; Eddaoudi, M. Advanced fabrication method for the preparation of mof thin films: Liquid-phase epitaxy approach meets spin coating method. *ACS Appl. Mater. Interfaces* **2016**, *8*, 20459-20464.
51. Chernikova, V.; Shekhah, O.; Spanopoulos, I.; Trikalitis, P.N.; Eddaoudi, M. Liquid phase epitaxial growth of heterostructured hierarchical mof thin films. *Chem. Commun.* **2017**, *53*, 6191-6194.
52. Liu, Y.; Ng, Z.; Khan, E.A.; Jeong, H.-K.; Ching, C.-b.; Lai, Z. Synthesis of continuous mof-5 membranes on porous α-alumina substrates. *Microporous Mesoporous Mater.* **2009**, *118*, 296-301.
53. Yoo, Y.; Jeong, H.K. Rapid fabrication of metal organic framework thin films using microwave-induced thermal deposition. *Chem. Commun.* **2008**, 2441-2443.
54. Kozachuk, O.; Yusenko, K.; Noei, H.; Wang, Y.; Walleck, S.; Glaser, T.; Fischer, R.A. Solvothermal growth of a ruthenium metal-organic framework featuring hkust-1 structure type as thin films on oxide surfaces. *Chem. Commun.* **2011**, *47*, 8509-8511.
55. Flugel, E.A.; Ranft, A.; Haase, F.; Lotsch, B.V. Synthetic routes toward mof nanomorphologies. *J. Mater. Chem.* **2012**, *22*, 10119-10133.

56. Hu, Y.; Lian, H.; Zhou, L.; Li, G. In situ solvothermal growth of metal-organic framework-5 supported on porous copper foam for noninvasive sampling of plant volatile sulfides. *Anal. Chem.* **2015**, *87*, 406-412.
57. Wu, M.; Ai, Y.; Zeng, B.; Zhao, F. In situ solvothermal growth of metal-organic framework-ionic liquid functionalized graphene nanocomposite for highly efficient enrichment of chloramphenicol and thiamphenicol. *J. Chromatogr. A* **2016**, *1427*, 1-7.
58. Yoo, Y.; Lai, Z.; Jeong, H.K. Fabrication of mof-5 membranes using microwave-induced rapid seeding and solvothermal secondary growth. *Microporous Mesoporous Mater.* **2009**, *123*, 100-106.
59. Albuquerque, G.H.; Herman, G.S. Chemically modulated microwave-assisted synthesis of mof-74(ni) and preparation of metal–organic framework-matrix based membranes for removal of metal ions from aqueous media. *Cryst. Growth Des.* **2017**, *17*, 156-162.
60. Centrone, A.; Yang, Y.; Speakman, S.; Bromberg, L.; Rutledge, G.C.; Hatton, T.A. Growth of metal-organic frameworks on polymer surfaces. *J. Am. Chem. Soc.* **2010**, *132*, 15687-15691.
61. Caro, J. Supported zeolite and mof molecular sieve membranes: Preparation, characterization, application. In *Zeolites and zeolite-like materials*, 2016; pp 283-307.
62. Hillman, F.; Brito, J.; Jeong, H.K. Rapid one-pot microwave synthesis of mixed-linker hybrid zeolitic-imidazolate framework membranes for tunable gas separations. *ACS Appl. Mater. Interfaces* **2018**, *10*, 5586-5593.
63. Venna, S.R.; Carreon, M.A. Highly permeable zeolite imidazolate framework-8 membranes for co2/ch4 separation. *J. Am. Chem. Soc.* **2010**, *132*, 76-78.
64. Nagaraju, D.; Bhagat, D.G.; Banerjee, R.; Kharul, U.K. In situ growth of metal-organic frameworks on a porous ultrafiltration membrane for gas separation. *J. Mater. Chem. A* **2013**, *1*, 8828-8835.
65. Kwon, H.T.; Jeong, H.K. In situ synthesis of thin zeolitic-imidazolate framework zif-8 membranes exhibiting exceptionally high propylene/propane separation. *J. Am. Chem. Soc.* **2013**, *135*, 10763-10768.
66. Mao, Y.; Li, J.; Cao, W.; Ying, Y.; Sun, L.; Peng, X. Pressure-assisted synthesis of hkust-1 thin film on polymer hollow fiber at room temperature toward gas separation. *ACS Appl. Mater. Interfaces* **2014**, *6*, 4473-4479.
67. Guerrero, V.V.; Yoo, Y.; McCarthy, M.C.; Jeong, H.K. Hkust-1 membranes on porous supports using secondary growth. *J. Mater. Chem.* **2010**, *20*, 3938-3943.
68. Mao, Y.; Shi, L.; Huang, H.; Cao, W.; Li, J.; Sun, L.; Jin, X.; Peng, X. Room temperature synthesis of free-standing hkust-1 membranes from copper hydroxide nanostrands for gas separation. *Chem. Commun.* **2013**, *49*, 5666-5668.
69. Nan, J.; Dong, X.; Wang, W.; Jin, W.; Xu, N. Step-by-step seeding procedure for preparing hkust-1 membrane on porous α-alumina support. *Langmuir* **2011**, *27*, 4309-4312.
70. Gascon, J.; Aguado, S.; Kapteijn, F. Manufacture of dense coatings of cu3(btc) (hkust-1) on α-alumina. *Microporous Mesoporous Mater.* **2008**, *113*, 132-138.
71. Kwon, H.T.; Jeong, H.K.; Lee, A.S.; An, H.S.; Lee, J.S. Heteroepitaxially grown zeolitic imidazolate framework membranes with unprecedented propylene/propane separation performances. *J. Am. Chem. Soc.* **2015**, *137*, 12304-12311.
72. Liu, X.; Demir, N.K.; Wu, Z.; Li, K. Highly water-stable zirconium metal-organic framework uio-66 membranes supported on alumina hollow fibers for desalination. *J. Am. Chem. Soc.* **2015**, *137*, 6999-7002.
73. Wang, N.; Mundstock, A.; Liu, Y.; Huang, A.; Caro, J. Amine-modified mg-mof-74/cpo-27-mg membrane with enhanced h2/co2 separation. *Chemical Engineering Science* **2015**, *124*, 27-36.

74. Lee, D.-J.; Li, Q.; Kim, H.; Lee, K. Preparation of ni-mof-74 membrane for co2 separation by layer-by-layer seeding technique. *Microporous Mesoporous Mater.* **2012**, *163*, 169-177.
75. Kang, Z.; Xue, M.; Fan, L.; Ding, J.; Guo, L.; Gao, L.; Qiu, S. "Single nickel source" in situ fabrication of a stable homochiral mof membrane with chiral resolution properties. *Chem. Commun.* **2013**, *49*, 10569-10571.
76. Neelakanda, P.; Barankova, E.; Peinemann, K.V. Polymer supported zif-8 membranes by conversion of sputtered zinc oxide layers. *Microporous Mesoporous Mater.* **2016**, *220*, 215-219.
77. Nian, P.; Cao, Y.; Li, Y.; Zhang, X.; Wang, Y.; Liu, H.; Zhang, X. Preparation of a pure zif-67 membrane by self-conversion of cobalt carbonate hydroxide nanowires for h2 separation. *CrystEngComm* **2018**, *20*, 2440-2448.
78. Huang, A.; Dou, W.; Caro, J. Steam-stable zeolitic imidazolate framework zif-90 membrane with hydrogen selectivity through covalent functionalization. *J. Am. Chem. Soc.* **2010**, *132*, 15562-15564.
79. Huang, A.; Bux, H.; Steinbach, F.; Caro, J. Molecular-sieve membrane with hydrogen permselectivity: Zif-22 in lta topology prepared with 3-aminopropyltriethoxysilane as covalent linker. *Angew. Chem. Int. Ed.* **2010**, *49*, 4958-4961.
80. Liu, Q.; Wang, N.; Caro, J.; Huang, A. Bio-inspired polydopamine: A versatile and powerful platform for covalent synthesis of molecular sieve membranes. *J. Am. Chem. Soc.* **2013**, *135*, 17679-17682.
81. Huang, A.S.; Liu, Q.; Wang, N.Y.; Caro, J. Highly hydrogen permselective zif-8 membranes supported on polydopamine functionalized macroporous stainless-steel-nets. *J. Mater. Chem. A* **2014**, *2*, 8246-8251.
82. Huang, A.; Liu, Q.; Wang, N.; Zhu, Y.; Caro, J. Bicontinuous zeolitic imidazolate framework zif-8@go membrane with enhanced hydrogen selectivity. *J. Am. Chem. Soc.* **2014**, *136*, 14686-14689.
83. Ben, T.; Lu, C.; Pei, C.; Xu, S.; Qiu, S. Polymer-supported and free-standing metal-organic framework membrane. *Chem. Eur. J.* **2012**, *18*, 10250-10253.
84. Huang, A.; Caro, J. Facile synthesis of lta molecular sieve membranes on covalently functionalized supports by using diisocyanates as molecular linkers. *J. Mater. Chem.* **2011**, *21*, 11424-11429.
85. Agrawal, K.V.; Topuz, B.; Pham, T.C.; Nguyen, T.H.; Sauer, N.; Rangnekar, N.; Zhang, H.; Narasimharao, K.; Basahel, S.N.; Francis, L.F., *et al.* Oriented mfi membranes by gel-less secondary growth of sub-100 nm mfi-nanosheet seed layers. *Adv. Mater.* **2015**, *27*, 3243-3249.
86. Ranjan, R.; Tsapatsis, M. Microporous metal organic framework membrane on porous support using the seeded growth method. *Chem. Mater.* **2009**, *21*, 4920-4924.
87. Hu, Y.; Dong, X.; Nan, J.; Jin, W.; Ren, X.; Xu, N.; Lee, Y.M. Metal-organic framework membranes fabricated via reactive seeding. *Chem. Commun.* **2011**, *47*, 737-739.
88. Sun, Y.; Zhang, R.; Zhao, C.; Wang, N.; Xie, Y.; Li, J.R. Self-modified fabrication of inner skin zif-8 tubular membranes by a counter diffusion assisted secondary growth method. *RSC Adv.* **2014**, *4*, 33007-33012.
89. Kusakabe, K.; Kuroda, T.; Morooka, S. Separation of carbon dioxide from nitrogen using ion-exchanged faujasite-type zeolite membranes formed on porous support tubes. *J. Memb. Sci.* **1998**, *148*, 13-23.
90. Aoki, K.; Tuan, V.A.; Falconer, J.L.; Noble, R.D. Gas permeation properties of ion-exchanged zsm-5 zeolite membranes. *Microporous Mesoporous Mater.* **2000**, *39*, 485-492.
91. Barankova, E.; Tan, X.; Villalobos, L.F.; Litwiller, E.; Peinemann, K.V. A metal chelating porous polymeric support: The missing link for a defect-free metal–organic framework composite membrane. *Angew. Chem. Int. Ed.* **2017**, *56*, 2965-2968.
92. Li, W.; Su, P.; Li, Z.; Xu, Z.; Wang, F.; Ou, H.; Zhang, J.; Zhang, G.; Zeng, E. Ultrathin metal-organic framework membrane production by gel-vapour deposition. *Nat. Commun.* **2017**, *8*.

93. Shekhah, O.; Fu, L.; Sougrat, R.; Belmabkhout, Y.; Cairns, A.J.; Giannelis, E.P.; Eddaoudi, M. Successful implementation of the stepwise layer-by-layer growth of mof thin films on confined surfaces: Mesoporous silica foam as a first case study. *Chem. Commun.* **2012**, *48*, 11434-11436.
94. Ladnorg, T.; Welle, A.; Heissler, S.; Woll, C.; Gliemann, H. Site-selective growth of surface-anchored metal-organic frameworks on self-assembled monolayer patterns prepared by afm nanografting. *Beilstein J. Nanotechnol.* **2013**, *4*, 638-648.
95. Shekhah, O.; Wang, H.; Zacher, D.; Fischer, R.A.; Wöll, C. Growth mechanism of metal–organic frameworks: Insights into the nucleation by employing a step-by-step route. *Angewandte Chemie International Edition* **2009**, *48*, 5038-5041.
96. Shekhah, O.; Hirai, K.; Wang, H.; Uehara, H.; Kondo, M.; Diring, S.; Zacher, D.; Fischer, R.A.; Sakata, O.; Kitagawa, S., *et al.* Mof-on-mof heteroepitaxy: Perfectly oriented $[zn_2(ndc)_2(dabco)]_n$ grown on $[cu_2(ndc)_2(dabco)]_n$ thin films. *Dalton Trans.* **2011**, *40*, 4954-4958.
97. Khanjani, S.; Morsali, A. Layer by layer growth of nano porous lead(ii) coordination polymer on natural silk fibers and its application in removal and recovery of iodide. *CrystEngComm* **2012**, *14*, 8137-8142.
98. Shekhah, O.; Wang, H.; Paradinas, M.; Ocal, C.; Schüpbach, B.; Terfort, A.; Zacher, D.; Fischer, R.A.; Wöll, C. Controlling interpenetration in metal-organic frameworks by liquid-phase epitaxy. *Nat. Mater.* **2009**, *8*, 481-484.
99. Darbandi, M.; Arslan, H.K.; Shekhah, O.; Bashir, A.; Birkner, A.; Wöll, C. Fabrication of free-standing ultrathin films of porous metal-organic frameworks by liquid-phase epitaxy and subsequent delamination. *Physica Status Solidi - Rapid Research Letters* **2010**, *4*, 197-199.
100. Shekhah, O.; Liu, J.; Fischer, R.A.; Wöll, C. Mof thin films: Existing and future applications. *Chem. Soc. Rev.* **2011**, *40*, 1081-1106.
101. Sapsanis, C.; Omran, H.; Chernikova, V.; Shekhah, O.; Belmabkhout, Y.; Buttner, U.; Eddaoudi, M.; Salama, K.N. Insights on capacitive interdigitated electrodes coated with mof thin films: Humidity and vocs sensing as a case study. *Sensors* **2015**, *15*, 18153-18166.
102. Chernikova, V.; Shekhah, O.; Eddaoudi, M. Advanced fabrication method for the preparation of mof thin films: Liquid-phase epitaxy approach meets spin coating method. *ACS Appl. Mater. Interfaces* **2016**, *8*, 20459-20464.
103. Caro, J. Are mof membranes better in gas separation than those made of zeolites? *Curr. Opin. Chem. Eng.* **2011**, *1*, 77-83.
104. Hijikata, T. Research and development of international clean energy network using hydrogen energy (we-net). Int. J. Hydrog. Energy **2002**, *27*, 115-129.
105. Yampolskii, Y.; Pinnau, I.; Freeman, B. *Materials science of membranes for gas and vapor separation*. John Wiley & Sons: 2006.
106. Hong, M.; Li, S.; Falconer, J.L.; Noble, R.D. Hydrogen purification using a sapo-34 membrane. *J. Memb. Sci.* **2008**, *307*, 277-283.
107. Nenoff, T.M.; Spontak, R.J.; Aberg, C.M. Membranes for hydrogen purification: An important step toward a hydrogen-based economy. *MRS Bull.* **2011**, *31*, 735-744.
108. Nenoff, T.M. Hydrogen purification: Mof membranes put to the test. *Nat. Chem.* **2015**, *7*, 377-378.
109. Guo, H.; Zhu, G.; Hewitt, I.J.; Qiu, S. "Twin copper source" growth of metal-organic framework membrane: Cu(3)(btc)(2) with high permeability and selectivity for recycling h(2). *J. Am. Chem. Soc.* **2009**, *131*, 1646-1647.

110. Zhou, S.; Zou, X.; Sun, F.; Zhang, F.; Fan, S.; Zhao, H.; Schiestel, T.; Zhu, G. Challenging fabrication of hollow ceramic fiber supported cu3(btc)2 membrane for hydrogen separation. *J. Mater. Chem.* **2012**, *22*, 10322.
111. Park, K.S.; Ni, Z.; Côté, A.P.; Choi, J.Y.; Huang, R.; Uribe-Romo, F.J.; Chae, H.K.; O'Keeffe, M.; Yaghi, O.M. Exceptional chemical and thermal stability of zeolitic imidazolate frameworks. *Proc. Nat. Acad. Sci. USA* **2006**, *103*, 10186-10191.
112. Banerjee, R.; Phan, A.; Wang, B.; Knobler, C.; Furukawa, H.; O'Keeffe, M.; Yaghi, O.M. High-throughput synthesis of zeolitic imidazolate frameworks and application to co2 capture. *Science* **2008**, *319*, 939-943.
113. Phan, A.; Doonan, C.J.; Uribe-Romo, F.J.; Knobler, C.B.; O'Keeffe, M.; Yaghi, O.M. Synthesis, structure, and carbon dioxide capture properties of zeolitic imidazolate frameworks. *Acc. Chem. Res.* **2010**, *43*, 58-67.
114. Chen, B.; Yang, Z.; Zhu, Y.; Xia, Y. Zeolitic imidazolate framework materials: Recent progress in synthesis and applications. *J. Mater. Chem. A* **2014**, *2*, 16811-16831.
115. Gong, X.; Wang, Y.; Kuang, T. Zif-8-based membranes for carbon dioxide capture and separation. *ACS Sustain. Chem. Eng.* **2017**, *5*, 11204-11214.
116. Bux, H.; Liang, F.; Li, Y.; Cravillon, J.; Wiebcke, M.; Caro, J. Zeolitic imidazolate framework membrane with molecular sieving properties by microwave-assisted solvothermal synthesis. *J. Am. Chem. Soc.* **2009**, *131*, 16000-16001.
117. Wu, X.; Liu, C.; Caro, J.; Huang, A. Facile synthesis of molecular sieve membranes following "like grows like" principle. *J. Memb. Sci.* **2018**, *559*, 1-7.
118. Li, Y.; Liu, H.; Wang, H.; Qiu, J.; Zhang, X. Go-guided direct growth of highly oriented metal-organic framework nanosheet membranes for h2/co2 separation. *Chem. Sci.* **2018**, *9*, 4132-4141.
119. Li, Y.-S.; Liang, F.-Y.; Bux, H.; Feldhoff, A.; Yang, W.-S.; Caro, J.r. Molecular sieve membrane: Supported metalâ "organic framework with high hydrogen selectivity. *Angew. Chem. Int. Ed.* **2010**, *122*, 558-561.
120. Wang, B.; Côté, A.P.; Furukawa, H.; O'Keeffe, M.; Yaghi, O.M. Colossal cages in zeolitic imidazolate frameworks as selective carbon dioxide reservoirs. *Nature* **2008**, *453*, 207-211.
121. Huang, A.; Chen, Y.; Wang, N.; Hu, Z.; Jiang, J.; Caro, J. A highly permeable and selective zeolitic imidazolate framework zif-95 membrane for h2/co2 separation. *Chem. Commun.* **2012**, *48*, 10981-10983.
122. Wang, N.; Liu, Y.; Qiao, Z.; Diestel, L.; Zhou, J.; Huang, A.; Caro, J. Polydopamine-based synthesis of a zeolite imidazolate framework zif-100 membrane with high h2/co2 selectivity. *J. Mater. Chem. A* **2015**, *3*, 4722-4728.
123. Knebel, A.; Wulfert-Holzmann, P.; Friebe, S.; Pavel, J.; Strauß, I.; Mundstock, A.; Steinbach, F.; Caro, J. Hierarchical nanostructures of metal-organic frameworks applied in gas separating zif-8-on-zif-67 membranes. *Chem. Eur. J.* **2018**, *24*, 5728-5733.
124. Zhang, F.; Zou, X.; Gao, X.; Fan, S.; Sun, F.; Ren, H.; Zhu, G. Hydrogen selective nh2-mil-53(al) mof membranes with high permeability. Adv. Funct. Mater. **2012**, *22*, 3583-3590.
125. Knebel, A.; Friebe, S.; Bigall, N.C.; Benzaqui, M.; Serre, C.; Caro, J. Comparative study of mil-96(al) as continuous metal-organic frameworks layer and mixed-matrix membrane. *ACS Appl. Mater. Interfaces* **2016**, *8*, 7536-7544.
126. Friebe, S.; Mundstock, A.; Unruh, D.; Renz, F.; Caro, J. Nh2-mil-125 as membrane for carbon dioxide sequestration: Thin supported mof layers contra mixed-matrix-membranes. *J. Memb. Sci.* **2016**, *516*, 185-193.
127. Li, W.; Zhang, Y.; Zhang, C.; Meng, Q.; Xu, Z.; Su, P.; Li, Q.; Shen, C.; Fan, Z.; Qin, L., *et al.* Transformation of metal-organic frameworks for molecular sieving membranes. *Nat. Commun.* **2016**, *7*, 11315.

128. Jin, H.; Wollbrink, A.; Yao, R.; Li, Y.; Caro, J.; Yang, W. A novel cau-10-h mof membrane for hydrogen separation under hydrothermal conditions. *J. Memb. Sci.* **2016**, *513*, 40-46.
129. Lee, D.J.; Li, Q.; Kim, H.; Lee, K. Preparation of ni-mof-74 membrane for co<inf>2</inf>separation by layer-by-layer seeding technique. *Microporous Mesoporous Mater.* **2012**, *163*, 169-177.
130. Nugent, P.; Belmabkhout, Y.; Burd, S.D.; Cairns, A.J.; Luebke, R.; Forrest, K.; Pham, T.; Ma, S.; Space, B.; Wojtas, L., *et al.* Porous materials with optimal adsorption thermodynamics and kinetics for co2 separation. *Nature* **2013**, *495*, 80-84.
131. Takamizawa, S.; Takasaki, Y.; Miyake, R. Single-crystal membrane for anisotropic and efficient gas permeation. *J. Am. Chem. Soc.* **2010**, *132*, 2862-2863.
132. Kang, Z.; Xue, M.; Fan, L.; Huang, L.; Guo, L.; Wei, G.; Chen, B.; Qiu, S. Highly selective sieving of small gas molecules by using an ultra-microporous metal-organic framework membrane. *Energy Environ. Sci.* **2014**, *7*, 4053-4060.
133. Fu, J.; Das, S.; Xing, G.; Ben, T.; Valtchev, V.; Qiu, S. Fabrication of cof-mof composite membranes and their highly selective separation of h2/co2. *J. Am. Chem. Soc.* **2016**, *138*, 7673-7680.
134. Li, Y.; Lin, L.; Tu, M.; Nian, P.; Howarth, A.J.; Farha, O.K.; Qiu, J.; Zhang, X. Growth of zno self-converted 2d nanosheet zeolitic imidazolate framework membranes by an ammonia-assisted strategy. *Nano Res.* **2018**, *11*, 1850-1860.
135. Peng, Y.; Li, Y.; Ban, Y.; Yang, W. Two-dimensional metal–organic framework nanosheets for membrane-based gas separation. *Angew. Chem. Int. Ed.* **2017**, *56*, 9757-9761.
136. Service, R.F. The carbon conundrum. *Science* **2004**, *305*, 962-963.
137. Koros, W.J.; Mahajan, R. Pushing the limits on possibilities for large scale gas separation: Which strategies? *J. Memb. Sci.* **2000**, *175*, 181-196.
138. Lin, H.; Freeman, B.D. Materials selection guidelines for membranes that remove co2 from gas mixtures. *J. Mol. Struct.* **2005**, *739*, 57-74.
139. D'Alessandro, D.M.; Smit, B.; Long, J.R. Carbon dioxide capture: Prospects for new materials. *Angew. Chem. Int. Ed.* **2010**, *49*, 6058-6082.
140. Lai, Z. Development of zif-8 membranes: Opportunities and challenges for commercial applications. *Curr. Opin. Chem. Eng.* **2018**, *20*, 78-85.
141. Bux, H.; Chmelik, C.; Krishna, R.; Caro, J. Ethene/ethane separation by the mof membrane zif-8: Molecular correlation of permeation, adsorption, diffusion. *J. Memb. Sci.* **2011**, *369*, 284-289.
142. Zou, X.; Zhang, F.; Thomas, S.; Zhu, G.; Valtchev, V.; Mintova, S. Co3(hcoo)6 microporous metal-organic framework membrane for separation of co2/ch4 mixtures. *Chemistry* **2011**, *17*, 12076-12083.
143. Liu, Y.; Zeng, G.; Pan, Y.; Lai, Z. Synthesis of highly c-oriented zif-69 membranes by secondary growth and their gas permeation properties. *J. Memb. Sci.* **2011**, *379*, 46-51.
144. Betard, A.; Bux, H.; Henke, S.; Zacher, D.; Caro, J.; Fischer, R.A. Fabrication of a co2-selective membrane by stepwise liquid-phase deposition of an alkylether functionalized pillared-layered metal-organic framework [cu2l2p](n) on a macroporous support. *Microporous Mesoporous Mater.* **2012**, *150*, 76-82.
145. Bohrman, J.A.; Carreon, M.A. Synthesis and co2/ch4 separation performance of bio-mof-1 membranes. *Chem. Commun.* **2012**, *48*, 5130-5132.
146. Xie, Z.; Li, T.; Rosi, N.L.; Carreon, M.A. Alumina-supported cobalt–adeninate mof membranes for co2/ch4 separation. *J. Mater. Chem. A* **2014**, *2*, 1239.
147. Zhao, Z.; Ma, X.; Kasik, A.; Li, Z.; Lin, Y.S. Gas separation properties of metal organic framework (mof-5) membranes. *Ind. Eng. Chem. Res.* **2013**, *52*, 1102-1108.

148. Rui, Z.; James, J.B.; Lin, Y.S. Highly co2 perm-selective metal-organic framework membranes through co2 annealing post-treatment. *J. Memb. Sci.* **2018**, *555*, 97-104.
149. Al-Maythalony, B.A.; Shekhah, O.; Swaidan, R.; Belmabkhout, Y.; Pinnau, I.; Eddaoudi, M. Quest for anionic mof membranes: Continuous **sod**-zmof membrane with co_2 adsorption-driven selectivity. *J. Am. Chem. Soc.* **2015**, *137*, 1754-1757.
150. Bernardo, P.; Drioli, E.; Golemme, G. Membrane gas separation: A review/state of the art. *Ind. Eng. Chem. Res.* **2009**, *48*, 4638-4663.
151. Xue, D.X.; Cadiau, A.; Weselinski, L.J.; Jiang, H.; Bhatt, P.M.; Shkurenko, A.; Wojtas, L.; Zhijie, C.; Belmabkhout, Y.; Adil, K., *et al.* Topology meets mof chemistry for pore-aperture fine tuning: Ftw-mof platform for energy-efficient separations via adsorption kinetics or molecular sieving. *Chem. Commun.* **2018**, *54*, 6404-6407.
152. Eldridge, R.B. Olefin/paraffin separation technology: A review. *Ind. Eng. Chem. Res.* **1993**, *32*, 2208-2212.
153. Li, K.; Olson, D.H.; Seidel, J.; Emge, T.J.; Gong, H.; Zeng, H.; Li, J. Zeolitic imidazolate frameworks for kinetic separation of propane and propene. *J. Am. Chem. Soc.* **2009**, *131*, 10368-10369.
154. Dechnik, J.; Gascon, J.; Doonan, C.J.; Janiak, C.; Sumby, C.J. Mixed-matrix membranes. *Angew. Chem. Int. Ed.* **2017**, *56*, 9292-9310.
155. Buonomenna, M.G.; Yave, W.; Golemme, G. Some approaches for high performance polymer based membranes for gas separation: Block copolymers, carbon molecular sieves and mixed matrix membranes. *RSC Adv.* **2012**, *2*, 10745-10773.
156. Li, J.R.; Sculley, J.; Zhou, H.C. Metal-organic frameworks for separations. *Chem. Rev.* **2012**, *112*, 869-932.
157. James, J.B.; Wang, J.; Meng, L.; Lin, Y.S. Zif-8 membrane ethylene/ethane transport characteristics in single and binary gas mixtures. *Ind. Eng. Chem. Res.* **2017**, *56*, 7567-7575.
158. Shah, M.N.; Gonzalez, M.A.; McCarthy, M.C.; Jeong, H.K. An unconventional rapid synthesis of high performance metal-organic framework membranes. *Langmuir* **2013**, *29*, 7896-7902.
159. Hara, N.; Yoshimune, M.; Negishi, H.; Haraya, K.; Hara, S.; Yamaguchi, T. Diffusive separation of propylene/propane with zif-8 membranes. *J. Memb. Sci.* **2014**, *450*, 215-223.
160. Liu, D.; Ma, X.; Xi, H.; Lin, Y.S. Gas transport properties and propylene/propane separation characteristics of zif-8 membranes. *J. Memb. Sci.* **2014**, *451*, 85-93.
161. Eum, K.; Ma, C.; Rownaghi, A.; Jones, C.W.; Nair, S. Zif-8 membranes via interfacial microfluidic processing in polymeric hollow fibers: Efficient propylene separation at elevated pressures. *ACS Appl. Mater. Interfaces* **2016**, *8*, 25337-25342.
162. Eum, K.; Ma, C.; Koh, D.-Y.; Rashidi, F.; Li, Z.; Jones, C.W.; Lively, R.P.; Nair, S. Zeolitic imidazolate framework membranes supported on macroporous carbon hollow fibers by fluidic processing techniques. *Adv. Mater. Interfaces* **2017**, *4*, 1700080-1700090.
163. Belmabkhout, Y.; Pillai, R.S.; Alezi, D.; Shekhah, O.; Bhatt, P.M.; Chen, Z.; Adil, K.; Vaesen, S.; De Weireld, G.; Pang, M., *et al.* Metal-organic frameworks to satisfy gas upgrading demands: Fine-tuning the soc-mof platform for the operative removal of H_2S. *J. Mater. Chem. A* **2017**, *5*, 3293-3303.
164. Suleman, M.S.; Lau, K.K.; Yeong, Y.F. Plasticization and swelling in polymeric membranes in co_2 removal from natural gas. *Chem. Eng. Technol.* **2016**, *39*, 1604-1616.
165. Robeson, L.M. The upper bound revisited. *J. Memb. Sci.* **2008**, *320*, 390-400.